Universitat Politècnica de Catalunya

UNIVERSITAT POLITÈCNICA DE CATALUNYA
BARCELONATECH

Tesi Doctoral

Aplicación de MALDI-TOF Imaging y HPLC-MS/MS al estudio de la degradación del polímero policaprolactonadiol en diferentes medios acuáticos

Presentada por

Daniel Rivas Becerra

Per a optar al títol de Doctor per la Universitat Politècnica de Catalunya

Supervisor: (IDAEA-CSIC): Prof. Dr. Antoni Ginebreda (IDAEA-CSIC)

Co-supervisors: Prof. Dr. Damià Barceló (IDAEA-CSIC)

2017

WE DECLARE:

That this Thesis entitled "Aplicación de MALDI-TOF Imaging y HPLC-MS al estudio de la degradación del polímero policaprolactonadiol en diferentes medios acuáticos", presented by Daniel Rivas Becerra to obtain a doctoral degree, has been completed under our supervision and meets the requirements to opt for an International Doctoral Degree.

For all intents and purposes, we hereby sign this document.

Prof. Dr. Antoni Ginebreda *Prof. Dr. Damià Barceló*

Barcelona, Septembre 2017

This Thesis was financially supported by the European Communities 7th Framework Programme funding under Grant Agreement No. 603629-ENV-2013-6.2.1-Globaqua. This work has also been supported by the Generalitat de Catalunya (Consolidated Research Groups "2014 SGR 418 - Water and Soil Quality Unit").

UNIVERSITAT POLITÈCNICA DE CATALUNYA
BARCELONATECH
Escola de Doctorat

Assessment results for the doctoral thesis

Academic year:

Full name

Doctoral programme

Structural unit in charge of the programme

Decision of the committee

In a meeting with the examination committee convened for this purpose, the doctoral candidate presented the topic of his/her doctoral thesis entitled _____

_____.

Once the candidate had defended the thesis and answered the questions put to him/her, the examiners decided to award a mark of:

☐ FAIL ☐ PASS ☐ GOOD ☐ EXCELLENT

(Full name and signature) Chairperson	(Full name and signature) Secretary

(Full name and signature) Member	(Full name and signature) Member	(Full name and signature) Member

_____, _____

The votes of the members of the examination committee were counted by the Standing Committee of the Doctoral School, and the result is to award the CUM LAUDE DISTINCTION:

☐ YES ☐ NO

(Full name and signature) Chair of the Standing Committee of the Doctoral School	(Full name and signature) Secretary of the Standing Committee of the Doctoral School

Barcelona, _____

International doctorate mention

- As the secretary of the examination committee, I hereby state that the thesis was partly (at least the summary and conclusions) written and presented in a one of the languages commonly used in scientific communication in the relevant field of knowledge, which must not be an official language of Spain. This rule does not apply to stays, reports and experts from a Spanish-speaking country.

(Full name and signature) Secretary of the Examination Committee

Agradecimientos

En primer lugar, me gustaría agradecer a los Profesores Antoni Ginebreda y Damià Barceló por darme la oportunidad de hacer esta Tesis.

En especial al Profesor Antoni Ginebreda por su dirección y su soporte incondicional y la confianza depositada, sobretodo en momentos donde todo no parecía tan fácil. Agradecer también su orientación, la ayuda recibida y por tener la puerta del despacho siempre abierta. El mundo no es un camino recto, es un entorno de 360º que no está ocupado solo por la ciencia.

Tengo que extender mi agradecimiento a la científica titular Sandra Pérez e investigadora contratada Carme Quero que me han ayudado en la realización de esta Tesis. A Sandra por su ayuda inestimable a lo largo de esta tesis y a Carme por enseñarme siempre con una sonrisa todo lo que se de MALDI.

I would like to acknowledge Professor György Marko-Varga from Lund Universitet (Sweden) for all the knowledge that he gave me and for giving me the opportunity to be part of his group.

Y ahora…y… 1…2…y 1...2…3…4

G/ G4 --- (Acompañado harmónica en G)

Yo vivía en la casa de mis sueños, pero una fría noche de otoño la casera me dijo que me tenía que ir, que tenía que abandonar la casa. Empaqué mis cuatro cosas, y me enfundé la chaqueta con dirección la calle. Me estaban esperando. Mis amigos estaban abajo para coger el coche y viajar. Viajamos juntos, y paramos en diferentes sitios. Sitios donde vivías experiencias, donde conocías gente. Gente de un rato, que duraban lo que duraba una nube en el cielo de Barcelona. Hubo una parada. Fue una sorpresa. Era la estación de tren. El revisor iba cantando que el tren estaba a punto de salir hacía una destinación llamada "Felicidad", y yo, no sé si por miedo, por sorpresa o simplemente porque no quería, me quedé quieto, contemplando como el tren partía. Al volver a la entrada de la estación pude comprobar que mis amigos seguían esperándome, así que me dieron un abrazo, nos montamos en el coche y seguimos nuestro camino con la hermana luna como compañera inseparable. Esta canción se la dedico a todos los que hemos nacido para correr (o perder).

Cambio y…1…2…3…

G/ D/ Em/ C

Nombre de reina, corazón de miel, voz radiofónica, corazón de oro, hasta yo sé que eres un tesoro.

La excelencia se alcanza con mi hermano haciendo este doctorado, yo no sé cuánto me has enseñado.

Alegría perenne, indecisa a muerte, fantasía loca ella no es de cantos, hasta mis armarios te echan de menos.

Pelo salvaje, fumando espera, inteligente siempre de manos negras, licor de menta, ella siempre, está a la espera.

Spuni, pelo de fuego o de castaño ella siempre tiene pelazo, y siempre se hace grande con un temazo.

Hermana gitana, alma soñadora, nómada poligonera deja que el viento te acompañe por la ladera.

La Croacia y el Serbía, dos personas dos países que yo quería, quien me dará por las noches mi rakía

Barcelona Sants- Ourense estación, otorrinos que vienen y van, no hay que acabar como con y "Vienen y van".

Bonachón sin son, al son de sus pensamientos que no van ni por asomo al ton-ton, que haría yo sin este dormilón.

Fuerte en palabras, alma indomable, mira a sus ojos siempre correctos, espero obtener tu sensatez con el medicamento.

Doctor de ojeras, pan de centeno, mala praxis con dolor de muelas, a ver si te pillo y te invito a unas birras.

Elegancia patoril, ahora mamá, seguirás bailando el cancán? sabes que "All along the watchtower" era de Dylan.

Aventurera de raza, mirada sigilosa, castellano paleta, ella sí que sabe montar una fiesta.

Mirada pícara, agujas en las palabras, simplemente genuino, donde llegaras sin haber visto el padrino.

Las flores de un jardín, un jardín que brilla y eso que no hay rastro de flor, seguir así curando el dolor.

Lecce, Bari y Bogotá una explosiva mezcla de bondad, gracias por darme vuestra afabilidad.

Fines de año, en barbacoas y festivales Que anarquía! que bien me caísteis desde el primer día.

Tenue sonrisa, de pequeña estatura, voz de pluma, como te diga algo te mete en la tumba.

De día en el bar de noche en el Dreblin con música siempre en la mente, Teruel existe que quede patente.

Voz tenue, corazón gigante, valiente con cuerpo de Hércules, siempre es un caballero cortés.

Mi primo-hermano bastardo, patrón de noches díscolas y enfermas, él siempre tiene en la manga un as.

Cambio a rock and roll G/ A/ G/ D

Y ahora me gustaría poder agradecer, a todo el mundo antes de que vuelva anochecer, así que los voy a nombrar de una vez; Àngels, Helena y Bozo para comenzar, Laia, Cayo y Kike también deben estar, Alex, Giselle y Alinne para continuar, y a todo el grupo de J.M. yo debo nombrar (Carmen, Yoli, Ana, Sandra, Xaxi, Dorde, Sergi y Víctor), Berta, Mº Pau y Gemma volvemos a empezar, Cristina, Thiago y Aléx seguimos para cantar, Paqui, Nicola y Jaume casi para acabar y Marianne, Josep y Marta para terminar.

Cambio C/ F < Extended Version>

Fin Riff en C

Abstract

Abstract

Water is essential for life, human activities and ecosystems. Currently, water scarcity is an issue of global concern, especially in arid or semi-arid land areas. The global climate change together the population increase causes an imbalance between the demand of water and the available water resources. To this quantitative decrease of the water resources, its qualitative deterioration caused by the contamination introduced by the human being must be added. All these factors lead to a increasing deterioration of human health and aquatic ecosystems.

The characterization of aquatic systems includes structural (biological, hydromorphological and physico-chemical) and functional aspects ("river metabolism"). In addition, it is necessary to emphasize the degradation of natural and anthropogenic organic matter. Wastewater treatment plants (WWTP) have been designed to remove biodegradable compounds, but they are not able to eliminate recalcitrant synthetic organic pollutants. Physico-chemical parameters such as chemical oxygen demand (COD), biochemical oxygen demand (BOD) or total organic carbon (TOC) are used to control the degradation of organic matter during the operation of WWTPs. On the other hand, aquatic ecosystem ecology uses the weight loss of natural organic devices such as dry leaves or fragments of standardized wood that has been exposed to the environment.

Bearing this in mind, the main objective of this thesis was to add more chemistry knowledge into the river ecology by using of a synthetic material probe to study its degradation in natural and engineering aquatic environments (fluvial ecosystems and water treatment plants). The device is based on a commercial polymer exposed for a while to different aquatic environments. The degradation of the synthetic material probe is collected and analyzed by using advanced mass spectrometry techniques such as high performance liquid chromatography mass spectrometry (HPLC-MS), Matrix-assisted laser desorption/ionization time of flight mass spectrometry (MALDI-TOF/MS) and MALDI IMAGING.

The thesis is divided into 7 chapters. Chapter 1 (Introduction) is distributed into three parts. The first presents the problems associated with the quality of the aquatic environment, their effects on ecosystems and succinctly describes the biotic and abiotic processes of degradation of organic matter and its application in WWTPs. In the second part there is a brief description of the polymers, their uses and degradation, as well as the analytical techniques used for their characterization. In the third part, we describe the mass spectrometry analytical techniques used in this thesis, emphasizing those that allow

the study of space in two dimensions, through the corresponding generation of images (IMAGING).

The main objectives of the thesis are described in Chapter 2.

Chapter 3 describes the selection of possible polymers to be used, and the optimization of the analytical methodologies used by MALDI-TOF/MS. The chosen polymer was (polycaprolactone 1250). Probes consisting of a plastic capsule-piston with a sample of the polymer were prepared. Exposure experiments were carried out at various points of the Ebro River. The results obtained showed different types of degradation. Finally, these results were compared with those obtained in parallel using classical methods (using tree leaves). Chapter 4 describes laboratory-scale experiments performed with the selected polymer (polycaprolactone 1250). These experiments consisted in exposing polymer samples for a time in aqueous systems, in sterile, aerobic and denitrifying conditions. The use of the novel MALDI IMAGING technique allowed the observation of degradation differences along the surface of the sample between the three types of conditions tested, obtaining images of the most interesting ions. Likewise, the statistical treatment of the results obtained was confirmed by the results of the images.

The success of the previous laboratory-scale experiment drove it to the next level and this experiment was applied it to wastewater samples. The WWTP El Prat de Llobregat was the site chosen, placing polymer probes in the secondary reactor, where the aerobic and denitrification (anaerobic) treatment are performed. The MALDI IMAGING technique was used to analyze the samples and high-resolution liquid chromatography coupled to mass spectrometry (HPLC-MS) was used as a complementary technique to elucidate the structures of the degradation compounds. The results obtained allowed to establish the degradation mechanisms and corresponding transformation products differentiated between the two types of environments studied. The description and results of this study is presented in Chapter 5.

Finally, in chapter 6 contains a general discussion of each experiment of this thesis. In addition, the future main problems of mass spectrometry analytical techniques (mainly MALDI IMAGING) are exposed offering solutions.

Resumen

Resumen

El agua es esencial para la vida y las actividades del ser humano y de los ecosistemas. Actualmente, la escasez de agua es uno de los temas más candentes que existen a nivel mundial, especialmente en las zonas terrestres de clima árido o semiárido. El cambio global climático junto al incremento constante de población hace que el desequilibrio entre la demanda de agua y los recursos hídricos disponibles se incremente. A esta limitación cuantitativa de los recursos hídricos debe añadirse su deterioro cualitativo causado por la contaminación de los mismos introducida por el ser humano. Todo ello redunda en un impacto creciente sobre la salud humana y los ecosistemas acuáticos.

La caracterización de los sistemas acuáticos incluye tanto aspectos estructurales (biológicos, hidromorfológicos y físico-químicos) como funcionales ("metabolismo fluvial"). Entre estos últimos hay que destacar la degradación de la materia orgánica, tanto natural como de origen antropogénico. Las estaciones depuradoras de aguas residuales (EDAR) están diseñadas para eliminar compuestos biodegradables, pero no son capaces de eliminar del todo un elevado número de contaminantes orgánicos sintéticos recalcitrantes. Para controlar la degradación de la materia orgánica durante la operación de las EDAR se utilizan parámetros globales como la demanda química de oxígeno (DQO), la demanda bioquímica de oxígeno (DBO) o carbono orgánico total (TOC). Por su parte, la ecología de sistemas acuáticos utiliza la pérdida de peso de soportes orgánicos naturales como hojas secas o fragmentos de madera estandarizados expuestos al medio.

Partiendo de esta idea el objetivo principal de esta tesis ha sido introducir más conocimiento químico dentro de la ecología de ríos utilizando una sonda basada en material sintético para estudiar su degradación en ambientes acuáticos, tanto naturales (ecosistemas fluviales) como ingenieriles (depuradoras). El dispositivo contiene un polímero comercial, el cual después de estar expuesto un tiempo en diferentes entornos acuáticos se recoge y se analiza su degradación utilizando técnicas avanzadas de espectrometría de masas, como son la cromatografía líquida de alta eficacia acoplada a espectrometría de masas (HPLC-MS), desorción/ionización láser asistida por matriz tiempo de vuelo acoplado a espectrometría de masas MALDI-TOF/MS y MALDI IMAGING.

La tesis se divide en 7 capítulos. El capítulo 1 (Introducción) está dividido en tres partes. En la primera se presenta la problemática asociada a la calidad del medio acuático, sus efectos sobre los ecosistemas y se describen sucintamente los procesos bióticos y abióticos de degradación de la materia orgánica y su aplicación en las EDAR. En la

segunda parte se realiza una breve descripción de los polímeros, sus usos y degradación, así como las técnicas analíticas que se usan para caracterizarlos. En la tercera parte, se describen las técnicas analíticas de espectrometría de masas empleadas en esta tesis, haciendo énfasis en aquellas que permiten el estudio espacial en dos dimensiones, mediante la correspondiente generación de imágenes (IMAGING).

Los objetivos principales de la tesis se detallan en el capítulo 2.

En el capítulo 3 se describe la selección de posibles polímeros a utilizar, así como la optimización de los correspondientes métodos de análisis mediante MALDI-TOF/MS. Con el polímero finalmente elegido (policaprolactonadiol 1250) se prepararon sondas consistentes en una cápsula-pistón de plástico con una muestra del polímero, y se realizaron experimentos de exposición en diversos puntos del río Ebro. Los resultados obtenidos evidenciaron diferentes tipos de degradación. Finalmente, éstos se compararon con los obtenidos en paralelo mediante métodos clásicos, empleando hojas de árbol. Con el polímero seleccionado (policaprolactonadiol 1250) se realizaron experimentos a escala de laboratorio, que se describen en el capítulo 4, consistentes en la exposición de muestras de polímero durante un tiempo concreto en sistemas acuosos en condiciones estériles, aeróbicas y desnitrificantes. El uso de la novedosa técnica MALDI IMAGING, permitió observar diferencias de degradación a lo largo de la superficie de la muestra entre los tres tipos de condiciones ensayadas, obteniendo imágenes de los iones más interesantes. Así mismo, el tratamiento estadístico de los resultados obtenidos confirmó las imágenes adquiridas.

El éxito del experimento anterior a escala de laboratorio, impulsó llevarlo al siguiente nivel y aplicarlo en muestras de aguas residuales. Así pues, las sondas de polímero se instalaron en el reactor secundario de la EDAR del Prat de Llobregat, donde se realiza un tratamiento de nitrificación (aerobio) y uno de desnitrificación (anaerobio). Para analizar las muestras se utilizó la técnica MALDI IMAGING, además de la cromatografía líquida de alta resolución acoplada a espectrometría de masas (HPLC-MS) para elucidar las estructuras de los compuestos de degradación. Los resultados obtenidos permitieron establecer los mecanismos de degradación y correspondientes productos de transformación en función de las condiciones estudiadas. La descripción y resultados de este estudio se presentan en el capítulo 5.

Finalmente en el capítulo 6 se encuentra la discusión general de cada experimento realizado extrayéndose unas conclusiones finales. Además se introduce el futuro de las técnicas analíticas de generación de imágenes por espectrometría de masas (fundamentalmente MALDI IMAGING), exponiéndose los principales problemas a solventar.

Índice

Lista de tablas

Lista de tablas suplementarias

Lista de figuras

Lista de figuras suplementarias

Abreviaciones

(es) Español / Spanish ---------- (en) Inglés / English

ADN (es)	Ácido desoxirribonucleico
AFDM (en)	total organic mass
AFM (en)	Atomic Force Microscopy
ATP (en)	Adenosine Triphosphate
BOD (en)	Biochemical Oxygen Demand
CHCA (en)	α-Cyano-4-hydroxycinnamic acid
COD (en)	Chemical Oxygen Demand
DCTB (en)	trans-2-[3-(4-tert-Butylphenyl)-2-methyl-2-propenylidene]malononitrile
DHB (en)	2,5-Dihydroxybenzoic acid
DIT (en)	Dithranol
EDAR (es)	Estación Depuradora Agua Residual
ESI (en)	Electrospray Ionization
ESR (en)	Electron Spin Resonance
FTIR (en)	Fourier-Transform Infrared Spectroscopy
GC	Gas Cromatography
GPC (en)	Gel Permeation Chromatography
***H* (en)**	Henry law's constant
HABA (en)	2-(4-hydroxyphenylazo)benzoic
HPLC	High-performance liquid chromatography
IAA (en)	trans-3-indoleacrylic acid
ITO (en)	Indium-Tin oxide
***Kd* (en)**	Soil-water distribution coefficient
***Koa* (en)**	Octanol-air partiotioning coefficient
***Koc* (en)**	Soil adsorption coefficient
***Kow* (en)**	Octanol-water partitioning coefficient
LC	Liquid Cromatography
LDI (es)	Laser Desorción/Ionización
MALDI	Matrix-Assisted Laser Desorption/Ionization
MS	Mass Spectrometry
MSI (en)	Mass Spectrometry mass Imaging
NIST (en)	National Institute of Standards and Technology

NMR (en) Nuclear Magnetic Resonance
PA (es) Poliamida
PAR (en) Photosynthetic Active Radiation
PBAT (es) Copoliesters aromáticos
PBSA (es) Copoliesters alifáticos
PC (es) Policarbonato
PCA (en) Principal Component Analysis
PCL (es) Policaprolactonas
PCLD (en) Polycaprolactone diol
PCP (es) Polycaprolactonediol
PDS (es) Polidioxanona
PE (es) Polietileno
PET (en) Positron EmissionTomogrphy
PEVE (en) Poly(Ethyl Vinyl Ether)
PGA (es) Ácido Poliglicólico
PHA (es) Polihidroxialcanoatos
PLA (es) Poliláctidos
PLLA (es) Ácido Poliláctico
PMM (es) Metil-propenato de metilo
PMMA (es) Polimetilmetacrilato
POL (en) ε-Polylysine
PP (es) Polipropileno
PPF (es) Polipropileno fumarato
PTFE (es) Politetrafluoroetileno
PU (es) Poliuretano
PVC (es) Policloruro de vinilo
RA (en) all-trans Retinoic Acid
RMS (en) Root Mean Square
ROI (en) Region Of Interest
SEC (en) Size-Exclusion Chromatography
SEM (en) Scanning Electron Microscopy
SIMS (en) Secondary Iom Mass Spectrometry
TEM (en) Transmission Electron Microscopy
TOC (en) Total Organic Carbon
TOF Time Of Flight
UNEP (en) United Nations Environment Programme
UV (en) Ultraviolet
VPO (en) Vapor Pressure Osmometry

WWTP (en)	Waste Water Treatment Plant
Yeff (en)	Effective quantum Yield

Capítulo 1

Capítulo 1. Introducción

1.1 El medio acuático

El agua ocupa dos terceras partes de la superficie terrestre. El volumen global de agua dulce se estima alrededor de los 35 millones de km^3 y representa aproximadamente el 2,5% del volumen total de agua existente en el planeta. Sin embargo, la cantidad de agua dulce necesaria para el desarrollo y mantenimiento de ecosistemas y civilización humana se cifra en 200.000 km^3, menos del 1% del volumen total (UNEP, 2004). Sin agua la vida en este planeta no es posible y es uno de los factores más importantes en el desarrollo de cualquier civilización.

En la Figura 1.1. se puede apreciar el ciclo del agua. Desafortunadamente debido al desarrollo industrial y al crecimiento de la población mundial, este ciclo se ve afectado tanto en lo que se refiere a la calidad (contaminación) como a la cantidad. Todo ello, hace que cada vez más los recursos hídricos de calidad disminuyan (Organization, 2011).

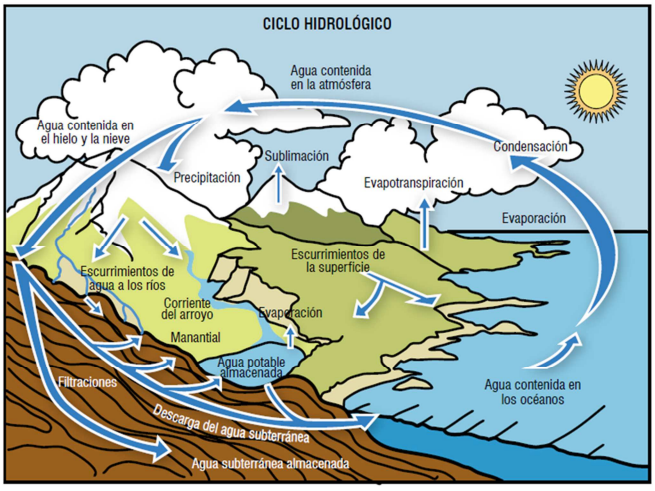

Figura 1.1: Ciclo hidrológico. https://www.siac.gov.co 2013.

Los sistemas de agua dulce de todo el planeta se encuentran en un estado precario debido a la actividad humana. Cerca de 500 científicos de todo el mundo han advertido que habrá escasez de agua dulce de calidad en tan solo dos generaciones si no se toman medidas oportunas (Hutton et al., 2004). La calidad del agua se determina mediante la comparación de parámetros físicos, químicos y biológicos de una muestra en relación a valores guía o estándares de calidad establecidos por los diferentes organismos competentes. Obviamente la calidad del agua depende del uso a que va destinado siendo el agua para consumo humano la que debe cumplir unos patrones de calidad más elevados.

Además, cabe mencionar que durante las últimas décadas se está produciendo un deterioro adicional, provocado por la contaminación química, que ya es detectable en una escala global y limita aún más una base de recursos hídricos que ya es limitada.

1.1.1 Contaminación en el medio acuático

Debido a todos los motivos anteriormente mencionados, el interés científico se ha incrementado por la posible contaminación en los diferentes medios acuáticos y sus efectos en los ecosistemas.

Hay dos tipos de fuentes de contaminación acuática:

Las fuentes puntuales son las que se refieren a los contaminantes que entran en un canal de agua; en esta categoría están las plantas de tratamiento de aguas residuales, los vertidos industriales o los drenajes de los núcleos urbanos.

Por otro lado están las fuentes difusas, que son las que no se originan de una fuente simple. Estas fuentes, difíciles de localizar en el espacio de forma concreta, suelen presentar efectos acumulativos en pequeñas cantidades de contaminantes recogidos en un área amplia. Las lixiviaciones de compuestos nitrogenados procedentes de las tierras agrícolas fertilizadas son un ejemplo.

Los principales parámetros de contaminación acuática son los patógenos, las sustancias químicas orgánicas (entre los que cabe destacar los

microcontaminantes orgánicos) y las sustancias químicas inorgánicas, como nutrientes, metales pesados etc. Dentro los patógenos se incluyen los microorganismos (bacterias, virus) responsables de la transmisión de enfermedades como tifus, cólera, salmonelosis etc. así como parásitos (helmintos).

Las sustancias químicas engloban desde los detergentes, insecticidas, herbicidas, hidrocarburos (orgánicos) a los metales pesados y los nutrientes en las aguas (inorgánicos).

Por otro lado, como hemos comentado están los microcontaminantes orgánicos. Estos contaminantes se nombran así debido a que su concentración se encuentran en niveles traza (ng L^{-1} - µg L^{-1}).

El origen de estos contaminantes puede ser natural o antropogénico (como son los insecticidas, fertilizantes, herbicidas, fármacos y productos de cuidado personal). Una de las vías más importantes de entrada de estos microcontaminantes es a través de las estaciones depuradoras de aguas residuales EDAR. A continuación en la figura 1.2 se muestran las diferentes vías de entrada de los microcontaminantes en el ciclo del agua.

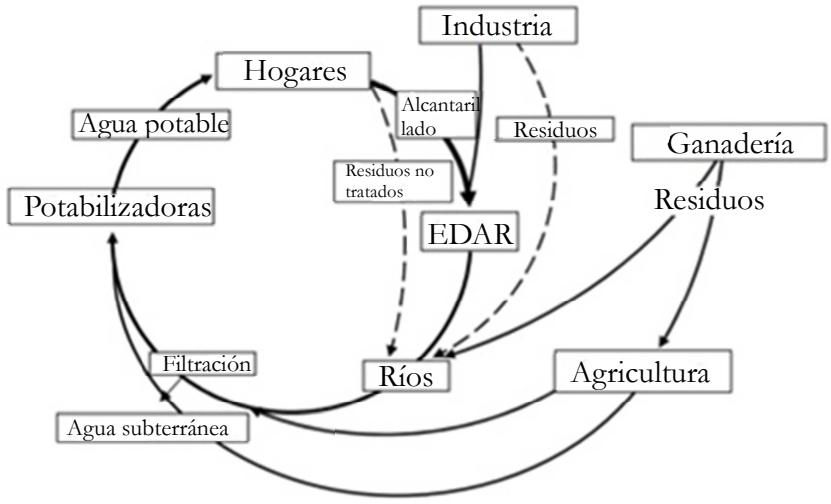

Figura 1.2: Vías de entrada de la contaminación en el ciclo del agua (UNEP, 2004).

Los microcontaminates orgánicos pueden migrar entre diferentes compartimentos ambientales.

Los procesos que pueden experimentar los microcontaminantes en el medio acuático pueden clasificarse en bióticos o abióticos en función de si están mediatizados por organismos vivos o no.

- Bióticos: Bioconcentración, biomagnificación y biodegradación
- Abióticos: Sorción, sedimentación, fotólisis y hidrólisis

Para cada compartimento ambiental puede haber diferentes procesos. Según cual sea el medio (acuático, terrestre o aéreo) hará falta tener en cuenta los diferentes parámetros y procesos que pueden tener lugar. A continuación, en la Tabla 1.1, se detallan los principales.

Tabla 1.1: Procesos y parámetros en los diferentes compartimientos ambientales (Calderón-Preciado et al., 2011).

Acuático	**Terrestre**	**Aéreo**
Solubilidad (S)	Solubilidad (S)	Volatilidad (P_v,H_c)
Volatilización (H_c, $t_{1/2}$)	Volatilización (Hc, $t_{1/2}$)	Tiempo de residencia atmosférico ($t_{1/2}$)
Adsorción a los sedimentos y materia en suspensión (K_{oc},K_d)	Adsorción a la materia orgánica (K_{oc},K_d) y a la materia inorgánica	Reactividad con radicales hidroxil, ozono (K_{oa}) y otros oxidantes
Fotolisis ($t_{1/2}$)	Contaminación en aguas subterráneas	Absorción UV
Hidrolisis	Factor de Bioconcentración	Fotolisis
Factor de Bioconcentración	Hidrolisis	Potencial de desaparición de ozono
Biodegradación	Biodegradación	Deposición

A continuación se resumen las propiedades físico-químicas y los procesos mencionados anteriormente:

Presión de vapor (Pv): Presión ejercida por el vapor de una substancia en equilibrio con su forma sólida o líquida. Proporciona información sobre la tendencia de una substancia a volatilizarse desde su estado puro. Las unidades típicas son mm Hg o torr.

Solubilidad (S): Cantidad máxima de una sustancia química pura que puede ser disuelta en una cantidad dada de agua pura en condiciones estándares de presión y temperatura. Las unidades típicas son mg L^{-1} o g L^{-1}

Tiempo de residencia atmosférica: La proporción de masa total de una sustancia química en un compartimiento atmosférico respecto al total de emisión bajo unas condiciones establecidas. Las unidades típicas son horas o días.

Biodegradación: Transformación de compuestos químicos por organismos vivos. No limitado a microorganismos (por ejemplo bacterias o hongos) pero principalmente por procesos microbianos dentro de la naturaleza. Las unidades típicas se expresan en términos de una constante de vida media.

Tiempo de vida media ($t_{1/2}$): Tiempo que se requiere para reducir la concentración de una sustancia al 50% de la concentración inicial. Las unidades típicas son horas o días.

Constante de Henry (H_c): Distribución de un compuesto entre una solución acuosa y la fase vapor en el equilibrio en un sistema cerrado. H_c puede ser medida directamente o estimada como una relación entre P_v i S y da información sobre la tendencia de un compuesto a volatilizarse desde el agua al aire o disolverse en agua desde el aire. H_c puede estar expresada adimensionalmente o bien en atm m^3 mol^{-1}.

Hidrólisis: Procesos de transformación química en el que una substancia reacciona con el agua.

Coeficiente de partición carbono orgánico-agua (K_{oc}): Proporción de la masa de un compuesto químico que esta adsorbido en el suelo por unidad de masa de carbón orgánico en el suelo respecto a la concentración en el equilibrio en solución. Valores elevados de K_{oc} significan que el compuesto esta adsorbido con fuerza, y por tanto, tiende a ser menos móvil en el medio ambiente.

Oxidación: En general, una reacción en la que los electrones son transferidos de un compuesto químico a un agente oxidante, o cuando un compuesto químico gana oxigeno de un agente oxidante.

Fotólisis: Transformación de un compuesto químico por energía luminosa.

Incorporación a los organismos vivos: Cantidad de compuesto químico que se ha incorporado a un organismo expresada en términos de un factor de bioconcentración (B_v), que es la proporción de la concentración en tejido de la planta respecto a la concentración en el suelo.

Coeficiente de distribución (K_d): Proporción de un compuesto químico adsorbido en la fase solida respecto a la fase liquida en el equilibrio. Las unidades típicas son L Kg^{-1}

Volatilización: Proceso de transporte en el que una sustancia química entra en la atmosfera por evaporación desde el suelo o el agua.

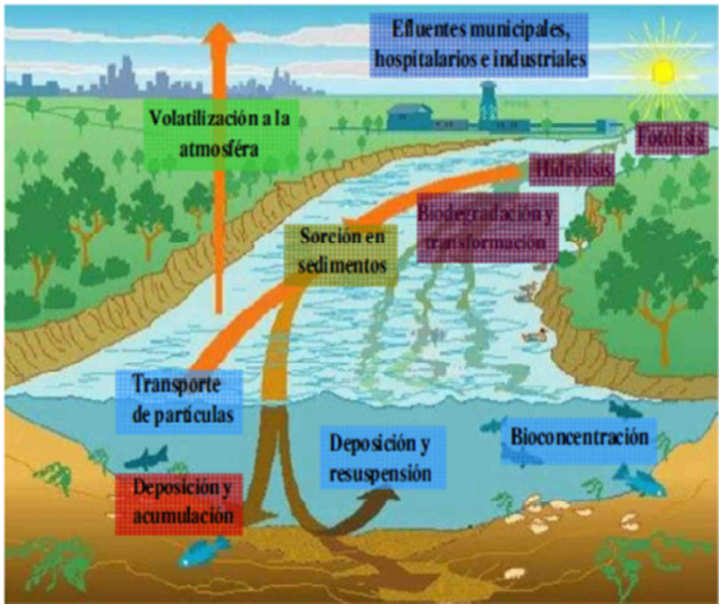

Figura 1.3: Procesos que pueden experimentar los contaminantes en el medio ambiente.

1.1.2 Descomposición de la materia orgánica

Una de las funciones de algunos microorganismos es la descomposición de la materia orgánica. Esta materia orgánica proviene de diferentes fuentes, como son los restos de animales, plantas y las excreciones de seres vivos. Las sucesivas generaciones de comunidades de estos microorganismos utilizan las células microbianas muertas como fuente de carbono. La heterogeneidad de los sustratos naturales crea muchos problemas a la hora de investigar la química de la materia orgánica y sus transformaciones (Mantzavinos and Kalogerakis, 2005).

Los microorganismos encuentran una variedad de sustancias que son física y químicamente heterogéneas debido a la diversidad de los materiales vegetales.

Los vegetales se pueden dividir en siete amplias categorías según su composición química (Wetzel et al., 1995):

- Celulosa, que contiene una concentración en peso seco entre el 15 y el 60%
- Hemicelulosa, que contiene una concentración en peso seco entre el 10 y el 30%
- Lignina, que contiene una concentración en peso de entre el 5 y el 30%
- Una fracción soluble en agua, en la que se incluye azúcares simples, aminoácidos y ácidos alifáticos, que contiene una concentración en peso seco entre el 5 y 30%
- Compuestos solubles en alcohol y éter, que pueden contener grasas, ceras, resinas y una serie de pigmentos
- Proteínas que contienen en su estructura nitrógeno y azufre
- Fracción mineral, los cuáles varían desde el 1 al 13 %

A medida que pasa el tiempo en las plantas sus componentes solubles en agua, minerales y proteínas decrece y la a abundancia de hemicelulosa, lignina y celulosa aumenta. La diversidad de estos compuestos constituye una amplia gama de sustratos que pueden ser utilizados por la comunidad detritívora en la descomposición del carbono. A ellos habría que añadir la materia orgánica sintética de origen antropogénico, cuya descomposición por parte de los microorganismos no solo tiene lugar de manera natural en el medio ambiente receptor, sino que también es aprovechada por el ser humano en el diseño de sistemas biológicos de depuración, como son las depuradoras de aguas residuales, compostaje etc.

1.1.3 Asimilación del carbono

Los microorganismos llevan a cabo la descomposición de la materia orgánica principalmente por dos motivos: como fuente de carbono para la formación del nuevo material celular y para tener suficiente energía para su crecimiento (Eswaran et al., 1993).

La mayoría de los microorganismos en sus células contienen aproximadamente, el 50% de su peso seco en carbono. El substrato que está siendo utilizado es la

principal fuente de este carbono. En microbiología la asimilación, es el proceso mediante el cual se convierte el substrato orgánico en carbono protoplasmático. En condiciones aeróbicas del 20 al 40% del carbono presente en el substrato es asimilado, el resto se puede acumular como productos de desecho o es liberado como CO_2. En ciertos campos y estudios se ha visto que la eficiencia se puede elevar hasta un 50-60%. El dióxido de carbono, los ácidos orgánicos, el metano y los alcoholes son algunos de los productos desechados y liberados en estos procesos.

En general se afirma que los hongos son más eficientes que las bacterias en la asimilación de carbono detrítico como se demuestra en los primeros estudios realizados en los ecosistemas terrestres. Por otro lado, los estudios realizados en ecosistemas acuáticos contradicen los estudios anteriormente descritos (Bertrand and Lallier-Vergès, 1993).

Las condiciones ambientales regulan la eficiencia de la síntesis celular y de un lugar a otro puede variar considerablemente. Así pues, si hay bajos niveles de nutrientes en el medio, se puede esperar un crecimiento lento de los microorganismos. Los organismos que están bajo unas condiciones concretas pueden liberar un producto que no se da en otras condiciones; por ejemplo, se pueden obtener otro tipo de productos dependiendo del pH del medio.

1.1.4 Factores que controlan la degradación del material orgánico

La mineralización de los materiales orgánicos se ve afectada por una serie de factores. Un detrito se oxidará más rápidamente dependiendo de las condiciones físico-químicas del medio así como de la idoneidad de los organismos descomponedores presentes. La velocidad de degradación de la materia orgánica viene dada por diferentes factores físicos y químicos, como la temperatura, el oxígeno, la humedad, los nutrientes inorgánicos y el pH. La relación C/N del residuo detrítico se considera el factor regulador más importante de la tasa de descomposición. El contenido de lignina, el grado de desintegración del substrato presentado a la microflora y la edad del propio detrito también regulan la descomposición (Parton et al., 1987).

Otro factor que afecta a la velocidad a la cual son metabolizados los materiales naturales es la temperatura. Debido a que la composición de la flora varía de una localidad a otra, es imposible encontrar una temperatura óptima para la degradación de un material. Unas temperaturas máximas aproximadas para la degradación se sitúan en 30-35ºC, a 37ºC y a 40ºC.

Las tasas de desasimilación son controladas por el oxígeno, el cual juega otro importante rol dentro del metabolismo microbiano (Harvey et al., 1986; Kalbitz et al., 2000).

Cuando no hay oxigeno existen otros "aceptores de electrones" distintos como el NO_3^-, el SO_4^{-2} o el CO_2, que dan lugar a procesos desnitrificadores, sulfatorreductores o metanogénicos y fermentativos.

Tabla 1.2: Procesos para la obtención de la energía de los diferentes tipos de microorganismos.

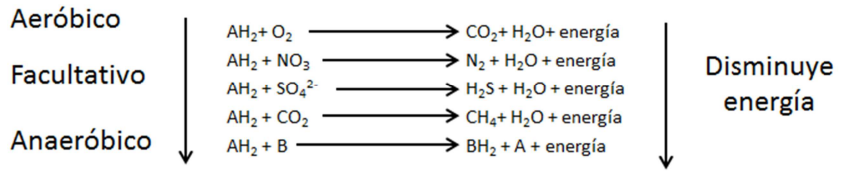

La humedad para que la descomposición proceda debe ser la adecuada. Donde el suministro de oxígeno es adecuado, normalmente en los medios líquidos, los microorganismos crecen con mayor facilidad., por otro lado, en los sedimentos se reduce las actividades de los microbios ya que hay altos niveles de humedad; esto se debe a que el agua interfiere en el movimiento del aire, y esto reduce el suministro de oxígeno.

Un nutriente clave para el crecimiento microbiano es el nitrógeno, y por tanto, para la degradación de la materia orgánica. La disponibilidad y cantidad de nitrógeno varía enormemente en los tejidos animales y vegetales, pero si el contenido del substrato es alto y el elemento es fácilmente utilizable, la microflora no necesita cantidades adicionales para satisfacer sus necesidades.

Algunos componentes que se forman sobre los productos naturales químicamente complejos son más persistentes a las enzimas microbianas que se

encuentran en la flora, mientras que otros desaparecen más rápidamente (Kalbitz et al., 2003; Kell et al., 1994; Moran et al., 2000).

Otro aspecto que afecta a la mineralización es el tipo y cantidad de arcillas ya que adsorben muchos compuestos orgánicos y enzimas extracelulares. La gran capacidad de retener el carbono que presentan las arcillas hace que se inhiba la descomposición. Además, la adicción a medios de cultivo inoculados con sedimentos de ciertas arcillas, retarda la degradación de una gran variedad de sustratos.

Sobre la descomposición no solo las arcillas influyen, sino el sedimento y la arena en general. El movimiento microbiano hacia los nutrientes orgánicos particulados se ve frenado por las barreras que crean estas estructuras, también previenen el contacto entre las células potencialmente activas.

1.1.5 Mineralización anaeróbica del carbono

La mineralización aeróbica del carbono da como principales productos el CO_2, H_2O, y como subproductos remanentes células y componentes húmicos. La formación de células microbianas por unidad de carbono degradado se ve disminuida ya que durante la fermentación anaeróbica la energía producida es baja. En condiciones anaeróbicas totales la degradación de la materia orgánica es más baja que en ambientes que mantienen el nivel de O_2 a concentraciones normales.

En suelos inundados las transformaciones aeróbicas se desplazan hacia las anaeróbicas. En estas zonas inundadas, aunque el O_2 está presente en la porción superior del suelo, el mayor porcentaje de la mineralización del carbono es anaeróbica. De la misma forma, en el medio acuático, si las aguas estancadas no se mueven se produce el mismo efecto, la mineralización del carbono se realiza mediante un proceso anaeróbico. La mayor parte del oxígeno se utiliza antes de que penetre demasiado profundamente en la capa líquido-fango, siempre y cuando haya suficientes carbohidratos disponibles, a medida que vamos profundizando las transformaciones se realizan prácticamente en condiciones anaeróbicas (Canfield et al., 1993; Kristensen et al., 1995).

1.1.6 Organismos descomponedores

La composición de la comunidad heterotrófica que un suelo contiene viene determinada por la cantidad, tipo y disponibilidad de la materia orgánica (Oades, 1984). La composición química de los sustratos añadidos hará variar la naturaleza de la flora, hay grupos microbianos que pueden predominar durante unos días, otros pueden mantener altos niveles poblacionales durante períodos de tiempos más largos (Balzer, 1984). El complejo de enzimas que permite oxidar un determinado grupo de compuestos químicos es único de cada organismo. Hay que tener en cuenta varios factores para que organismos que tienen potenciales enzimáticos similares sobrevivan unos por encima de otros. Estos factores son la competitividad, los predadores y parásitos que se encuentran en estos hábitats (Thomas, 1997).

La flora primaria la forman los microorganismos que son favorables a los componentes de las sustancias orgánicas añadidas. También se desarrolla una flora secundaria, que crecen sobre los compuestos producidos por los agentes primarios o sobre las células muertas o vivas de la flora inicial. La maquinaria bioquímica de este grupo de organismos es diferente al del inicial (Oades, 1989; Van Veen and Kuikman, 1990).

La evolución del CO_2 en relación al número de microorganismos no se ha podido comprobar completamente. La abundancia de microorganismos depende de la materia orgánica, al haber más microorganismos debería haber más presencia de CO_2 pero muchos estudios, demuestran lo contrario. Esto se debe a la múltiple existencia de diferentes comunidades de microorganismos y a las diferentes vías de entrada del carbono que hay en los diferentes compartimentos ambientales.

1.1.7 Caracterización funcional de los ecosistemas fluviales

Para realizar una adecuada caracterización de los ecosistemas fluviales se debe tener en cuenta tanto los aspectos estructurales como los funcionales (Gessner and Chauvet, 2002) (Palmer and Febria, 2012). Sin embargo, la evaluación clásica de la salud de los ecosistemas de agua dulce se basa en las variables físico-químicas (oxígeno disuelto, nutrientes, acidez, conductividad,

contaminantes), las características hidromorfológicas de los ríos, y sobre todo en propiedades estructurales tales como la composición de las comunidades biológicas (Bunn et al., 1999), como está reflejada en la actual legislación (Directiva Marco del Agua, Directiva 2000/60/EC). (Costanza et al., 1997) (Sweeney et al., 2004). Comparativamente se ha prestado mucha menos atención a aquellos aspectos que caracterizan el funcionamiento de los ecosistemas (Feld et al., 2011) (Friberg et al., 2011).

El funcionamiento de los ecosistemas de ríos abarca una variedad de procesos tales como la producción, la retención y la descomposición de la materia orgánica, o la retención y el reciclaje de nutrientes (Elosegi et al., 2010).

El uso de la descomposición de hojarasca como una herramienta de medida funcional se ha empleado ampliamente debido tanto a su sensibilidad a una gran variedad de factores estresantes tales como la presencia de nutrientes (Ferreira et al., 2015), los cambios de uso del suelo (Martínez et al., 2015) o la regulación del agua (Mendoza–Lera et al., 2012), como a su simplicidad experimental (Bärlocher, 2005). Por lo tanto, es el método más utilizado en comparación a otros indicadores para el control de rutina del funcionamiento de los ecosistemas fluviales (Feio et al., 2010); (Gessner and Chauvet, 2002).

Como alternativa, las hojas se han sustituido por otros materiales más estandarizados como tiras de algodón (Imberger et al., 2010);(Tiegs et al., 2007) o palos de madera (McTammany et al., 2008) ; (Tank and Winterbourn, 1996); (Young et al., 2008);. (Arroita et al., 2012) si bien todos estos sustratos reflejan ciertamente la descomposición de la materia orgánica natural, proporcionan poca información acerca de la degradación de la materia orgánica sintética de origen antropogénico.

Dado que muchos de los ecosistemas de agua dulce están hoy en día muy expuestos a la contaminación antropogénica (Vorosmarty et al., 2010) parece conveniente desarrollar nuevos materiales para evaluar los ríos de los ecosistemas fluviales y ver cómo responden a tales perturbaciones y en qué medida son capaces de degradar la materia orgánica sintética. Con este fin, los polímeros pueden constituir candidatos adecuados para ser utilizados como sustratos.

1.1.8 Estaciones de aguas residuales

Una de las formas más comunes de reducir la polución del agua en son las estaciones depuradoras de aguas residuales (EDAR). La mayoría de países avanzados disponen de sistemas de saneamiento compuestos por un vasto sistema de colectores de aguas residuales, estaciones de bombeo, y de plantas de tratamiento que tienen como finalidad recoger el agua residual de los hogares, empresas e industrias, y a través del sistema de colectores, conducir el agua residual a las plantas de tratamiento. El agua tratada es devuelta al medio o puede ser objeto de reutilización. Sin embargo, todavía en muchas áreas de mundo, especialmente en los países en vías de desarrollo, las aguas residuales son vertidas en el medio acuático sin tratamiento alguno.

El proceso más comúnmente utilizado en el tratamiento de aguas residuales, es el denominado "biológico", cuya función básica no es otra que acelerar los procesos naturales por los que se purifica el agua, mediante el uso de la tecnología. Hay tres etapas básicas en el tratamiento de las aguas residuales, denominadas respectivamente tratamientos primario, secundario y terciario (ver figura 1.4). En la etapa primaria, los sólidos se dejan sedimentar y se eliminan de las aguas residuales. La etapa secundaria utiliza procesos biológicos para purificar aún más las aguas residuales, eliminando la materia orgánica mediante un proceso aerobio y en algunos casos nitrógeno en un proceso de desnitrificación anaerobio. A veces, estas etapas se pueden combinar en una operación.

Las aguas residuales entran al tratamiento primario a través de un filtro que elimina los objetos flotantes grandes tales como trapos y palos que podrían obstruir las tuberías o dañar los diferentes equipos presentes en la depuradora. Después de someter las aguas residuales a este procedimiento, pasan un decantador, donde las materias en suspensión se sedimentan en el fondo.

Cuando el proceso de separación se ha completado y la arena ha sido eliminada del agua residual, ésta sigue conteniendo materia orgánica e inorgánica con otros sólidos en suspensión.

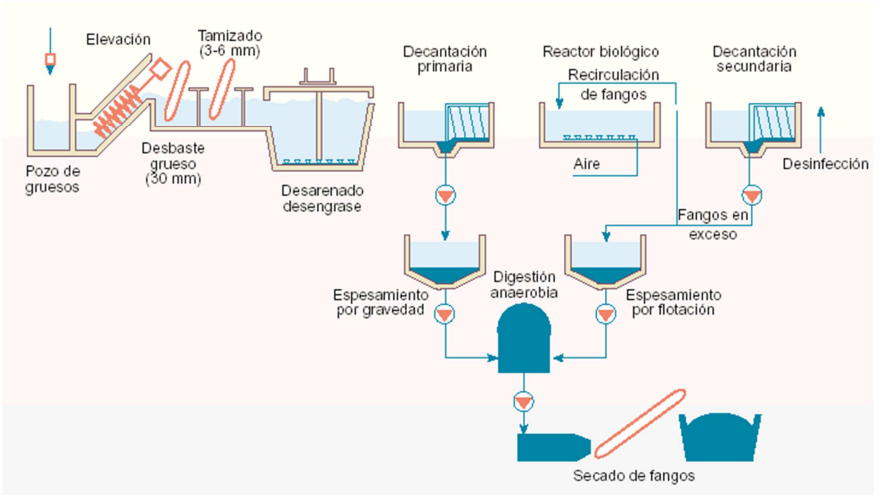

Figura 1.4: Esquema de los diferentes tratamientos en una EDAR

Los microorganismos como las bacterias y los protozoos se pueden usar para disolver las partículas pequeñas y la materia orgánica que no se ha eliminado en tratamiento primario, un ejemplo podría ser la comida. El tratamiento secundario o biológico se realiza en un tanque que contiene una mezcla líquida de microbios denominado lodo activado. Los microorganismos del lodo activado son aeróbicos, y por eso en el tanque donde se realiza el proceso hay bombas que suministran el oxígeno. Los microorganismos presentes en este tanque usan el material particulado y la materia orgánica para crear más microorganismos. Así, los materiales de desecho que no fueron eliminados en el tratamiento primario se transforman en microorganismos que pueden ser recogidos y separados del agua en la siguiente etapa.

La tendencia actual es hacia el uso del proceso de lodo activado en lugar de filtros de goteo. El proceso de lodos activados acelera el trabajo de las bacterias al poner el aire y los lodos cargados con bacterias en contacto estrecho con las aguas residuales. Después de que las aguas residuales abandonen el tanque de sedimentación en la etapa primaria, se bombea hacia un tanque de aireación, donde se mezcla con aire y se mantiene durante varias horas. Durante este tiempo, las bacterias descomponen la materia orgánica en subproductos inofensivos. El lodo, ahora activado con bacterias y otros microorganismos, se decanta en un tanque de sedimentación. Una parte de los lodos se recircula al tanque de aireación para mantener el proceso biológico.

Para completar el tratamiento secundario, hace falta hablar de la desnitrificación. La desnitrificación es el proceso biológico en el cual los nitratos son convertidos en nitrógeno y otros gases como productos finales. Los requerimientos que se necesitan para llevar el proceso a cabo es que el nitrógeno presente este en forma de nitratos y tengamos una fuente de carbono orgánico, además el medio para efectuar el proceso tiene que ser anaeróbico. Los principales procesos que actualmente se utilizan para eliminar los nitratos son el bescanviador iónico y la desnitrificación biológica.

Eventualmente, y sobre todo en función del uso posterior a que se destine el agua tratada, el efluente del tanque de sedimentación puede someterse a desinfección antes de su vertido final. El cloro es el método de desinfección más empleado. La luz ultravioleta o el uso de ozono son otro tipo de técnicas usadas para la desinfección, ya que en muchos casos la presencia de cloro en el agua de los efluentes puede afectar a la fauna y flora del medio receptor.

Los lodos en una depuradora se generan principalmente en los procesos de decantanción primaria y secundaria y en la eliminación del nitrógeno y fósforo. Los lodos primarios y secundarios se mezclan dando lugar a lodos mixtos y estos se juntan con los lodos terciarios, que provienen del tratamiento de eliminación de N_2 y P. Hay varios tratamientos para los lodos generados en la depuradora, el tratamiento por espesamiento consiste en la acción de la gravedad, que actúa depositando el lodo en el fondo y dejando el agua arriba. El tratamiento por digestión anaeróbica, donde en esta fase, toda la materia orgánica se biodegrada en ausencia de oxigeno por acción de microorganismos dando como resultado biogás, y un lodo que puede utilizarse como abono. Finalmente se aplica un tratamiento de deshidratación donde se intenta extraer la máxima cantidad de agua/humedad para reducir su volumen y su peso para facilitar el transporte. En esta fase se utilizan medios mecánicos como presión, centrifugado o filtros.

Los nuevos problemas de contaminación plantean nuevos retos en los sistemas de tratamiento de aguas residuales. Los contaminantes actuales, como metales pesados, compuestos químicos y sustancias tóxicas, son más difíciles de eliminar del agua. La creciente demanda de agua sólo agrava el problema. El aumento en la reutilización del agua requiere un mejor tratamiento de aguas residuales. Estos desafíos se están logrando mediante mejores métodos de eliminación de

contaminantes en las plantas de tratamiento, o mediante la prevención de la contaminación en origen. El pretratamiento de efluentes industriales, por ejemplo, elimina muchos contaminantes problemáticos al principio.

Para devolver el agua más saludable al medio receptor, se están desarrollando nuevos métodos para eliminar los contaminantes. Las técnicas avanzadas de tratamiento de residuos en uso o en desarrollo de separación físico-química tales como filtración, ultrafiltración, adsorción sobre carbón activo, aplicación de técnicas electroquímicas y ósmosis inversa. Estos procesos de tratamiento de aguas residuales, solos o en combinación, pueden alcanzar casi cualquier grado de eliminación de contaminación deseado, siendo únicamente su coste económico el factor limitante de su viabilidad práctica. Los efluentes sometidos a estos tratamientos, pueden ser utilizados para fines industriales, agrícolas o recreativos, o incluso como agua potable.

1.2 Polímeros

1.2.1 Introducción

Los polímeros (del griego poly: «muchos» y mero: «parte», «segmento») son macromoléculas formadas por la unión de moléculas más pequeñas llamadas monómeros.

De forma general puede decirse dos tipos de polímeros, los polímeros naturales y los sintéticos, creados por el hombre (Brandrup,1999).Los materiales poliméricos como el ámbar, la lana, la seda y el caucho natural han sido utilizados a lo largo de los siglos. Existe así mismo una gran variedad de otros polímeros naturales, como la celulosa, la cual, es la mayor constituyente de la madera y el papel. En cuanto a los polímeros sintéticos, en su mayor parte se basan en la química del carbono, y en menor medida de otros elementos como el silicio (siliconas etc.). Los avances de la Química Orgánica del pasado siglo han permitido disponer de una variedad enorme de ellos (véase Tabla 1.3), y puede decirse que hoy día son materiales fundamentales, objeto de múltiples usos y aplicaciones.

Tabla 1.3: Ejemplos de polímeros naturales y sintéticos junto a los monómeros por los que están formados y algunos de sus usos más comunes.

Polímeros Naturales	Monómeros	Uso
Celulosa (polisacáridos)	Glucosa	Papel, algodón
Almidón (polisacáridos)	Glucosa	Almacenamiento de energía en vegetales
Glicógeno (polisácaridos)	Glucosa	Almacenamiento de energía en animales
ADN	Ácido nucleico	Material genético
Proteína	Aminoácido	Proteínas estructurales y funcionales
Seda (poliamidas)	Amida	Tejidos y telas
Lana (proteína)	Aminoácido (proteína pelo y piel de oveja)	Tejidos y telas
Caucho natural	Isopreno	Fabricación de neumáticos, artículos impermeables y aislantes

Polímeros sintéticos	Monómeros	Uso
Polietileno	Eteno	Bolsas, juguetes
Polipropileno	Propeno	Películas, utensilios de cocina, aislante eléctrico
Policloruro de vinilo	Cloro de etano	Ventanas, sillas, aislantes
Poliestireno	Fenileten	Embalajes, aislante térmico y acústico
PTFE (teflón)	Tetrafluoreteno	Antiadherente, aislante
Cloropreno o neopreno	2- clorobutadieno	Aislante térmico, neumáticos
Poliacrilonitrilo	Propenonitrilo (Acrilonitrilo	Tapicerías, alfombras, tejidos
PMM (Plexiglás)	Metil-propenato de metilo (metacrilato de metilo)	Muebles, lentes y equipos ópticos
Nailon	Amidas (Poliamidas)	Plásticos, fibras
Caucho sintético	Butadieno	Fabricación de tubos, correas.

1.2.2 Polímeros en el medio ambiente

El impacto en el medio ambiente causado por la vasta industrialización creada por el hombre y el saqueo de los recursos naturales que éste ejerce sobre el mismo hace que la industria de los polímeros no sea una excepción. El mayor daño proviene de la producción de polímeros. Para contrarrestar los efectos de estas instalaciones, las empresas han hecho esfuerzos para reducir los residuos y el uso de recursos, como el consumo de agua y la energía consumida. Sin embargo, los polímeros pueden ayudar al medio ambiente también. Por una parte, son reciclables, ahorrando espacio en los vertederos. En segundo lugar, su bajo peso ahorra energía durante el transporte, mediante la reducción del uso de combustible. Por último, hacen que los vehículos sean más ligeros, lo que reduce las emisiones de carbono procedentes de la quema de gas y diésel.

La economía es un tema global importante y en constante cambio. . El petróleo crudo es necesario para la producción de polímeros lo que ha generado importantes ganancias a la industria petrolera. Los polímeros también han proporcionado productos totalmente nuevos, creando industrias que no habrían sido posibles sin estos materiales. Véase en la figura 1.5 el crecimiento vertiginoso de producción de plásticos a nivel mundial.

Figura 1.5: Producción mundial de plásticos en millones de toneladas desde 1950-2013.(http://www.plasticseurope.org/plastics-industry/marketandeconomics.aspx?)

Además, los polímeros también han reducido el costo de muchos productos, aumentando la rentabilidad de los procesos. En este sentido, los polímeros han revolucionado no sólo la industria sino también multitud de aspectos prácticos de la vida doméstica de todo el mundo.

1.2.3 Biopolímeros y polímeros biodegradables

Aunque los seres humanos han tomado medidas para reducir el impacto medioambiental de los polímeros sintéticos, los avances recientes han ido un paso más allá. La producción de polímeros se puede hacer con materiales totalmente biológicos, haciendo que los productos finales sean biodegradables y renovables, lo que elimina la necesidad del petróleo por parte de la industria. El almidón, un hidrato de carbono común que se encuentra en el maíz, la patata y el trigo, se puede utilizar para crear papel, cartón, textiles y adhesivos. El colágeno es una proteína que se encuentra en los mamíferos que también puede convertirse en gelatina y además es usada en el campo de la fotografía. La caseína, que se encuentra en la grasa de la leche, se puede utilizar en adhesivos, revestimientos protectores y aglutinantes. Los poliésteres producidos por ciertas bacterias han demostrado ser útiles para los productos biomédicos.

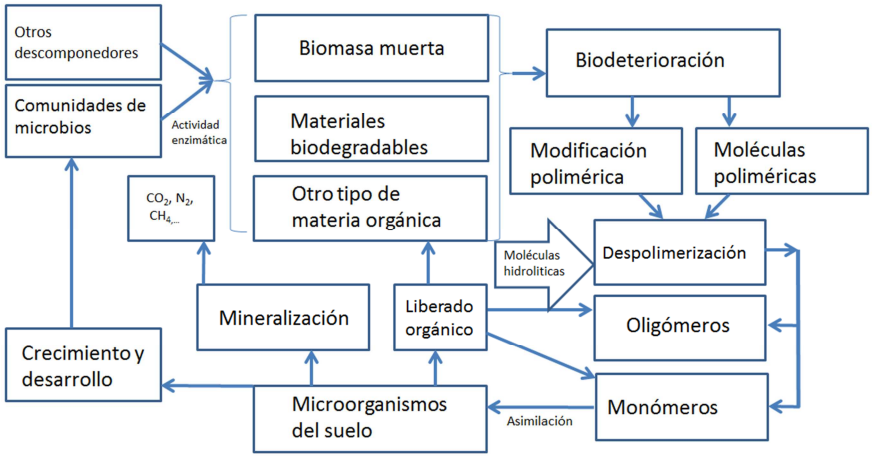

Figura 1.6: Esquema de la biodegradación de polímeros.

Los polímeros presentan un panorama prometedor, en el campo de la biomedicina. El objetivo principal es encontrar materiales no tóxicos para el cuerpo humano y que sean biocompatibles. Estos nuevos materiales tienen que presentar una degradación adecuada y que los productos de esta degradación no sean nocivos para al organismo. Los polímeros biocompatibles tienen un gran

rango de aplicaciones en base a sus propiedades físico químicas. Los estudios que más han profundizado en el tema son los que tienen que ver con los poliésteres y los polihidroxialcanoatos (Albertsson and Varma, 2002).

Quizás el material polimérico más usado en medicina es el hilo para suturar y los clips para los huesos y las placas. El material más usado para suturar es Dexon®, un material que contienen PGA (ácido poliglicólico), el Vicryl® es muy usado también y es un copolímero compuesto por PLLA (ácido poliláctico) (8%) y PGA (92%), finalmente el PDS® , sería el tercero más utilizado siendo un polidioxanona.

Tabla 1.4: Principales polímeros biodegradables y biopolímeros

Origen	**Polímeros Biodegradables**
Productos de Biomasa (agropolímeros)	Polisacáridos
	Proteinas
Microorganismos	Polihidroxialcanoatos (PHA)
Biotecnología	Polilácticos (PLA)
Sínteticos	Policaprolactonas (PCL)
	Poliestaramidas (PEA)
	Copoliesters alifáticos (PBSA...)
	Copoliesters aromáticos (PBAT…)

Biopolímeros		
Naturales	Proteínas	Colageno
		Fibrinogeno
		Proteina de soja
		Seda
	Polisacaridos	Celulosa
		Ácido hilarunoico
Sintéticos	No degradables	PE
		PP
		PA
		PU
		PC
		PVC
		PMMA
		PTFE
	Degradables	PGA
		PLA
		PDS
		PCL
		PPF

El uso de implantes biodegradables para la fijación de fracturas de huesos ha sido estudiado por Hofmann (Hofmann, 1995) y contrastado con el uso de placas metálicas.

Además el transporte y liberación de medicamentos controlados, es otra aplicación en la cual, los polímeros están presentes en la medicina (Rossi et al., 2014). La liberación controlada de medicamentos, se extiende también a campos como a la veterinaria o a la industria agroalimentaria.

Actualmente se depositan en los diferentes compartimientos ambientales toneladas de residuos plásticos generados por el ser humano, con el consiguiente efecto nocivo que provoca. Por ello, los polímeros biodegradables son importantes como alternativa medioambientalmente sostenible.

Las bolsas de plástico son una de las mayores entradas de plásticos al medio ambiente. Las bolsas de basura están hechas de diferentes polímeros. En estos años recientes se han estudiado las propiedades de estas bolsas de plástico para acelerar la biodegradación mitigar su impacto negativo en el medio ambiente (Greene, 2007).

De todas formas, es importante conocer las propiedades de los polímeros, ya que muchos plásticos están presentes en los alimentos que comemos. Los plásticos, debido a sus propiedades de transparencia y aislantes, son utilizados masivamente para empaquetar los alimentos que pueden contaminarse, y llegar al ser humano debido a su ingesta. En el futuro previsiblemente solo se utilizarán bioplásticos para el empaquetamiento de comida. Los bioplásticos presentan varias ventajas: no generan productos nocivos para el organismo y pueden ser fisiológicamente eliminables (Siracusa et al., 2014).

También se pueden encontrar nuevos usos en los cuales se aplican los polímeros biodegradables dentro del campo de la medicina. Los biosensores, que son dispositivos analíticos que detectan componentes biológicos, tienen un gran uso en las ciencias medioambientales. La medicina intenta hacer lo mismo en el cuerpo humano y poder detectar irregularidades o simplemente usarlos para monitorizar ciertos parámetros.

También se pueden encontrar polímeros en el uso de detergentes. Se ha demostrado que la eficiencia de diferentes productos de limpieza tiene que ver con la composición polimérica que estos contienen (Uner and Yilmaz, 2015).

1.2.4 Métodos analíticos de estudio de la degradación de polímeros

Los polímeros presentan una amplia variedad de estructuras, pueden ser lineales, cíclicas, pueden tener ramas en su cadena, estar compuestos por una mezcla de

polímeros (copolímeros). Alternativamente también pueden ser nanomateriales (dendrímeros, etc.) normalmente para la caracterización estructural de una muestra de polímero se evalúan la masa molar media, la distribución de la masa molecular, la secuencia de copolímeros, el final de cadena del polímero investigado y la detección de impurezas y aditivos que pueda contener.

Hay diferentes métodos para la caracterización de polímeros, ya sean sintéticos o naturales. Las técnicas espectroscópicas más usadas son la transformada de Fourier (FTIR), resonancia de espín electrónico (ESR), y la resonancia magnética nuclear (NMR) de protón (^{1}H) y carbono ^{13}C.

Para caracterizar el peso molecular se suele utilizar las propiedades coligativas de las sustancias, así se utilizan la osmometría de presión de vapor (VPO), así como el viscosímetro o la cromatografía de gel (GPC) o la cromatografía de exclusión molecular (SEC).

Hay muchas técnicas microscópicas para el estudio de la superficie de los polímeros durante su biodegradación, como son los microscopios ópticos, los de transmisión y los de barrido (TEM y SEM). Se pueden encontrar estudios con microscopios de fuerza atómica (AFM).

La cromatografía de líquidos y la de gases (HPLC y GC) se usa para analitos que provienen de la mezcla generada por la degradación de los productos.

El análisis de polímeros puede envolver muchos diferentes aspectos incluyendo, la caracterización detallada de las estructuras químicas y la composición así como la determinación de la media de la masa molecular (Rizzarelli and Carroccio, 2014)

La espectrometría de masas, ofrece la oportunidad de explorar minuciosamente los detalles estructurales del polímero (Bahr et al., 1992; Cotter et al., 2004; Montaudo et al., 2006; Nielen, 1999; Pasch and Rode, 1995; Peacock and McEwen, 2004; Schriemer and Li, 1996).

1.3 La técnica MALDI TOF/MS (Matrix Assited Laser Desorption Ionization) y afines: Teoría y aplicaciones.

1.3.1 Introducción: descripción de la técnica

En los últimos años se ha incrementado el rango de masas del Matrix assisted laser desorption/ionization time-of- flight (MALDI TOF), esto supone que se pueden resolver espectros de masa de 50 a 70 KDa, permitiendo la detección de grandes moléculas en bajas concentraciones (Montaudo et al., 2006). Estos avances han logrado que en los últimos años se haya incrementado el uso del MALDI TOF/MS en la caracterización de materiales, abarcando aspectos tan variados como polímeros, tejidos biológicos, bacterias etc.

La identificación de los finales de cadena del polímero es una de las principales ventajas que se presenta en la caracterización de polímeros. La identificación del grupo final es crucial en el análisis de polímeros (Montaudo et al., 2006; Pasch and Rode, 1995) .

A la hora de usar MALDI TOF/MS hay que tener en cuenta una serie de cosas, como es la preparación de la muestra, que incluye la matriz, el solvente y el agente cationizante, así como las proporciones que se usan (Jagtap and Ambre, 2005).

1.3.2 Detector y analizador

La espectrometría de masas de tiempo de vuelo (TOF/MS) es un método de espectrometría de masas en el que la relación masa-carga de un ión se determina mediante una medición de tiempo. Los iones son acelerados por un campo eléctrico de fuerza conocida. Esta aceleración da como resultado un ion que tiene la misma energía cinética que cualquier otro ion que tenga la misma carga. La velocidad del ion depende de la relación masa-carga (los iones más pesados de la misma carga alcanzan velocidades más bajas). Se mide el tiempo que toma

posteriormente para que el ion alcance un detector a una distancia conocida. Este tiempo dependerá de la velocidad del ion, y por lo tanto es una medida de su relación masa-carga. A partir de esta relación y parámetros experimentales conocidos, se puede identificar el ion.

El detector es muy importante al usar la fuente de ionización MALDI ya que amplifica la señal en un factor de10^7. Esta amplificación de señal no se puede conseguir sin la presencia de una *pool*, cuya función principal es vaciar los electrones para que el amplificador no tenga una sobrecarga. Este efecto molesto se llama saturación del detector. La presencia de compuestos de bajo peso molecular en las muestras puede causar la saturación del detector, y hacer que las señales disminuyan. Este efecto se hace evidente en muestras que presentan dificultad a la hora de desorber sus compuestos cuando se aplica una potencia de laser moderada. El usuario tiene varias posibilidades de intentar evitar la saturación del detector o por lo menos de reducirlo (Ashcroft et al., 2004; Pasch and Rode, 1995).

Los espectrómetros de masas del MALDI TOF/MS están equipados con un instrumento electrostático, el deflector, el cual actúa como freno para que los compuestos de bajo peso molecular no lleguen al detector. La eficacia de este instrumento es alta y por eso el uso del deflector es muy popular.

1.3.3 Resolución

La mayoría de instrumentos MALDI TOF/MS tienen un instrumento para aumentar la resolución, el reflectrón, el cual consiste en una serie de electrodos puestos al final del tubo de "vuelo". El reflectrón tiene que ser usado en conjunción con un detector adicional (usualmente llamado el reflectrón detector) que se encuentra en la cara opuesta con respecto al otro detector ordinario. En la figura 1.7 y figura 1.8 se muestra el esquema del reflectrón en el espectrómetro de masas MALDI TOF/MS (Cotter et al., 2004). Cuando los electrodos están en modo *off*, los espectros del MALDI TOF/MS son registrados en el modo lineal, mientras que si están en modo *on* los espectros se registran en el modo reflectrón. El reflectrón causa una disminución en la sensibilidad, y no puede ser usado con los polímeros que presentan una desorción recalcitrante, como por ejemplo el dimetisilaferrocenofano

(Kloninger and Rehahn, 2004) , polímeros de alta masa molecular (40 KDa) (Pasch and Rode, 1995) , polímeros terminados por grupos voluminosos como la terpiridina (Andres and Schubert, 2004; Holder et al., 2004) y polímeros substituidos por dibutil tiofenos (Welsh et al., 2002).

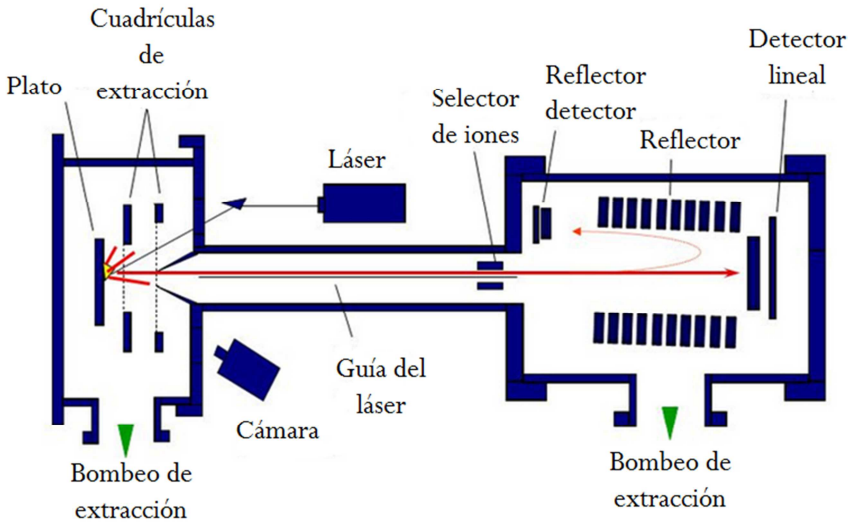

Figura 1.7: Diagrama de un instrumento de MALDI TOF

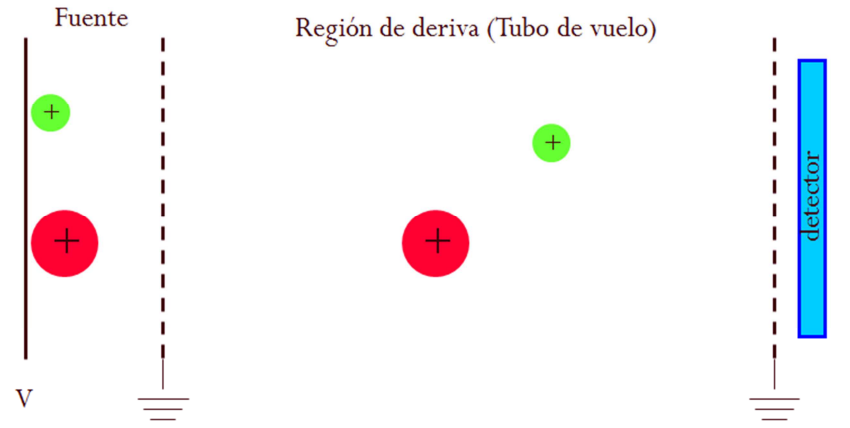

Figura 1.8: Diagrama del analizador de masa de Tiempo de Vuelo

Los instrumentos comerciales MALDI TOF tienen problemas de resolución espectral lo que dificulta las identificaciones estructurales, ya que la resolución

no es la mejor para realizar este tipo de estudios. Sin embargo, los últimos MALDI TOF/MS de diferentes casas comerciales han conseguido solventar este problema y ofrecen a sus clientes una gran resolución (40000 y 1 ppm).

1.3.4 Matrices MALDI

En los análisis de MALDI TOF/MS, una solución diluida del material a analizar se mezcla con una solución de matriz. El número de moléculas formadas en la desorción/ionización cuando el láser irradia la muestra, baja de forma muy significativa a medida que irradiamos en el mismo sitio. La elección de la matriz para una muestra particular es crucial para el éxito en su caracterización. En general la selección preliminar de la matriz a utilizar se realiza a partir de la literatura, procediéndose después a la elección definitiva a partir de pruebas experimentales de tanteo. Lo que se suele hacer para tener una buena caracterización de la estructura de nuestro polímero es ir probando diferentes cantidades y proporciones de analito, solvente y matriz. Una gran ayuda para comenzar es buscar en la literatura existente un polímero parecido al de la muestra objetivo y comenzar utilizando esas "recetas".

En la tabla 1.5 se encuentran las matrices para MALDI TOF/MS según la hidrofobicidad de las muestras poliméricas que se tengan.

Tabla 1.5: Matrices más comunes para MALDI TOF/MS (Rizzarelli and Carroccio, 2014)

Matrices		Polímeros
	Hidrofílico	
2,5 - Ácido Dihidroxibenzoico	↑	Polipropilenglicol
Ácido α-Ciano Hidroxicianamico		Polivinil acetato
Ácido Ferulico		Politetrametilenglicol
Ácido Indoleacrilico		Polimetilmetracrilato
Ditranol		Poliestireno
Ácido trans-Retinoico		Polibutadiano
Difenilbuta ieno	↓	Polidimetilsi oxano
	Hidrofóbico	

En la tabla 1.5 se listan matrices como el Ácido α-Ciano Hidroxicianamico la cual se suele utilizar para experimentos de fragmentación de polímeros (Hoteling et al., 2003; Hoteling and Owens, 2004; Neubert et al., 2003) esto es debido a que contiene iones con una gran energía interna. Otras matrices, como el Ácido trans-Retiónico, son particularmente sensibles a las impurezas mientras que otras matrices como el Ditranol, la pérdida que sufren en su eficiencia es nimia.

Como se ha comentado anteriormente es difícil encontrar la "receta" para que caracterizar una muestra determinada con MALDI.TOF/MS Esta búsqueda se tiene que hacer a base de ensayo y error, ya que el rol que juega la matriz en la muestra no se acaba de comprender totalmente. A pesar de este desconocimiento, se cree que hay tres acciones claves que la matriz hace en el polímero, que consiste en la incorporación del analito dentro de los cristales de la matriz y la acción de ionización/desorción que se produce en los cristales (Bauer et al., 2002; Zhang and Zenobi, 2004). La matriz ideal para analizar la muestra debería tener las siguientes características: una gran capacidad de absorber la longitud de onda del láser, una gran estabilidad en el vacío, baja presión de vapor, una buena solubilidad en el solvente , que pueda disolver al analito y finalmente, una buena miscibilidad con el analito en estado sólido.

1.3.5 Preparación de muestra

En la mayoría de casos se utiliza el sistema denominado *dried droplet* (Bahr et al., 1992; Jagtap and Ambre, 2005; Schriemer and Li, 1996). Las solución de matriz, el analito y los agente cationizantes se mezclan y se depositan en un *spot* del plato de MALDI TOF/MS.

Bajo estas condiciones de *dried droplet*, la cristalización es relativamente lenta, además se incrementa el riesgo del fenómeno de segregación del analito, de la matriz o del agente cationizante. Si la segregación ocurre, produce variaciones de picos y de sus intensidades y además la resolución y la precisión de la masa también se ven afectadas. Los resultados óptimos se obtienen cuando el polímero y la matriz son solubles en el mismo solvente.

El método *dried droplet* no se puede usar para análisis de muestras de polímeros ya que en general son muy poco solubles o insolubles en solventes orgánicos.

1.3.6 Agentes cationizantes

La ionización de polímeros sintéticos suelen producirse por clústeres metálicos. Los polímeros normalmente presentan una alta afinidad por los cationes, además no necesitan que haya una alta concentración de cationes, simplemente necesitan que estén presentes en las impurezas de la matriz, en los reactivos, en los solventes etc. Para mejorar la ionización lo más utilizado es la adición de soluciones de sales alcalinas (LiCl, NaCl, KCl). Para escoger la mejor sal para adicionar a la muestra de polímero se hace de forma experimental, como por ejemplo (Jagtap and Ambre, 2005; Trimpin et al., 2001) que para obtener el mejor espectro de la polivinilpirrolidina utilizó como agentes cationizantes el Na, K , Li y la Ag.

1.3.7 MALDI IMAGING

La caracterización de polímeros así como el cálculo de sus masas moleculares y los índices de valores de la polidispersidad presentan una técnica robusta y rápida para su análisis; la espectrometría de masas de ionización débil. Poder observar la composición de la superficie de una muestra polimérica es muy importante para entender las propiedades que presenta. La técnica de espectrometría de masas MALDI IMAGING (MSI) se presenta como una gran opción (Barner-Kowollik et al., 2012; Crecelius et al., 2009; Rivas et al., 2016)

Sin embargo, la mayoría de las publicaciones que hay se centran en el campo de las plantas y de las aplicaciones biomédicas en tejidos. El campo que más destaca la utilización de la técnica MSI en polímeros es en la investigación de la composición de los copolímeros. El uso combinado de la técnica MSI junto a otras técnicas de alta resolución nos permite obtener información estructural de la muestra y como están distribuidos los diferentes compuestos que la forman superficialmente.

1.3.8 Funcionamiento del MALDI MSI

La técnica MSI (Mass Spectrometry Imaging) funciona básicamente como un MALDI TOF/MS convencional, la fuente luz que emite el láser, incide sobre la superficie de la muestra desorbiendo los diferentes iones.

Las principales diferencias con respecto al MALDI TOF/MS están en que el análisis se realiza directamente sobre la muestra, por lo que no se necesita homogeneizarla con un solvente, bastando simplemente aplicar la matriz y proceder a obtener el análisis.

Los iones generados se separan en el analizador y son detectados. El analizador más común en MSI es el tiempo de vuelo (TOF) en el cual se mide el tiempo que necesitan los diferentes iones para llegar detector. Los iones de masa más grande tardan más en recorrer la distancia que hay entre la muestra y el analizador. Para obtener la imagen del material de la muestra, no solo se analiza una posición como se hace en el MALDI TOF/MS normal, sino que se realiza un escáner de la superficie de la muestra, es decir, el instrumento se desplaza a lo largo de los ejes "X" y "Y" de la muestra, haciendo un barrido de todos los iones y generando la imagen de la muestra en dos dimensiones. El último paso es analizar los datos y crear imágenes de los diferentes iones a través de las masas de interés, utilizando diferentes paquetes de software de tratamiento de imagen, los cuales pueden adquirirse de las diferentes casas comerciales existentes o como opción más barata, obtenerse de internet, de fuentes no comerciales.

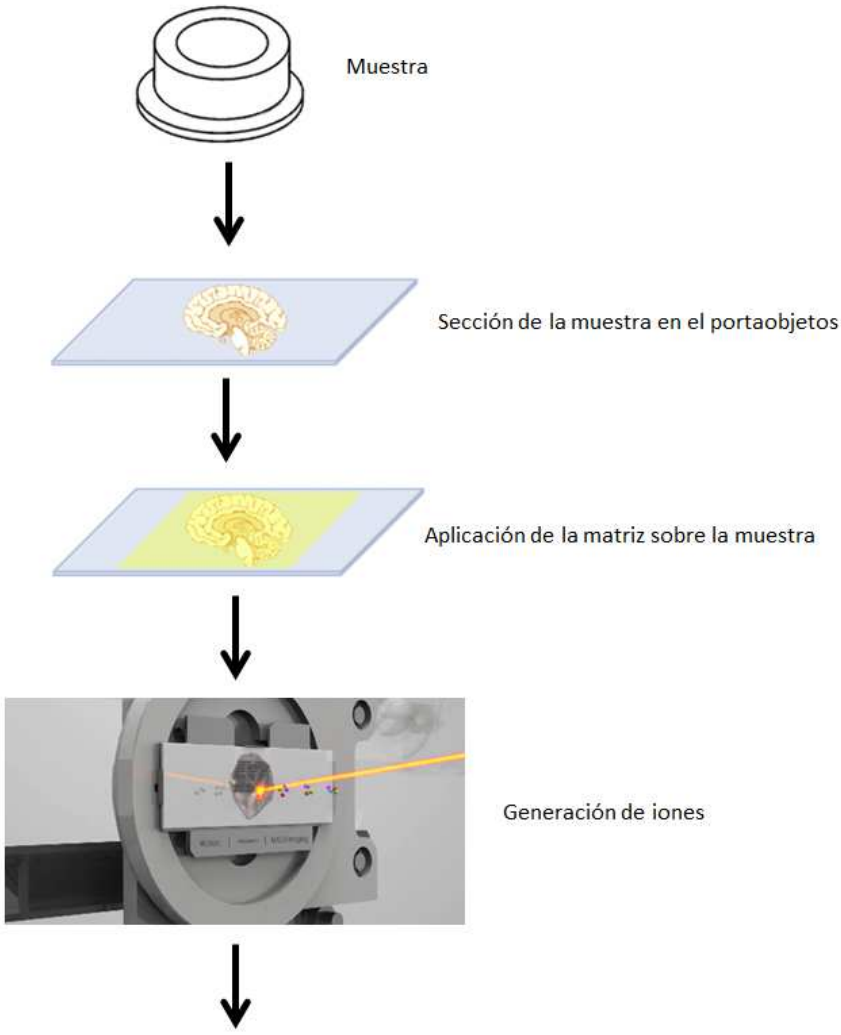
Muestra
Sección de la muestra en el portaobjetos
Aplicación de la matriz sobre la muestra
Generación de iones

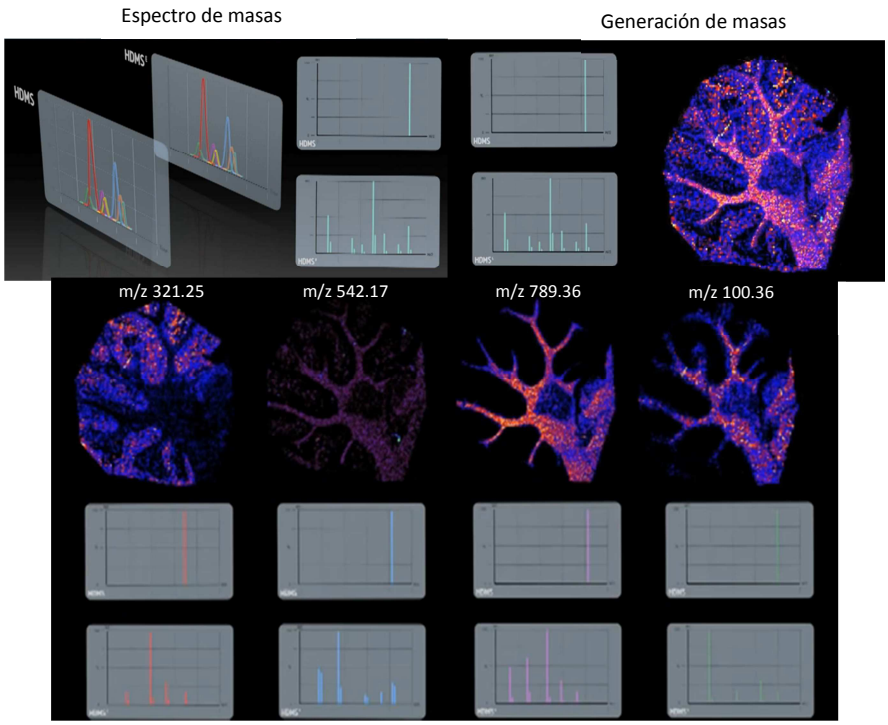

Figura 1.9: Diagrama de trabajo para los experimento en MSI. Pasos del pretratamiento de la muestra que incluye el corte, el montaje de la muestra sobre el portaobjetos y la deposición de la matriz. Los espectros de masa son generados en los ejes de coordenadas "X" y "Y". Se pueden obtener imágenes de iones concretos.

Para el análisis de polímeros se utilizan principalmente dos fuentes de ionización, MALDI y SIMS (secondary ion mass spectrometry).El análisis con TOF-SIMS consiste en bombardear una muestra solida con un haz de iones primarios. Los iones atómicos y moleculares son emitidos desde las capas externas de la superficie y extraídos. Su masa es medida por el detector TOF. Este análisis cíclico se repite a altas frecuencias para generar el espectro de masas completo. Las dos técnicas de ionización son complementarias.

La principal ventaja que presente el MALDI-MSI es el gran rango m/z que presenta debido al analizador TOF y su suave ionización, que apenas daña a la muestra. Sin embargo, MALDI-MSI no puede competir con la resolución espacial que tiene SIMS-MSI, que puede llegar hasta los 100 nm (Hoshi and

Kudo, 2003). La resolución máxima que se llega actualmente en MALDI-MSI es de1-5 μm (Guenther et al., 2011; Zavalin et al., 2012). La contra de la técnica MALDI-MSI radica en que la muestra tiene que estar cubierta por una matriz orgánica. Por esta razón, se encuentran muchas interferencias en los picos por debajo de m/z 300. Los principales inconvenientes de la técnica SIMS-MSI son, por una parte, la gran fragmentación que induce la fuente de ionización y por otra, debido a su alta resolución, solo se pueden analizar zonas muy concretas de las muestras.

Si bien la técnica SIMS ofrece una excelente sensibilidad en la superficie, requiere un paso de *clean-up* para evitar la contaminación en la preparación de la muestra. Para lograr una alta sensibilidad e incrementar el rango de m/z para SIMS-MSI la superficie se puede cubrir con una matriz orgánica común para MALDI como DHB o CHCA (Altelaar et al., 2006). Para incrementar la sensibilidad se puede depositar la matriz usando *electrospray*, de esta forma se logran obtener cristales muy pequeños, aumentando la resolución espacial por debajo de los 3 μm (por ejemplo, usando una matriz del estilo DHB) y logrando un rango de masas de 2500 m/z en experimentos con MSI. Otra posibilidad para mejorar la sensibilidad es evaporar metales, como por ejemplo oro, en la superficie del polímero. Con este pretratamiento de muestra por ejemplo se han obtenido muy buenos resultados en SIMS-MSI sobre muestras de polistereno de masa molecular 1000 (Delcorte et al., 2003). Finalmente la combinación de las dos técnicas (el recubrimiento de la superficie con una matriz orgánica de MALDI y seguida de recubrimiento de metales) mejora el rango de masas sin bajar la resolución espacial como en el caso de (Altelaar et al., 2006) donde recubrieron con oro secciones de tejidos de rata.

La preparación de muestra que se requiere para MALDI-MSI es crucial para obtener una buena imagen sobre la superficie de los polímeros. La homogeneidad de la mezcla matriz-polímero, es esencial para obtener un buen registro de la muestra (Weidner et al., 2011; Weidner and Falkenhagen, 2009). La temperatura tiene un gran efecto sobre la muestra, si se trabaja con el sistema *dried droplet*.

La selección de la matriz óptima para el análisis del polímero deseado es muy importante también. Por ejemplo, si se usa el Ditranol para analizar poliestireno, solo se ven fragmentos sin el grupo final de cadena. Para observarlo todo se

debería usar DHB (Lepoittevin et al., 2000). De todas formas, la División de Polímeros del Instituto Nacional de Estándares y Tecnología (National Institute of Standards and Technology, NIST) ha desarrollado una biblioteca, de acceso público en su página web (https://www.nist.gov/), donde se pueden encontrar recomendaciones sobre el tipo de matriz a utilizar en una base de datos de polímeros. El uso de metales como el polvo de cobalto u oro son algunas de las nuevas ideas que se barajan para mejorar el análisis de polímeros por MSI (Dufresne et al., 2013; NIST; Yalcin et al., 2002).

Hay muchos estudios en los que se ha investigado la mejor forma para depositar la matriz en la muestra, desde el uso de la sublimación, al empleo de dispositivos como el ImagePrep™ (Bruker Daltonics), el cual se basa en la programación de varios parámetros para que un robot deposite la matriz automáticamente, o la utilización de un aerógrafo, en todos ellos no se ha llegado a una conclusión sobre cuál es la mejor opción debido a las múltiples variables que hay en el proceso de preparación de muestra, que van desde el corte de la muestra, la elección de la matriz a la propia naturaleza de la muestra en sí. Por ejemplo en el estudio de Weidner (Weidner et al., 2011) llegaron a la conclusión de que usando la deposición por *electrospray* se obtenían los mejores resultados para su mezcla de polímeros.

1.3.9 Diferentes aplicaciones de la técnica MSI

Los estudios realizados en los campos de la biomedicina y de la biología superan con creces a los realizados sobre polímeros mediante la técnica MSI. A favor, los últimos estudios realizados y publicados en este campo tienen una calidad superior debido al desarrollo continuo de la espectrometría de masas.

Para efectuar un análisis correcto utilizando la técnica MSI de polímeros y biomoleculas hay tener en cuenta la preparación de la muestra, la cual se presenta como uno de los pasos cruciales (Crecelius et al., 2014). La poca resolución que se obtiene al utilizar esta técnica, es uno de los principales problemas que se encuentran. Así por ejemplo, uno de los primeros estudios que se llevaron a cabo (van Hove et al., 2010) fue el análisis simultaneo de polietilenglicol y rodamina, con adición de una matriz orgánica.

La revisión realizada por (Gruendling et al., 2010) para el análisis con la técnica MALDI MSI, aporta una gran ayuda para la preparación de muestras y obtención de imágenes en superficie de polímeros.

Los componentes en la mayoría de mezclas de polímeros binarios son inmiscibles entre ellos (Robeson, 2007). Al no mezclarse los polímeros hacen que las técnicas MALDI-MSI y SIMS-MSI sean muy adecuadas para el estudio de localización espacial de los componentes de la muestra. En la tabla 1.6 se muestra una variedad de sistemas mixtos estudiados mediante la técnica IMAGING.

Tabla 1.6: Lista para sistemas de mezcla de polímeros caracterizados por MALDI-MSI y SIMS-MSI (adapted from (Crecelius et al., 2014))

Sistema de Mezcla	Fuente de ionización	Referencia
Polietilenglicol 5000/Polietilenglicol 1050 PEG /PEG	MALDI	(Kooijman et al., 2017)
Polivinilcloruro/polimetil metacrilato PVC/PMMA	SIMS	(Jackson and Short, 1992; Short et al., 1993)
Polimetil metacrilato- *b* -(2- perfluorohexil etil)acrilato) PMMA-b-PFHEA/PMMA	SIMS	(Marien et al., 1993)
Tetra-etileno fluoretileno/poli(metil metacrilato) ETFE/PMMA	SIMS	(Weng et al., 1998)
Glicoproteinas / Polímero Parafina	MALDI	(Powers et al., 2014)
Poliestireno/poli(metil metacrilato) PS/PMMA	SIMS	(Kailas et al., 2004)
Policaprolactona/polivinilcloruro PCL/PVC	SIMS	(Cheung et al., 2005)
Polimetilmetacrilato 2400/ Polimetilmetacrilato 6950 PMMA/PMMA	MALDI	(Kooijman et al., 2017)
Poli(l-ácido láctico)/proteína PLLA	SIMS	(Mahoney et al., 2006)
Poliestireno/ Polivinilpiridina PS/P2VP	SIMS	
Polietileno/polipropileno PE/PP	SIMS	(Miyasaka et al., 2008)
Poliestireno/polibutadieno PS/PB	SIMS	(Kono et al., 2008)
Poliestireno/poli(2-vinilpiridina) PS/P2VP	SIMS	(Torrisi et al., 2010)

Además, SIMS-MSI permite caracterizar películas generadas mediante un solo polímeros y obtener imágenes de cómo se organiza su estructura (Chan et al., 2014; Yunus et al., 2007), habiéndose utilizado también para el estudio analítico de procesos fotolitográficos (Dubey et al., 2009).

Utilizando la técnica MALDI-MSI se pueden obtener imágenes de los diferentes iones de interés, lo que permite localizarlos sobre la superficie de la muestra. En el estudio de Crecelius et al. (Crecelius et al., 2012) se investiga la localización exacta del PCB sobre un circuito eléctrico. Este material es muy caro e interesa localizarlo en una zona determinada.

Los polímeros no solo juegan un papel importante en los sistemas binarios como los descritos anteriormente, sino que también se pueden encontrar en recubrimientos. Los pigmentos comerciales cobran una especial atención en la industria de las pinturas. En el estudio llevado a cabo por Kawasaki (Kawasaki et al., 2012) se utiliza la técnica IMAGING para la detección directa de pequeños analitos de tinta sobre papel impreso. La técnica LDI-MSI presenta una ventaja sobre la técnica MALDI-MSI y es que no necesita matriz orgánica para la preparación de la muestra y permite una alta resolución. En el estudio de Brentan (Brentan Silva et al., 2017) se analizaron varias plantas de girasol con LDI-MSI llegando a una resolución espacial de 35 μm.

Otros usos frecuentes de la técnica LDI aplicada a polímeros es la determinación de la composición de hidrogeles (Sosnik et al., 2006; Takahashi et al., 2008).

En la actualidad hay diferentes instrumentos comerciales para realizar los análisis de MALDI-MSI que presentan unas mejoras sustanciales respecto a los primeros. A pesar de esto el software para tratar los datos es el principal problema que se encuentran los usuarios, ya que son exclusivos de las diferentes casas comerciales que suministran los equipos. Afortunadamente en internet se encuentran diferentes bases de datos realizadas con los diferentes instrumentos de IMAGING del mercado, y son bases de datos (https://ms-imaging.org/wp/) que se pueden consultar libremente y pueden ser de gran ayuda para los usuarios (Paschke et al., 2013).

Como hemos comentado hay otras grandes áreas donde se utiliza la técnica MALDI MSI, como lo son el campo de la medicina y de la biología.

1.3.10 Aplicación del MALDI MSI al estudio de plantas

Actualmente es posible localizar los complejos procesos bioquímicos que ocurren en las células, órganos y tejidos de las plantas con la técnica MALDI MSI dejando intactas las secciones de tejido que se analizan, lo que permite ver la distribución de las moléculas de posible interés, incluyendo metabolitos y péptidos, además de estimar su abundancia relativa.

La principal ventaja que tiene el MALDI MSI en frente a las otras técnicas que producen imágenes, es el mapeado que se puede hacer de muchos compuestos que se encuentran en la superficie de las diferentes muestras biológicas. Como consecuencia de este hecho, se puede generar una gran cantidad de información sin invertir demasiado en la preparación de muestra (Groseclose et al., 2007). Como ya se ha comentado el principal problema que tiene el MALDI MSI es la baja resolución que presentan las imágenes y la dificultad para tener una alta sensibilidad debido a que cada preparación de muestra se tiene que optimizar. A pesar de todo, las diferentes firmas comerciales actualmente trabajan en mejorar el tamaño del haz del láser para mejorar la resolución espacial y ser cada vez más preciso en la adquisición de datos. Actualmente ya hay estudios en que la resolución espacial es de 2-3 μm como en el estudio (Kompauer et al., 2017).

Para la preparación de muestras de plantas hay que tener en cuenta la contaminación de los materiales ya que pueden causar interferencias en el análisis de masas. El proceso más crítico es el de la preparación de las secciones. Normalmente se usan fijadores y desfijadores en los protocolos para las preparaciones de muestras, donde el principal problema es el desconocimiento del efecto que pueden ejercer sobre la reproducibilidad. En la mayoría de protocolos para la preparación de muestras para la técnica MALDI MSI se recomienda una congelación rápida de la muestra (entre -20ºC y -80ºC) para asegurar que el material químico de la planta quede lo menos alterado posible. Para hacer los crio-cortes se recomienda la adición de resinas o polímeros para fijar la muestra, lo que conlleva el riesgo de posibles interferencias en el análisis de las muestras (Goodwin et al., 2008; Kim et al., 2017). Para evitar la adición de estas sustancias, se puede utilizar agua, ya que a las temperaturas de crio-corte (-15ºC a -25ºC) se transforma en hielo, y sirve como fijador. No obstante hay muestras como por ejemplo las hojas, los granos de maíz, o el polen que son difíciles de fijar, y se han tenido que utilizar otros fijadores como una cinta

adhesiva especial (Kawamoto, 2003). Este material da mejores resultados para la mayoría de muestras, y genera menos distorsión y dislocación de las secciones que si no se usa ningún tipo de fijador. Este método ha sido utilizado con éxito, por ejemplo, para el análisis de granos de arroz (Zaima et al., 2010).

Además del uso o no de fijador, las secciones tienen que tener una anchura determinada para que el análisis tenga algún valor. Normalmente en los estudios publicados las medidas varían entre 50-100 mm aunque gracias a los avances tecnológicos en la instrumentación hay estudios en que se puede reducir a los 10-20mm (Crecelius et al., 2017b).

Por lo que a la introducción de muestra en el analizador se refiere, se suele llevar a cabo mediante porta-objetos recubiertos con óxidos metálicos, especialmente óxido de indio y estaño (Indium-Tin oxide, ITO).

La técnica MALDI TOF/MS es ideal para analizar sustancias polares como por ejemplo fosfolípidos y colina, y sustancias no polares como son los triglicéridos y el colesterol, en los espectros de masas del MALDI TOF/MS suelen salir los aductos de sodio y potasio protonados (Sugiura and Setou, 2010). Los aminoácidos, azucares y los compuestos fosforilados también se pueden identificar en los espectros (Francese et al., 2009). Al analizar metabolitos por MALDI MSI se requieren los mismos cuidados que para analizar proteínas con tal de mantener su localización espacial y evitar la degradación de los compuestos de interés (Aziz et al., 2017). Para evitar el riesgo de supresión iónica, al analizar proteínas y péptidos se recomienda hacer un pretratamiento de lavado (Francese et al., 2009; Goodwin et al., 2008). El problema de este pre tratamiento es que puede deslocalizar las moléculas de metabolitos (Sugiura and Setou, 2010). En la mayoría de protocolos, las muestras se deshidratan antes de aplicar la matriz. Para analizar este tipo de metabolitos se suelen usar matrices comunes como CHCA o DHB (dos Santos et al., 2017; Fowble et al., 2017; Kompauer et al., 2017).

Para una buena detección de péptidos normalmente se hace un pretratamiento de lavado a la muestra para eliminar la contaminación de sales y azúcares. Etanol al 70% en frío es la solución más utilizada para lavar la muestra, seguida normalmente de un segundo lavado de etanol al 90-100% para asegurar la deshidratación y prevenir la proteólisis (Chaurand et al., 2004; Schwartz et al., 2003). Hay variaciones en los protocolos en los que se utilizan otras

proporciones de disolventes y se juega con la temperatura y el número de lavados. En general, la prioridad es mejorar la relación de señal/ruido y minimizar la pérdida de los analitos que interesan. Las proteínas de masa molecular alta se analizan previo fraccionamiento de la misma efectuado mediante la acción de encimas proteolíticas. Ello da lugar a una serie de péptidos característicos de masa menor, que constituyen una "huella dactilar" de la proteína original

Tabla 1.7: Diferentes ejemplos representativos de aplicaciones de la técnica MALDI MSI al análisis de plantas y frutas.

Organismo / Tejido	**Compuesto**	**Referencia**
Soja / hoja, Tallo	Metabolito	(Mullen et al., 2005)
Fresa	Metabolito	(Crecelius et al., 2017a)
Trigo / Tallo	Metabolito	(Robinson et al., 2007)
A. Thaliana / Piel	Péptido	(Kondo et al., 2006)
Fresa / Fruta	Metabolito	(Li et al., 2007)
Lino / Semilla	Metabolito	(Dalisay et al., 2015)
Limón / Piel	Metabolito	
Trigo/ Grano	Metabolito	(Burrell et al., 2006)
A. Thaliana / Hoja	Metabolito	(Shroff et al., 2008)
Girasol / Tallo	Metabolito	(Anderson et al., 2009)
Banana / Tallo	Metabolito	(Hölscher et al., 2015)
Berenjena	Metabolito	(Goto-Inoue et al., 2010)
N.Tabacum /Hoja	Metabolito	(Ibáñez et al., 2010)
Tomate / Semilla	Metabolito	(Debois et al., 2014)
A. Thaliana / Flor, Tallo, Raíz	Metabolito	(Jun et al., 2010)
A. Thaliana / Flor, Pétalo	Metabolito	(Sinha et al., 2008)
A. Thaliana / Hoja	Metabolito	(Vrkoslav et al., 2010)
Tomate , Manzana , Neftarina	Polímero (Cutícula)	(Veličković et al., 2014)
Arroz / Grano	Metabolito	(Zaima et al., 2010)

1.3.11 Aplicación del MALDI MSI al estudio de fármacos

Los estudios de drogas y fármacos intentan detallar la actividad farmacológica, los efectos toxicológicos y su distribución a lo largo de los tejidos de los individuos tratados. La localización de estos compuestos o de los metabolitos es de suma importancia en los seres vivos, ya que es imprescindible saber si llegan a sus receptores y son eliminados adecuadamente o si, por el contrario, se bioacomulan provocando efectos no deseados en los organismos (Lanao and Fraile, 2005; Langer and Muller, 2004; Mouton et al., 2007). La técnica MSI es una herramienta que se utiliza tanto a nivel industrial como académico y proporciona información complementaria a los métodos tradicionales que se usan para los estudios de distribución de estos compuestos.

La técnica MALDI MSI se ha revelado como una tecnología pionera para la localización de drogas y metabolitos en tejidos biológicos. A pesar que al principio solo se utilizaba para la localización de péptidos y proteínas, actualmente se ha extendido su aplicación a analitos de bajo peso molecular como son los fármacos. El principal problema que presenta la metodología para analizar drogas y metabolitos en tejidos biológicos es la baja concentración en que se encuentran y las muchas interferencias que se producen debido a las sustancias endógenas y a efectos de matriz.

El conocimiento sobre la localización y distribución de los compuestos y sus metabolitos en el organismo es necesario para los estudios de absorción, distribución, metabolismo y excreción. Hay varios estudios en los que se ha analizado como se distribuye y localiza un fármaco marcado radiactivamente a lo largo del cuerpo de un animal. Este método, denominado auto radiografía, presenta una resolución espacial de 100 μm.. El principal problema que presenta esta técnica es su poca especificidad, ya que solo se puede medir el compuesto marcado radioactivamente. Además la síntesis de dichos compuestos suele ser costosa y los tiempos de experimento requeridos largos (típicamente desde días a varias semanas) si se quieren tener imágenes suficientemente buenas para los estudios de distribución. Sin embargo, esta técnica permite obtener imágenes múltiples de diferentes secciones de tejidos y combinándola con otras técnicas como LC-MS/MS se pueden llegar a cuantificar los compuestos y los metabolitos que están en los tejidos, teniendo en cuenta que la información espacial que se obtiene está limitada al tamaño de tejido previo a su

homogenización. Existen otras tecnologías alternativas para obtener imágenes en vivo, como es la Tomografía por Emisión de positrones (Positron EmissionTomogrphy, PET). Con esta técnica el fármaco está marcado radioactivamente antes de la administración al ser vivo. Las ventajas del PET es que las imágenes que se obtienen son en tiempo real, pudiendo seguir la sustancia marcada a través del organismo. Sin embargo, la especificidad sigue siendo baja y los metabolitos no se pueden distinguir del compuesto padre. Además, si bien el PET presenta una baja resolución espacial (aproximadamente 1mm) su principal ventaja respecto a MSI está en que siempre se puede cuantificar (Riemann et al., 2008). Como se ha dicho anteriormente, la técnica MSI permite el barrido de los compuestos y metabolitos interesantes de la muestra, así como la obtención de las imágenes sobre los ejes "X" y "Y", donde cada pixel es un espectro de masas.

No hace falta decir que la fuente de ionización más utilizada para analizar tejidos es el MALDI. La preparación de muestra se realiza como en los otros casos con una matriz que extrae los compuestos de la muestra y son desorbidos hacia el analizador. Las resoluciones que se alcanzan en este tipo de muestras varían de los 50-200 μm. Normalmente estas medidas se llevan a cabo en condiciones de vacío aunque hay varios experimentos descritos realizados en condiciones intermedias y a presión atmosférica (Garrett et al., 2007; Guenther et al., 2011). La técnica MALDI MSI tiene la ventaja de ser muy sensible pero puede sufrir muchas interferencias debido a la matriz, además de especies endógenas como lípidos y péptidos, lo cual dificulta mucho el análisis del rango de masa deseado. Para intentar disminuir estos problemas se suele aplicar MS/MS a los experimentos de fármacos para asegurar que el compuesto observado coincide efectivamente con el que se desea analizar. Sin embargo, siempre se aprecian efectos de supresión iónica debido a las matrices, que hacen que la cuantificación sea más difícil.

Tabla 1.8: Lista de estudios con la técnica MSI de drogas y metabolitos.

Analito	Metabolito	Tejido / Organismo	Método de Ionización	Método de detección	Analizador de Masas	Reference
Heroina	Si	Cerebro (Rata)	MALDI	MS/MS	TOF/TOF	(Teklezgi et al., 2017)
Lípidos	Si	Cerebro (Ratón)	MALDI	MS/MS	TOF/TOF	
Ácido Artesunato	No	Pastillas	DESI	MS	LCQ	(Nyadong et al., 2009)
ATP (metabolitos primarios)	Si	Cerebro (Rata)	MALDI	MS MS/MS	TOF/TOF	(Atkinson et al., 2007; Benabdellah et al., 2009)
β-péptido	Si No	Tejido Tumoral (Humano) Cuerpo entero (Ratón)	MALDI MALDI	MS MS	QqTOF TOF/TOF	(Stoeckli et al., 2007)
Biflavonoides	Si	Planta *A. thaliana* y *Hypericum*	LDI	MS MS/MS	TOF/TOF	(Hölscher et al., 2009)
BMS-X-P	Si	Hígado, corazón, Pulmón (Rata)	MALDI	MS/MS	LTQ	(Drexler et al., 2007)
Metal anticáncer	No	Cultivos celulares	MALDI/ SIMS	MS/MS	TOF/TOF	(Lee et al., 2017)
Cloroquina	No	Ojo (Rata)	MALDI	MS/MS	QqTOF	(Yamada et al., 2011)
Cimetidina	No	Pulmón (Rata)	MALDI	MS	TOF/TOF	(Shariatgorji et al., 2012)
Glicoesfingolípido	Si	Cerebro (Ratón)	MALDI	MS/MS	FTCIR	(Jones et al, 2017)
	Si	Pelo (Humano)	MALDI	SRM	QqQ	
Clozapina	Si	Cerebro (Rata)	NIMS	MS	TOF/TOF	(Northen et al., 2007; Porta et al., 2011) (Hsieh et al., 2010) (Goodwin et al., 2010; Goodwin et al., 2008; Wiseman et al., 2008)
	Si	Cerebro (Rata)	MALDI	SRM	QqTOF	
	Si	Cerebro, pulmón, hígado (Rata)	DESI	MS/MS	LTQ	

Analito	Metabolito	Tejido / Organismo	Método de Ionización	Método de detección	Analizador de Masas	Reference
Dexamethasona	No	Riñón (Rata)	MALDI	MS	TOF/TOF	(Mains et al., 2011)
				MS/MS		
	No	Ojo (Ovino)	SIMS	MS	TOF	
Metabolitos de la cera Epiticular	Si	Planta (*Arabidopsis*)	LDI	MS	LTQ	(Cha et al., 2009)
	No	Túmor de pulmón (humano)	MALDI	MS	LTQ Orbitrap	(Marko-Varga et al., 2011)
				MS/MS		
Flavonoides	Si	Planta (*A. thaliana* and *Hypericum*)	LDI	MS	TOF/TOF	(Hölscher et al., 2009)
				MS/MS		
Gerfitinib	No	Túmor de pulmón (Humano)	MALDI	MS	LTQ Orbitrap	(Marko-Varga et al., 2011)
				MS/MS		
Receptor agonista Glucocorticoide	No	Piel (Porcina)	MALDI	MS/MS	TOF/TOF	(Marshall et al., 2010)
Ifosfamida y imatinib	No	Riñón (Ratón)	MALDI	MS	LTQ Orbitrap	(Römpp and Spengler, 2013)
Proteina	Si	Ratón	MALDI	MS/MS	FTCIR	(Dilillo et al., 2017)
Imipramina	No	Pulmón (Rata)	MALDI	MS	TOF/TOF	(Shariatgorji et al., 2012)i
Ipratropium	No	Pulmón(Humano)	MALDI	MS	LTQ Orbitrap	(Fehniger et al., 2011)
				MS/MS		
Isoniazida	No	Pulmón (Conejo)	MALDI	MS/MS	LTQ	(Manier et al., 2011)
Rifampicina	Si	Hígado (Conejo)	MALDI	MS/MS	TOF	(Prentice et al., 2017)
Dinorfina	Si	Cerebro (Rata)	MALDI	MS/MS	TOF	(Bivehed et al., 2017)
Lapatinib	Si	Riñón (Perro)	MALDI	MS	FTICR	(Castellino et al., 2011)
Loperamida	No	Cerebro (Ratón)	MALDI	MS/MS	QqTOF	(Shin et al., 2011)
3-Metoxisalicilamina	No	Riñón, Hígado (Ratón)	MALDI	MS/MS	LTQ	(Chacon et al., 2011)
Moxifloxacin	No	Pulmón (Conejo)	MALDI	SRM	QqQ	(Prideaux et al., 2010)
Brimonidina		Ojo (Conejo)	MALDI	MS/MS	TOF	(Grove et al.)
Varios components farmacéuticos	No	Formulación de Comprimidos	MALDI	MS	QqTOF	(Earnshaw et al., 2010)

Analito	Metabolito	Tejido / Organismo	Método de Ionización	Método de detección	Analizador de Masas	Reference
Naftodiantronas	Si	Planta (*A. thaliana* and *Hypericum*)	LDI	MS MS/MS	TOF/TOF	(Hölscher et al., 2009)
Nelfinavir	No	Células (Mono Mac 6)	MALDI	MS	TOF/TOF	(Dekker et al., 2009)
Olanzapina	Si No	Cuerpo entero (Rata) Hígado (Rata)	MALDI MALDI	MRM MS/MS	QqTOF QqTOF	(Khatib-Shahidi et al., 2006) (Koeniger et al., 2011)
Oxaliplatino	Si	Riñón (Rat)	MALDI	MS	TOF/TOF	(Bouslimani et al., 2010)
Doxorubicin	Si	Cultivos celulares	MALDI	MS	TOF	(Lukowski et al., 2017)
Metabolitos Primarios	Si	Plantas	LAESI	MS MS/MS	QqTOF	(Nemes et al., 2009)
Propranolol	No	Cuerpo entero (Ratón)	DESI	SRM	QqQ	(Kertesz et al., 2008)
Componente en desarrollo	Si	Cuerpo Entero (Rata)	MALDI	MS MS/MS	TOF/TOF	(Stoeckli et al., 2007)
Racloprida	No No	Cuerpo Entero (Ratón) Cerebro, Riñón (Rata)	MALDI MALDI	MS/MS MS/MS	LTQ TOF/TOF	(Takai et al., 2012) (Goodwin et al., 2011)
Rapamicina	No	Ácido Poli(lactic-co-glicolico)	SIMS	MS	TOF	(Belu et al., 2008)
Saquinavir	No	Celúlas (Mono Mac 6)	MALDI	MS	TOF FTICR	(Dekker et al., 2009)
SCH 23390	No	Cerebro (Rata)	MALDI	MS MS/MS	TOF/TOF QqTOF FTICR	(Goodwin et al., 2011)
Sirolimus	No	Ácido Poli (lactico-glicolico)	SIMS	MS	ToF	(Fisher et al., 2009)
Enalapril / Verapamil	Si	Revestimiento de control de fármacos	MALDI	MS/MS	TOF/TOF	(Prentice et al., 2017)
Antibióticos Streptomicetas	Si	Capullo *Beewolf larvae*	LDI	MS	QqTOF	(Kroiss et al., 2010)
Terfenadina	Si	Cuerpo entero (Rata, Ratón)	MALDI	MS MS/MS	QqTOF	(Hsieh et al., 2008)
Cocaina	Si	Pelo	MALDI	MS/MS	TOF/TOF	(Flinders et al., 2017)

Analito	Metabolito	Tejido / Organismo	Método de Ionización	Método de detección	Analizador de Masas	Reference
Tetraciclina	No	Revestimiento de control de fármacos	SIMS	MS	TOF	(McDermott et al., 2010)
Teofilina	No	Fármacos	SIMS	MS	TOF	(Belu et al., 2008)
Tiotropium	No	Pulmón (Rata)	MALDI	MS/MS	TOF/TOF	(Nilsson et al., 2010; Végvári et al., 2010)
	No	Pulmón (Rata)	MALDI	MS	LTQ Orbitrap	
				MS/MS		
Vinblastina	No	Cuerpo entero (Rata)	MALDI	IM-MS/MS	QqTOF	(Trim et al., 2010)

La preparación de muestra se realiza de forma similar a las anteriores comentadas. Las secciones interesantes a analizar del tejido u órgano del animal se cortan usando un criotomo utilizando o no un fijador para que el corte sea lo más preciso posible. En algunos estudios se utiliza una cinta adhesiva de fijación (Prideaux et al., 2010). Esta cinta adhesiva presenta el inconveniente de que no es compatible con los analizadores TOF, ya que no posee una superficie conductora imposibilitando por consiguiente el análisis. Para soslayar este inconveniente se puede rociar oro después de la deposición de la matriz sobre la muestra. Sin embargo lo más corriente es utilizar los portaobjetos de ITO. El único problema a tener en cuenta, es la posible pérdida de muestra al pasar el tejido al portaobjetos o que la deposición sobre el portaobjetos no sea precisa, dando lugar a interferencias en el análisis. Se han probado varios materiales para fijar las muestras siendo el más utilizado la carboximetilcelulosa (Solon et al., 2010). Hay otras alternativas como usar agua (Khatib-Shahidi et al., 2006), gelatina (Chen et al., 2009) y poli [N-(2-hidroxipropilo) metacrilamida] (Strohalm et al., 2011). En cuanto a los cortes, deben presentar un grosor en el rango de 10-15 μm.

Los solventes que se utilizan en los pasos de preparación de muestra para péptidos y proteínas no son adecuados cuando se pretende analizar fármacos, ya que les puede afectar y como resultado perder gran parte de la información espacial. Sin embargo, si se ajusta el pH usando una solución tampón, se puede ampliar la señal en el tejido eliminando interferencias como las que producen las sales endógenas (Shariatgorji et al., 2012). En definitiva, si se ajusta el pH a

niveles que los compuestos de los fármacos son insolubles, la descolocación que pueda sufrir el analito se minimiza.

Como en toda preparación de muestra la matriz es un elemento crucial para obtener un buen análisis en MALDI MSI. Las matrices más utilizadas para este tipo de muestras son el ácido α-Ciano-4-hidroxicinamico y el ácido 2,5-dihidroxibenzoico. Además el método de deposición de la matriz es muy importante en este tipo de muestras. Cuando se aplica la matriz disuelta en un solvente en forma de spray es muy importante que esté lo suficientemente húmeda para que los analitos puedan salir de la superficie de la muestra hacia los cristales de la matriz, pero no excesivamente para impedir que estos analitos se deslocalicen de sus posiciones iniciales, y evitar así la pérdida de información espacial. Los métodos de aplicación de matriz seca disminuyen este problema y se han utilizado para el estudio de lípidos en tejidos. El uso de este método no sirve para cualquier compuesto, y los protocolos existentes son muy concretos con los compuestos que se pueden utilizar. Además hace falta optimizar la matriz para el compuesto que se quiere analizar.

Para la deposición de la matriz se utilizan varios métodos con diferentes características de reproducibilidad y de grados de cristalización de matriz. Si la matriz presenta una alta concentración de material orgánico, el uso de nebulizadores funciona muy bien, aunque se corre el riesgo de su obturación (Trim et al., 2010). La deposición por spray se ha utilizado en muchos estudios y es muy rápida y barata. Por el contrario presenta una muy baja reproducibilidad a la hora de repetir los experimentos, ya que se considera un método semi-manual. El sistema de *dried droplet*, es un método que ofrece una baja resolución debido al tamaño de las propias gotas. Por otro lado, aporta una gran sensibilidad ya que la extracción del analito es muy buena. La capacidad que presenta un compuesto para ionizarse es un requisito muy importante a la hora de tener un IMAGING de gran calidad. En general, si el compuesto tiene una baja afinidad para protonarse se recomienda una derivatización química en tejido (Chacon et al., 2011; Manier et al., 2011). En este tipo de método, el derivatizante es añadido al tejido mezclado con el solvente.

Para optimizar la deposición de matriz se ejecutaron varios experimentos durante mi estancia científica en la universidad de Lund (Suecia). El

experimento se llevó a cabo utilizando un nebulizador y modificando una serie de parámetros.

Figura 1.10: Nebulizador TM-Sprayer de la marca HTX- Imaging, utilizado en los experimentos de optimización de la deposición de matriz.

Los parámetros a modificar fueron los siguientes: matriz, concentración de matriz, temperatura de deposición de la matriz, número de veces que el nebulizador deposita la matriz por encima de la muestra, el solvente utilizado en nuestra matriz, el flujo a la que el nebulizador deposita la matriz encima de la muestra, la velocidad del nebulizador que pasa por encima de la muestra, el recorrido que sigue nuestro nebulizador por encima de la muestra, y el tiempo de secado entre deposición de matriz del nebulizador.

Una vez optimizados estos parámetros, se utilizó el nebulizador para depositar la matriz sobre una muestra biólogica.

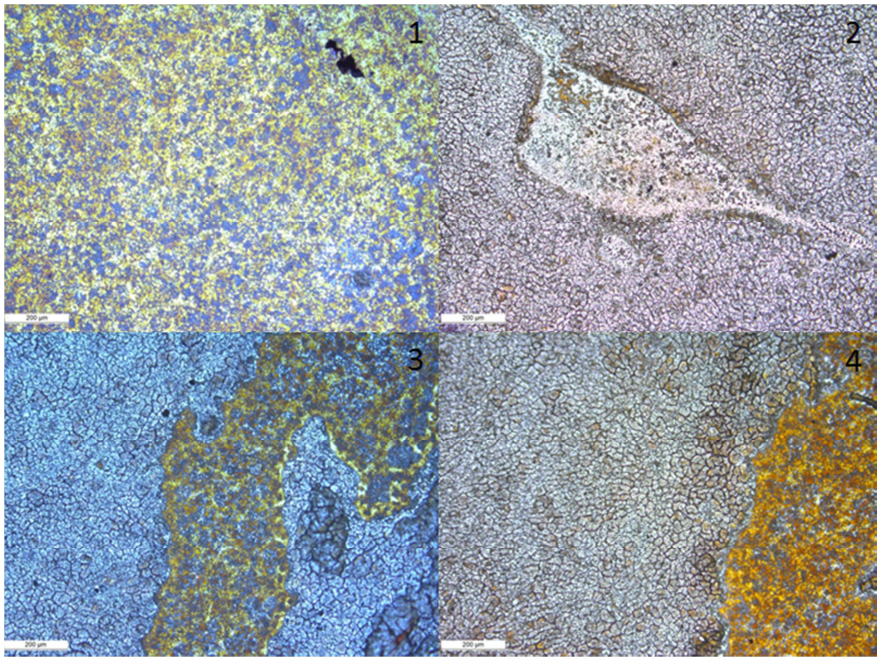

Figura 1.11: Matriz CHCA depositada utilizando un nebulizador sobre una muestra biológica. (1) Matriz depositada sobre el cristal del portaobjetos, (2) Matriz depositada sobre una vesícula del tejido, (3) Matriz depositada sobre células tumorales, (4) Matriz depositada en el límite del cristal del portaobjetos y de las células del tejido.

En la figura 1.11 se puede apreciar la diferente cristalización de la matriz según se deposite en los tejidos de la muestra biológica, esta cristalización de la matriz es diferente debido a las sustancias endógenas.

Para realizar una buena identificación en tejido de fármacos y metabolitos y evitar las interferencias debidas a las sustancias endógenas y a los tejidos se recomienda utilizar compuestos estándares.

Hay que tener en consideración para cualquier experimento en Imaging la concentración depositada del metabolito o fármaco estudiado debido a la posibilidad de que se produzcan las interferencias mencionadas anteriormente. Los efectos de supresión iónica son la razón principal de la pérdida de intensidades en la señal, y ocurre en muchos tipos de tejidos. Los efectos de supresión iónica se dan también a causa de las sustancias endógenas como los

lípidos, o por la presencia de las sales de los tejidos biológicos (Deininger et al., 2011). Los efectos de la supresión iónica son realmente problemáticos cuando se quieren obtener diferentes imágenes de la localización de los analitos, por ejemplo cuando se quiere comparar la distribución de un analito en un tejido con un tumor *versus* un tejido sano. Estos efectos se aprecian claramente cuando en una superficie homogénea se observan intensidades diferentes de un mismo analito (Stoeckli et al., 2007). Hay muchos factores que afectan a la supresión iónica, como es el caso de la matriz aplicada sobre la muestra, ya que la extracción de los analitos puede ser diferente debido a que un tejido contiene diferentes estructuras biológicas. Además hay que añadir los parámetros experimentales, el solvente aplicado y el método de aplicación. El tipo de cristalización de la matriz también afecta a la composición y estructura del tejido, como se puede apreciar en la figura 1.11. Por todos estos factores se dice que la técnica MSI da una información muy útil sobre la localización de los compuestos analizados y sus metabolitos, pero que no es cuantitativa sino semi-cuantitativa. No obstante se han propuesto varias aproximaciones para hacer cuantificaciones de compuestos que consisten esencialmente en el cálculo de los efectos de supresión iónica y la normalización de las señales. En la cuantificación por supresión iónica, la imagen obtenida corresponde a los compuestos estándar que se encuentran depositados sobre la superficie de la muestra de una forma homogénea. Para cada área del tejido de interés, se mide la intensidad de la señal. Las intensidades medidas de la muestra biológica dopada se escalan con el factor de supresión para compensar la supresión del tejido (Stoeckli et al., 2007).

Si se realiza una normalización para cuantificar, la señal de los iones en cada espectro del fármaco o el metabolito, se normalizan a un pico de referencia, o sino al *total ion current* (TIC) (Deininger et al., 2011). Sin embargo existe el problema de la abundancia de especies endógenas como las fosfatidilcolinas que no suelen estar distribuidas sobre la muestra de forma homogénea, produciendo errores si las señales del fármaco están normalizadas respecto a ellas. Para evitar este efecto se suele aplicar un estándar con una eficacia de ionización similar para compensar y corregir los efectos de supresión en la ionización en tejidos (Prideaux et al., 2010). Debido a todos los problemas que afectan a la cuantificación en MSI, casi todos los estudios se respaldan en otras técnicas como LC-MS/MS para mejorarla. Por otro lado se pueden encontrar muchos

estudios donde la correlación de las concentraciones encontradas con MSI son parecidas a las determinadas con LC-MS/MS.

Para cuantificar pitavastatin en hígado de ratón se realizó un experimento en el centro de investigación de biomedicina en Lund. Se llevó a cabo una cuantificación por normalización a TIC, donde primero se observó el límite de detección del analito sobre la muestra. Dos replicados presentaron un límite de detección de 10 µM de pitavastatin, véase figura 1.12, en cambio la tercera réplica presentó un límite de detección de 20 µM. Este resultado se debe a la supresión iónica que presenta la muestra, como se ha comentado anteriormente.

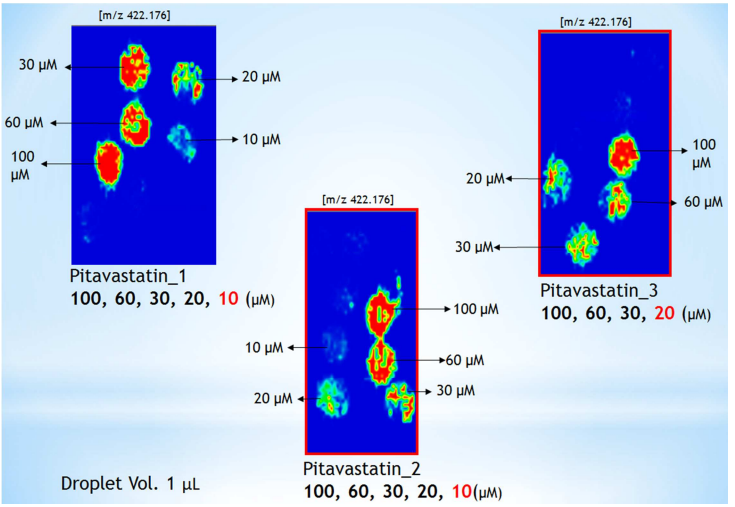

Figura 1.12: Imágenes de Pitavastatin (m/z 422.176) sobre hígado de ratón a diferentes concentraciones.

Finalmente, se adicionó un estándar (Pitavastatin d5) obteniendo una buena recta de calibrado como se aprecia en la figura 1.13.

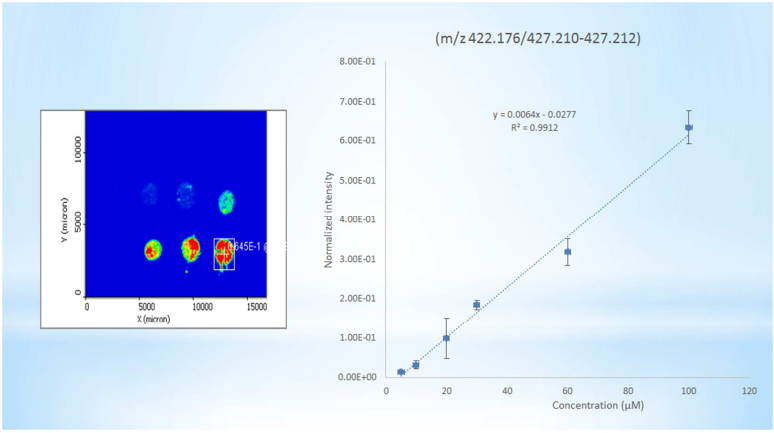

Figura 1.13: Calibración en hígado de ratón con el estándar Pitavastatin d5.

Por último en el centro de investigación biomédica de Lund se desarrolló un experimento para localizar e identificar metabolitos *non target* cancerosos. Se realizó el análisis de una muestra histológica de melanoma y se identificó las posibles regiones de interés como se puede apreciar en la figura 1.14.

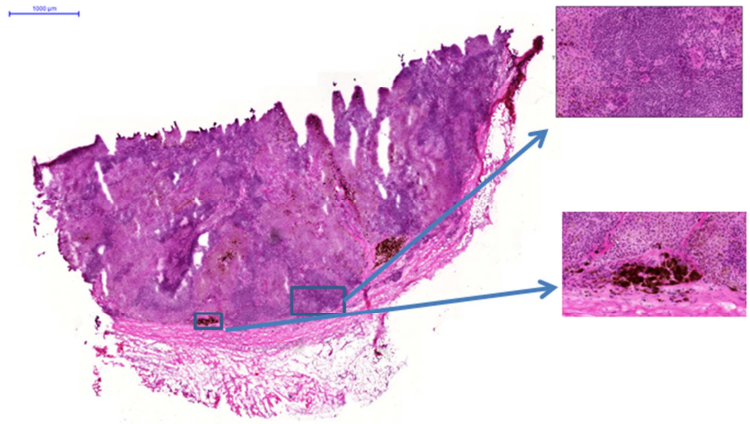

Figura 1.14: Muestra histológica de melanoma y sus dos regiones de interés.

Un análisis con la técnica MSI localizando varios metabolitos sospechosos procedió a la búsqueda de sus masas en librerías y bibliografía para una posible identificación de los compuestos. Finalmente una superposición de imágenes (histológica e imagen del ión interesante obtenida por MALDI IMAGING)se

realiza para observar su posición encima de la muestra, y observar si se situa en algún compartimento clave biológico de la muestra.

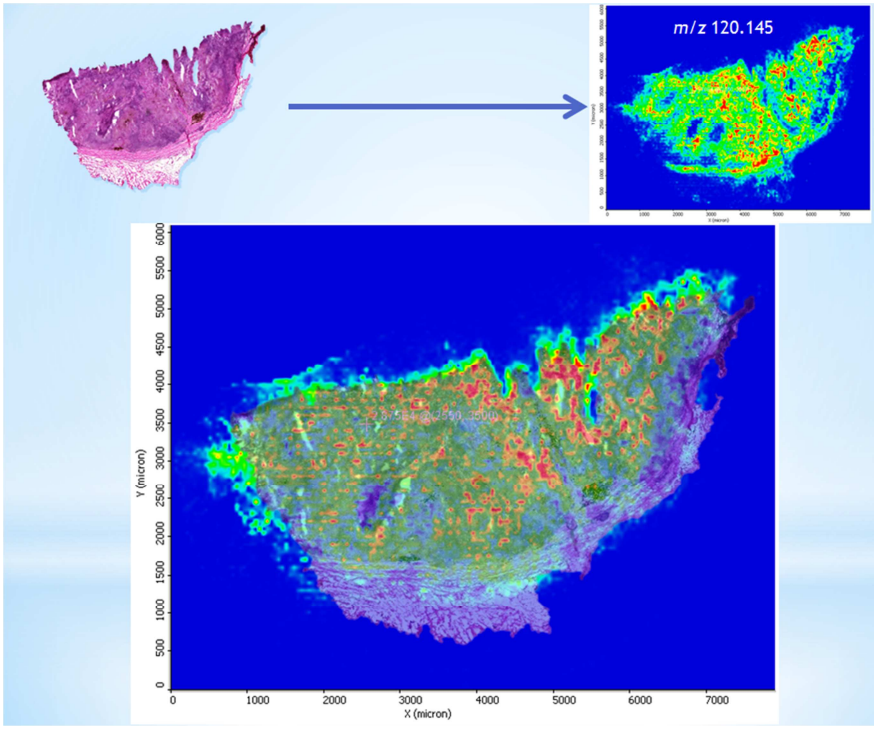

Figura 1.15: Superposición de imágenes de la histológica contra la del ión m/z 120.145.

Chapter 2

Capítulo 2. Objetivos

The overall aim of this Thesis is the application of MALDI-TOF Imaging and HPLC-MS to the study of the degradation of polycaprolactone diol polymer in different aquatic environments. Therefore, this general aim will be met by achieving the following specific objectives:

- To select different commercially available homopolymers to be used as possible candidates in the development of the probe.

- For the finally selected homopolymer to develop analytical methods based on advanced mass spectrometry techniques, such as MALDI-TOF, MALDI IMAGING and HPLC-MS.

- To study the behavior of the selected homopolymer in exposure experiments, first at laboratory and mesocosms scale and subsequently in field experiments in natural (river) and engineered (wastewater treatment plants) systems, so that different aquatic environments are covered.

- To study the 2D spatial degradation patterns of the polymer and its transformation products by MALDI-TOF MS IMAGING.

- To provide complementary information to MALDI-TOF MS Imaging results regarding the identification of transformation products and their quantification by HPLC-MS. To assess the application of different analytical software to process the raw imaging data obtained in MALDI-TOF MS IMAGING analytical determinations.

Chapter 3

Capítulo 3. Using a polymer probe characterized by MALDI-TOF/MS to assess river ecosystem functioning: From polymer selection to field tests

This chapter is based on the article:

Rivas D, Ginebreda A, Elosegi A, Pozo J, Pérez S, Quero C, et al. Using a polymer probe characterized by MALDI-TOF/MS to assess river ecosystem functioning: From polymer selection to field tests. Science of The Total Environment 2016; 573: 532-540.

3.1 Highlights

• Four polymers were characterized by MALDI-TOF/MS.

• Polycaprolactonediol 1250 polymer was used as probe to assess ecosystem functioning.

• Polycaprolactone diol 1250 probes were tested in mesocosoms and in river.

• MALDI-TOF/MS spectra reflect changes undergone by probes after exposure.

3.2 Abstract

Characterization of river ecosystems must take into consideration both structural and functional aspects. For the latter, a convenient and simple approach for routine monitoring is based on the decomposition of organic matter measured in terms of breakdown of natural organic substrates like leaf litter, wood sticks. Here we extended the method to a synthetic organic material using polymer probes characterized by MALDI-TOF/MS. We first characterized several commercial available polymers, and finally selected polycaprolactonediol 1250 (PCP 1250), a polyester oligomer, as the most convenient for further studies. PCP 1250 was first tested at mesocosms scale under conditions simulating those of the river, with and without nutrient addition for up to 4 weeks. Differences to the starting material measured in terms of changes in the relative ion peak intensities were clearly observed. Ions exhibited a different pattern evolution along time depending on their mass. Greatest changes were observed at longest exposure time and in the nutrient addition treatment. At shorter times, the effect of nutrients (addition or not) was indistinguishable. Finally, we performed an experiment in 11 tributaries of the Ebro River during 97 days of exposure. Principal Component Analysis confirmed the different behavior of ions, which were clustered according to their mass. Exposed samples were clearly different to the standard starting material, but could not be well distinguished among each other. Polymer mass loss rates, as well as some environmental variables such as conductivity, temperature and flow were correlated with some peak intensities. Overall, the interpretation of field results in terms of environmental conditions remains elusive, due to the influence of multiple concurrent factors. Nevertheless, breakdown of synthetic polymers opens an interesting field of research, which can complement more traditional breakdown studies to assess river ecosystem functioning.

3.3 Graphical abstract

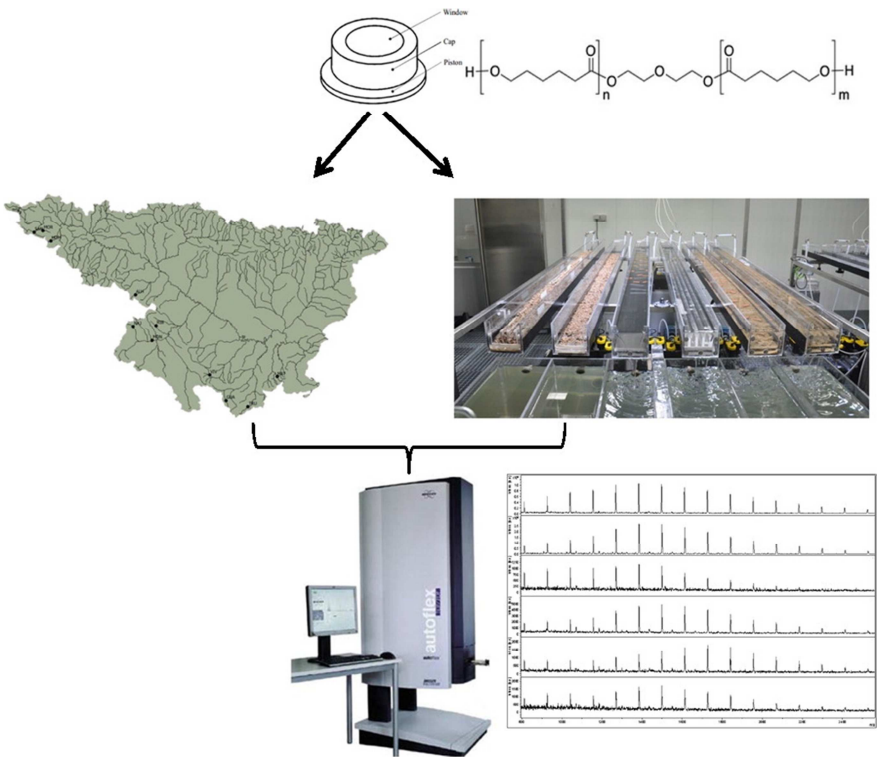

3.4 Introduction

It is widely recognized that an adequate characterization of river ecosystems must take into consideration both structural and functional aspects (Gessner and Chauvet, 2002) (Palmer and Febria, 2012). However, classical health assessment of freshwater ecosystems is mainly based on physicochemical variables (dissolved oxygen, nutrients, acidity, conductivity, pollutants), river hydromorphological characteristics, and other structural properties such as the composition of biological communities (Bunn et al., 1999), as it is reflected in the current legislation (Water Framework Directive, Directive 2000/60/EC). Despite its relevance as driver of ecosystem services (Costanza et al., 1997) (Sweeney et al., 2004), much less attention has been devoted to ecosystem functioning (Feld et al., 2011) (Friberg et al., 2011). Stream ecosystem functioning encompasses a variety of processes such as production, retention and

decomposition of organic matter, or retention and recycling of nutrients (Elosegi et al., 2010). The use of leaf-litter decomposition as a functional tool is greatly spread because of its sensitivity to a great variety of stressors such as nutrient addition (Ferreira et al., 2015), land-use changes (Martínez et al., 2013) or water regulation (Mendoza–Lera et al., 2012), and its experimental simplicity (Bärlocher, 2005). Thus, decomposition of organic matter measured in terms of breakdown of leaf litter has been often preferred to other indicators for routine monitoring (Feio et al., 2010); (Gessner and Chauvet, 2002). Alternatively, leaves have been replaced by other more standardized materials such as cotton strips (Imberger et al., 2010); (Tiegs et al., 2007) or wooden sticks (McTammany et al., 2008); (Tank and Winterbourn, 1996); (Young et al., 2008); (Arroita et al., 2012). While all these substrata reflect the decomposition of natural organic matter, they yield little information about the degradation of synthetic organic matter. Since many freshwater ecosystems are nowadays heavily exposed to anthropogenic pollution (Vörösmarty et al., 2010) it seems worth developing probes to assess how stream ecosystems respond to such perturbation and to what extent they are able to degrade synthetic organic matter. To this end, polymers may constitute suitable candidates to be used as substrates.

Polymer degradation is a complex process encompassing both abiotic (mechanical, thermal, chemical, photolysis) and biotic (biodeterioration, biofragmentation, assimilation) phenomena that often are concurrent (Göpferich, 1996) (Molero et al., 2008). Typically after an initial abiotic step, biotic degradation proceeds through the action of enzymes excreted by the microorganisms (bacteria, fungi etc.). In contrast to abiotic processes, biotic degradation usually starts at the polymer's surface where an initial depolymerisation step takes place by means of extracellular enzymes. When broken polymer chains are small enough, they may be uptaken by the microorganisms and metabolized until complete mineralization (Eubeler et al., 2010). Polymer biodegradation has been the object of several reviews (Swift, 1997; Shah et al., 2008; Lucas et al., 2008; Eubeler et al., 2010). These reviews usually focus on two main aspects, namely, the biodegradation of the different polymer groups and standardized test methods and procedures employed to characterize polymer biodegradation. Studied groups include, among others, polyolefins, polyethylene glycols, polyurethanes, polyamides, polyimides, polyisoprene, acrylic polymers, polyvinyl alcohol, polyvinyl pyrrolidone and polyesters, being the latter by far the most studied (Tokiwa and Calabia, 2007) (Eubeler et al., 2010) as they are the main constituents of biodegradable polymeric materials ("bioplastics"). Remarkably, most of the research on the biodegradation of polyesters has been focused on soil and compost, while

water environments (seawater, freshwater and wastewater) have been much less investigated (Eubeler et al., 2010).

Polymer degradation studies include monitoring of changes occurred in physico-chemical and rheological characteristics of the material (intrinsic viscosity, average molecular weight, (Pitt and Zhong-wei, 1987)), as well as the application of analytical chemical methods such as infrared spectroscopy, nuclear magnetic resonance, gas chromatography coupled to mass spectrometry, liquid chromatography mass spectrometry and Matrix-assisted laser desorption ionization time-of-flight mass spectrometry (MALDI-TOF/MS) (Eubeler et al., 2009). These analytical techniques provide information about the molecular structure of polymers, and maybe useful for monitoring changes over time. MALDI-TOF/MS, originally developed to study peptides and proteins, has also been successfully applied to synthetic polymers (Favier et al., 2004). This technique enables analysing polymers in a broad range of molecular weight. However, its resolution and mass accuracy are best for relatively low-mass polymers (Nielen, 1999) (Schriemer and Li, 1996). MALDI-TOF/MS is particularly suitable for polymer analysis because of simple acquisition of the mass spectra which show mainly single-charged quasi-molecular ions with hardly any fragmentation (Rizzarelli and Carroccio, 2014). Moreover, simple sample preparation, short analysis times, the variety of available matrices and low sample consumption are further advantages of this technique (Montaudo et al., 2006). Nevertheless, MALDI-TOF/MS has been seldom used to study polymer degradation in water. Some examples of MALDI-TOF/MS to study polymer degradation include the hydrolytic degradation of poly(ethylene terephthalate) in water (Weidner et al., 1997), the aerobic biodegradation of poly(vinylpyrrolidone) on a laboratory-scale fixed-bed bioreactor run with river water (Trimpin et al., 2001) and the aerobic biodegradation of polyethylene glycols in seawater and wastewater (Bernhard et al., 2008).

The general aim of the present article was to use a polymer substrate as a probe for characterizing river ecosystem functioning. To the best of our knowledge, this approach had not been yet tested for that purpose. Specific objectives sought in the present study were: (i) to select commercially available synthetic polymers to be used as probes in degradation studies in freshwater; (ii) to compare the starting polymers with potentially modified structures following its exposure to aquatic environments using MALDI-TOF/MS at lab (mesocosm) scale; (iii) to use the selected polymer probe in real field experiments. To this end, an exposure experiment was carried out in the Ebro river basin in parallel to another study using leaf litter (Monroy et al., 2016).

3.5 Methods

3.5.1 Materials

Selected polymers: ε-Polylysine (POL) 4000 Da (physical aspect: powder), was obtained from Zhengzhou Bainafo Bioengineering CO LTD (Zhengzhou city, Henan Province, P.R. China). Polycaprolactonediol (PCP) 1250 Da (physical aspect: waxy), and PCP 2000 Da (physical aspect: waxy), were obtained from Polysciences USA (Warrington, PA18976) and poly(ethyl vinyl ether) (PEVE) 3800 Da (physical aspect: viscous oil), from Aldrich (Steinheim, Germany). Matrices: all-trans retinoic acid (RA), trans-3-indoleacrylic acid (IAA), 2-(4-hydroxyphenylazo)benzoic (HABA), dithranol (DIT) and trans-2-[3-(4-tert-Butylphenyl)-2-methyl-2-propenylidene]malononitrile (DCTB) were obtained from Aldrich (Steinheim, Germany). 2,5-dihydroxy benzoic acid (DHB) was obtained from Bruker (Bruker Daltonik GmbH, Bremen, Germany). Metal Salts: silver trifluoroacetate (Ag-TFA), sodium trifluoroacetate (Na-TFA) and potassium trifluoroacetate (K-TFA) were purchased from Aldrich (Steinheim, Germany). Solvents: the employed solvent Tetrahydrofuran (p.a.) (THF) and trifluoroacetic acid (TFA) were obtained from Sigma-Aldrich (St. Louis, MO, USA). Acetonitrile and water (p.a.) were obtained from J. T. Baker (Teugseweg 20-Deventer, Netherlands). The cap units used in the degradation exposure experiments were purchased from Exposmeter AB (Tavelsjo, Sweden). Each capsule unit consists of a plastic piston (3.9 cm external diameter) a plastic cap (2.5 cm diameter) with a window (2 cm diameter) (Fig. S3.1, Supplementary data).

The Four commercially available polymers selected (POL, PEVE, PCP 1250 and PCP 2000) were characterized using MALDI-TOF/MS as described in Section 3.6.

3.5.2 Mesocosm degradation experiments

Mesocosm degradation experiments were carried out by placing capsules filled with PCP 1250 (20–80 mg) in two artificial streams (mesocosm) located at the indoor Experimental Streams Facility of the Catalan Institute for Water Research (Girona, Spain), with two treatments differing in their nutrient concentration. The artificial streams were 2 m long, had a rectangular cross-section of 50 cm^2 and were set up as an open system with constant slope and steady, uniform flow. They operated with water at a constant flow of 60 mL s^{-1}, resulting in mean water velocity of 0.9 ± 0.3 cm s^{-1}, and a water depth over the plane bed between 2.2 and 2.5 cm. The artificial streams were filled with approximately 100 L of sand (mean diameter = 0.37 mm).

Sand was sterilized in a Presoclave-II 30 L autoclave (120 °C for 20 min) (JP Selecta S.A., Barcelona, Spain) and evenly distributed in the artificial stream to create a plane bed that facilitated the growth of biofilm. Biofilm inocula were obtained from an unpolluted segment of Segre River (Puigcerdà, Girona, Spain), after scraping 10–12 cobbles. New inocula were provided twice a week to each channel during the first three weeks of the colonization period.

The artificial streams run with rainwater collected in a tank and filtered through activated carbon filters. One of the streams had no nutrients added, whereas in the other the concentrations of phosphate and ammonium were raised (0.038 mg L^{-1} P-PO_4^{3-} and 0.035 mg L^{-1} N-NH_4^+; Table S3.1, Supplementary data), by means of an injection of concentrated solutions (KH_2PO_4 and NH_4Cl, respectively) via a peristaltic pump (IPC Ismatec, Glattbrugg, Switzerland). Daily cycles of photosynthetic active radiation (PAR) were defined as 9-h daylight + 15-h darkness. PAR was held constant at 150 μE m^{-2} s^{-1} during the daytime. Water temperature was held constant at 20 °C by means of a cryo-compact circulator (Julabo CF-31, Seelbach, Germany). Total exposure time was 28 days. Samples (three capsules) were collected every 7 days. The following physico-chemical and biological parameters were monitored: Temperature, pH, conductivity, dissolved oxygen, nitrates, nitrites, chlorophyll, fluorescence, effective quantum yield (Yeff) and total organic mass (AFDM). (See Figs. S3.2–S3.5 and Table S3.1, Supplementary data).

3.5.3 River exposure experiments

Once the degradation device was evaluated in the mesocosm study, a decomposition experiment was performed at 11 sites across the Ebro River basin, which had relatively good water quality (Ccanccapa et al., 2016; López-Serna et al., 2012; Roig et al., 2015), well preserved channel and riparian zones, but which were spatially distributed along a variable precipitation gradient, ranging from 380 up to 621 mm/y (Fig. 3.1). We deployed three caps filled with PCP 1250 (20–80 mg/caps) at each site, and recovered them 97 days later. After collection, samples were stored at low temperature (4 °C), air dried at room temperature and weighted prior to MALDI-TOF/MS measurements (described in Section 3.6). Degradation rate constants Kd (d^{-1}) were calculated from weight loss assuming first-order kinetics at time = 97 days.

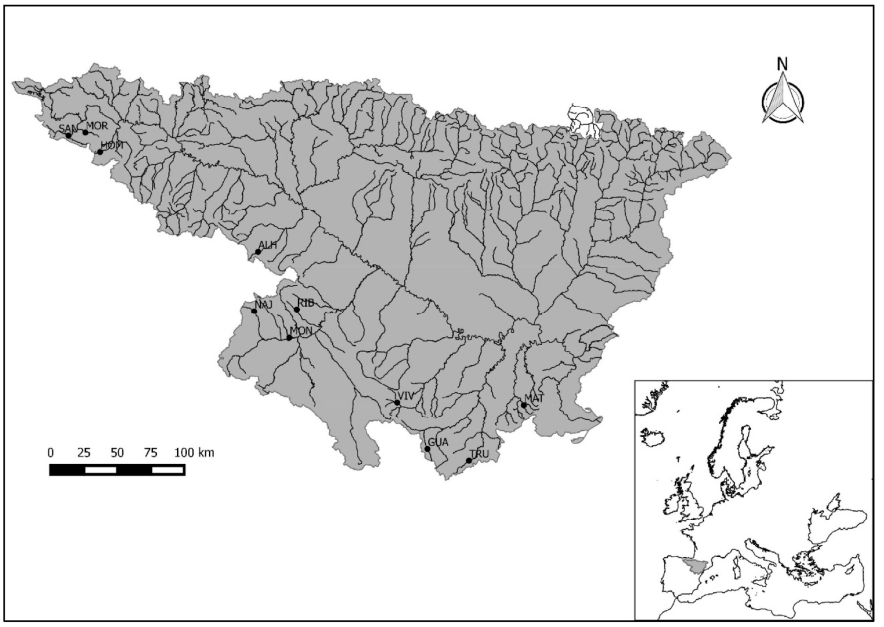

Figure 3.1: Ebro River basin map showing the location of the study sites.

Water temperature was recorded every hour during the experiment with data loggers (Onset Optic StowAway or ACR SmartButton). Electrical conductivity, dissolved oxygen and pH were measured (WTW Multi 350i) on three occasions at each site. On the same occasions, water was collected and transported chilled to the laboratory. Unfiltered water was used to determine ammonium concentration and alkalinity within 48 h of collection, while filtered (Millipore 0.45 μm) water was frozen for later analyses of nitrate, nitrite and soluble reactive phosphorus (SRP) concentrations. Nitrate was determined by capillary ion electrophoresis (Agilent CE); ammonium and nitrite concentrations were determined with automatic analyzers (Dionex DX-120 and Traacs 800). SRP concentration was determined by the ascorbic acid method (APHA, 1998). Alkalinity was estimated by titration with H_2SO_4 to an end point pH of 4.5 (APHA, 1998). Daily mean flow values for all studied sites were obtained from nearby gauging stations for the period 2005–2015 (data from Ebro Hydrographic Confederation; http: \\www.chebro.es). Results of physico-chemical and environmental variables are given in Table S3.2 (Supplementary data).

3.6 MALDI-TOF/MS

MALDI-TOF mass spectra were recorded using an Autoflex III MALDI-TOF mass spectrometer (Bruker Daltonik GmbH, Bremen, Germany) equipped with a 200 Hz smartbeam laser (337 nm). Different parameters were tested in order to find the optimal conditions for further analysis (Table 3.1). Six different matrices (RA, IAA, HABA, DIT, DHB and DCTB) were prepared in THF or in 30%ACN/0.1%TFA at different concentrations in order to analyze four polymers with different average molecular weight that oscillated between 1200 and 4000 Da. Three metal salts (Ag-TFA, K-TFA and Na-TFA) were tried as cationization agents. Matrix, polymer and cationization agent were mixed at three different ratios (10:10:1,10:25:1, 10:50:1 and 10:100:01), then 1 μL of the mixture was deposited onto the stainless steel target plate, which was then dried in air before insertion into the ion source chamber. The analytical conditions for the MALDI-TOF/MS analysis were set as follows: positive reflector ion mode; ion source 1 voltage, 19.2 kV; ion source 2 voltage, 16.2 kV; lens voltage, 8.5 kV; and mass range, 600–4000 m/z. The mass spectra were acquired by averaging 1000 laser shots. Laser irradiance was maintained slightly above threshold.

Tabla 3.1: Different parameters to optimize for MALDI-TOF/MS characterization of the target polymers

Parameters							
Matrix	Name	RA[1]	IAA[2]	HABA[3]	DIT[4]	DHB[5]	DCTB[6]
	Solvent	THF			30%ACN/0.1%TFA (TA30)		
	Concentration	10 mg/mL		20 mg/mL		50 mg/mL	
Analytes	Name	PCP[7]		PCP[7]	PEVE[8]		POL[9]
	Mw	1250		2000	3800		4000
	Concentration	1 mg/mL			5 mg/mL		
Cationization agent	Metal	K		Na		Ag	
	Concentration	2 mg/mL					
Matrix : analyte : Cat. agent		10:10:01		10:25:01	10:50:01		10:100:01

RA1: All-trans retinoic acid, IAA2: trans-3-indoleacrylic acid, HABA3: 2-(4-hydroxyphenylazo) benzoic, DIT4: dithranol, DHB5: 2,5-dihydroxybenzoic acid, DCTB6: t-2-(3-(4-t-Butyl-phenyl)-2-

methyl-2-propenylidene)malononitrile, PCP7: polycaprolactonediol, PEVE8: poly (ethyl vinyl ether), POL9: ε-polylysine.

3.7 Statistical analysis

Data analysis was carried out on both mesocosm and river experiments using as variables the normalized ion intensities zi defined as $zi = xi/\sum xi$, where xi designates the intensity of ion i in a given sample. Statistical treatment was performed with IBM SPSS Statistics Package 21.0. For mesocosm exposure experiments Levene test was first applied to evaluate the homogeneity of variances of the results. Significant differences were determined by one-way ANOVA (with treatment as a factor) at a significance level lower than 0.05 ($p < 0.05$). When significant differences were found for treatment factor, the Tukey and Games - Howell test (significance, $p < 0.05$) was used as post hoc comparison between controls and treatment. Principal Component Analysis was applied to both mesocosms and river exposure experiments.

3.8 Results and discussion

3.8.1 Polymer selection and characterization

In the present study, four polymers were chosen for further MALDI-TOF/MS characterization, namely, POL, PEVE, PCP 1250 and PCP 2000. Selection was done on the basis of two criteria: (a) molecular weight range (1000–10,000 Da), as it is the most suitable for MALDI-TOF/MS analysis and (b) their commercial availability and economic affordability. It is worth noting that their MALDI-TOF/MS characterization was not previously reported.

Sample preparation is crucial in MALDI-TOF/MS and greatly influences the quality of the spectra. In a typical preparation approach, appropriate amounts of polymer, matrix and cationizing agent dissolved in compatible (preferably identical) solvent are mixed to yield a matrix: analyte molar ratio in a specific range for each polymer.

In MALDI-TOF/MS analysis, a dilute solution of the analyte polymer is mixed with a more concentrated matrix solution. The choice of a matrix tailored for a particular kind of polymer sample is crucial for its successful characterization. Optimal matrix selection is usually found by trial and error since the exact role of the matrix is still not fully understood. General requirements for an ideal matrix performance are the following: high electronic absorption at the employed laser wavelength, good vacuum stability, low vapor pressure, good solubility in solvents that also dissolve the analyte,

and good miscibility with the analyte in the solid state. In contrast to biopolymers, the ionization of syntethic polymers usually occurs by cationization rather than protonation. Different cations (such as lithium, sodium, potassium and cesium) and transition metal salts (such as $Ag^+ X^-$, $Cu^{2+} X^{2-}$) that efficiently wrap around the polymer can be used and are added in the form of cationizing agents. Finally, after the selection of the MALDI matrix, cationizing agent and solvent, several options are available for transferring the mixture onto the MALDI target plate (Aparna et al., 2015). In the present study the dried droplet method was selected. In this method the three solutions are mixed, and 1 μL of the mixture is applied to the target plate and air-dried at room temperature. Under these conditions crystallization is relatively slow, thereby increasing the risk of segregation among sample, matrix and cationizing agent (Montaudo et al., 2006). Matrix, cationizing agent and solvent as well as optimal experimental conditions are summarized in Table 3.2. Detailed MALDI-TOF/MS spectra of the four polymers studied are given in Figs. 3.2A to 3.2D. It is worth noting that even though Ag was added as cationizing agent, sodium and potassium adducts (M_n + 23 and M_n + 39 respectively) are the predominant species appearing in the spectra in the case of PCP 1250, PCP 2000 and POL (Figs. 3.2A–C) (Liu et al., 1999). Main peaks observed for PEVE were tentatively identified as K adducts of HM_{n-1}–CH_2–CHO (see Fig. 3.2D and the insert therein) (Katayama et al., 2001; Kumagai et al., 2008).

Table 3.2: Optimized conditions for MALDI-TOF/MS characterization of the target polymers.

Sample	Proportion	Matrix	Cationizing agent	Solvent
POL[1] 1 mg/mL	10:10:01	DHB[4] 10 mg/mL	AgTFA 2 mg/mL	TA 30
PEVE[2] 1 mg/mL	10:10:01	All trans retinoic acid 10 mg/mL	KTFA 2 mg/mL	TA 30
PCP[3] 1250 MW 1 mg/mL	10:10:01	DCTB[5] 10 mg/mL	NaTFA 2 mg/mL	THF
PCP[3] 2000 MW 1 mg/mL	3:20:01	DCTB[5] 20 mg/mL	AgTFA 2 mg/mL	THF

POL[1]: ε-polylysine. PEVE[2]: poly (ethyl vinyl ether). PCP[3]: polycaprolactonediol. DHB[4]: 2,5-dihydroxybenzoic acid, DCTB[5]: t-2-(3-(4-t-Butyl-phenyl)-2-methyl-2-propenylidene)malononitrile.

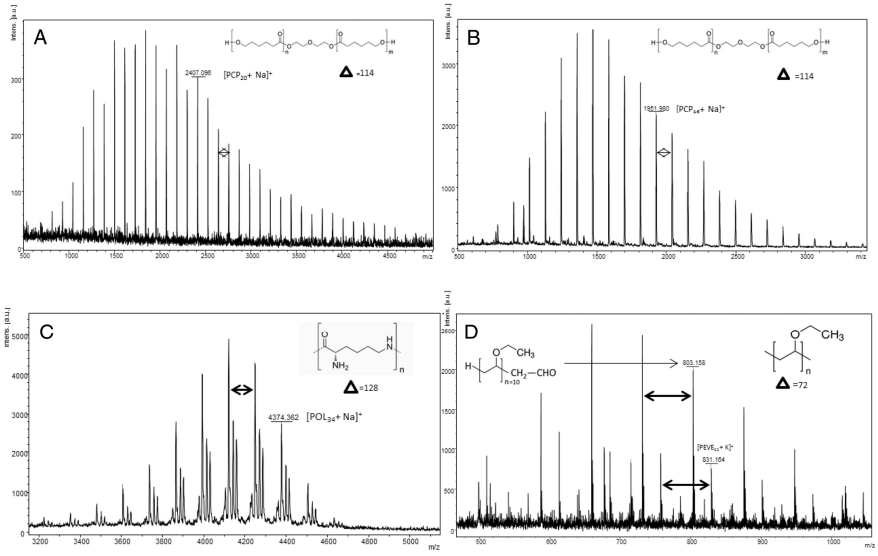

Figure 3.2: MALDI-TOF/MS spectra of the studied polymers. (A) polycaprolactonediol 1250 (PCP 1250); (B) polycaprolactonediol 2000 (PCP 2000); (C) polylysine (POL); (D) polyethylvinyl ether (PEVE). M + Na and M + K adducts are observed for PCP 1250, PCP 2000 and POL. Main species observed for PEVE are tentatively identified as K adducts of structure shown in the insert (Katayama et al., 2001; Kumagai et al., 2008).

High matrix effects were observed for PEVE when the polymer:matrix:cationizing agent ratios used were of 10:50:01 and 10:100:01. This means that if high laser energies are used only very weak spectra intensities are obtained (Rizzarelli and Carroccio, 2014). The best conditions for this polymer were finally set at a ratio 10:10:1 (Table 3.2). These data suggest that the polymer might have undergone degradation by some cause (i.e. photo-degradation) (Göpferich, 1996; Rizzarelli and Carroccio, 2014). As seen in Table 3.1, even though the only apparent difference between PCP 1250 and PCP 2000 is molecular weight, the optimal conditions for MALDI-TOF/MS characterization of PCP 2000 were remarkably different, thus indicating that the polymer molecular weight may influence the crystallization process (Bahr et al., 1992).

Owing to its physico-chemical properties, commercial affordability, degradability, manipulation advantages and easy MALDI-TOF/MS characterization, PCP 1250, a polyester oligomer, was finally selected as testing material to be further used in mesocosms and field experiments.

3.8.2 Mesocosms experiments

In the artificial streams experiment we focused on the possible role of nutrients, since the development of river biological communities is strongly dependent on nutrient availability (Ponsatí et al., 2016; Sabater et al., 2016). Physico-chemical and biological variables measured are reported in Table S3.1 and Figs. S3.2–S3.5 respectively (Supplementary data). The three first components of a PCA performed using the normalized intensities of the 25 most abundant ions in the range m/z 700–3436 present in the MALDI-TOF/MS spectra captured 79.7% of the total variance (51.9%, 16.3% and 11.5% respectively) (Fig. 3.3). In the loading plot ions appeared well separated (Fig. 3A) in three groups corresponding to low (m/z 700–1700), medium (m/z 1700–2800) and high masses (m/z > 2800). The scores plot (Fig. 3.3B) did not differentiate samples neither in terms of exposure time nor treatment (nutrient concentration). However, the starting material seemed different from the rest, indicating that exposed samples had undergone some structural changes.

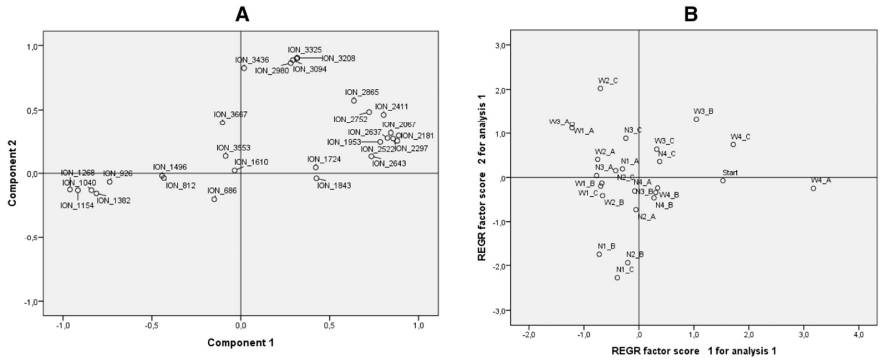

Figure 3.3: Principal Component Analysis plots of mesocosms experiments. Samples corresponding to the treatment with nutrient addition are labeled 'N', those of the treatment without nutrient addition are labeled 'W'. Ions are indicated by their m/z. (A) Loadings plot; (B) Scores plot.

The evolution of the relative intensities of different ions along time depended on the ion mass (Fig. 3.4). Whereas small ions apparently increased their relative intensity during the first two weeks and decayed afterwards, the opposite behavior was observed for larger ones. Note that relative intensities only allow a comparison of the mass distributions (in the studied range) of the remaining polymer, but do not inform about other possible deeper absolute changes undergone by the polymer during the

water exposition. The differences in relative intensities between a given ion of an exposed sample with respect to the standard material at different exposure times were checked for both treatments (ANOVA, Levene test $p < 0.05$) (Table 3.3). In the first three weeks, the number of ions showing statistically significant differences with respect to the standard was similar in both treatments and decreased over time. However, in the fourth week the trend was reversed and the number of statistically different ion intensities with respect to the standard material increased, but in the presence of nutrients the change was remarkably more pronounced (3 different peak intensities in the treatment without nutrients; 11 different peak intensities with nutrients). Furthermore, a direct comparison of peak intensities for both experiments at a given time was performed (ANOVA, Levene test $p < 0.05$) only showing statistically significant differences for peaks m/z 2411 and 2865 at week 4. Overall, under the conditions examined, differences in the degradation of polycaprolactonediol attributable to the presence of nutrients were seemingly statistically relevant only at longest exposure times. This result is consistent with the differences observed on biofilm development between both treatments (see Supplementary data, Figs. S3.2–S3.5, parameters Chlorophyll-a, organic biomass, photosynthetic activity and fluorescence) that were likewise more perceptible at longer exposure times (weeks 3 and 4).

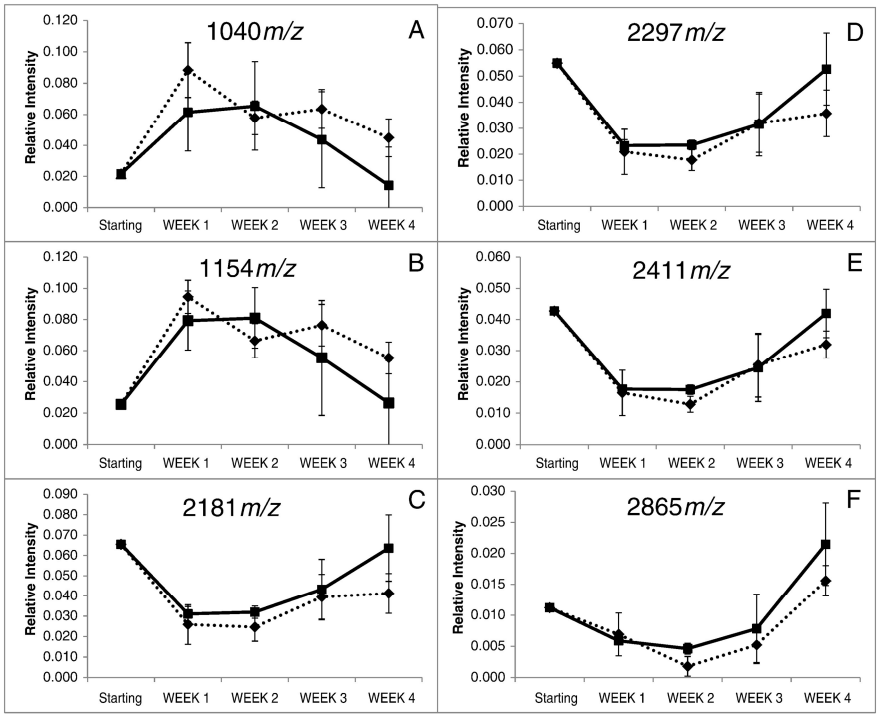

Figure 3.4: Time course of relative peak intensities of some representative ions in mesocosm experiments with nutrients (full line) and without nutrient addition (dotted line). Error bars correspond to mean ± standard deviation (n = 3).

Table 3.3: Summary of ANOVA results comparing experiments with and without nutrient addition against standard material. Relative peak intensities of each ion at a given time (week 1 to 4) are compared to those of the standard material.

Week	Number of statistical significant peaks[a]	
	Nutrient	Without nutrients
1	7	11
2	4	6
3	1	1
4	11	3

[a]Levene test of homogenity of variance.

3.8.3 River experiments

After 97 days of exposure, the composition of the polymer probes differed from the starting material, but the extent of changes was highly variable among samples. In general, changes were evident in terms of weight loss Table S3.3 (Supplementary data) as well as in their MALDI-TOF/MS spectra (see some representative examples in Fig. 3.5). The spectral changes detected were of two types: (i) different distribution of the polymer chain lengths, the most transformed samples showing a shift of the maximum towards longer chains and (ii) a decrease of the overall peak intensity (in the examples shown in Fig. 3.5, this fact is manifested in the different attenuation factors needed to acquire the spectra). A preliminary interpretation of the results was obtained by PCA using the normalized intensities of the main 25 ions in the m/z range 700–3436 present in the MALDI-TOF/MS spectra of the samples. The first three axes explained 78.5% of the total variance (51.2%, 21.4% and 5.9%, respectively) (Fig. 3.6). Remarkably, the loadings plot (Fig. 3.6A) followed a similar pattern to that obtained in the mesocosm PCA (Fig. 3.3A), i.e. ions clustered in three groups corresponding to low (m/z 700–1300), medium (m/z 1300–1900) and high masses (m/z > 2000), with ranges slightly shifted towards low masses. As observed in the mesocosm experiments, the PCA scores plot (Fig. 3.6B) allowed differentiating samples among sites. Starting material, characterized by positive PC1 and negative PC2 scores, appeared clearly separated from the river-exposed samples. Polymer weight loss (quantified as Kd) was comprised between $17.6 \cdot 10^{-2}$ and $2.52 \cdot 10^{-3}$ $days^{-1}$ corresponding the lowest value to stream TRU, one of the most severely affected (together with VIV) by flow reduction during the experiment (VIV Kd was $3.97 \cdot 10^{-3}$ $days^{-1}$). This behavior was also observed in litter degradation measurements done in parallel (Monroy et al., 2016), thus pointing to the relevance of local-scale hydrological conditions as proposed by these authors. The relative intensities of some peaks were correlated to Kd (Fig. 3.7); thus, whereas larger m/z peaks were negatively correlated, medium ones showed a less pronounced trend. Regarding the influence of environmental conditions, conductivity, mean temperature, river flow and nutrients ($N\text{-}NH_4^+$, DIN and SRP) showed a correlation with the intensities (Table S3.4, Supplementary data). Again, as previously mentioned, low and high mass ions exhibited in some cases opposite trend correlations.

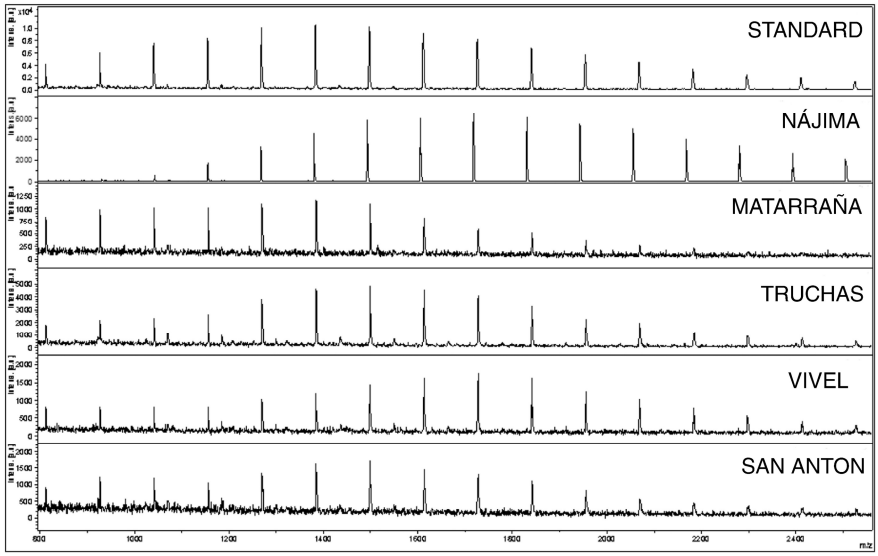

Figure 3.5: Representative MALDI-TOF/MS spectra of polymer probes of different river exposed samples. Spectrum of standard material is included for comparison purposes. Note that intensity scales correspond to different attenuation factors. Differences among spectra of are perceptible both in absolute intensities of peaks and in their respective distribution (shifting of maxima).

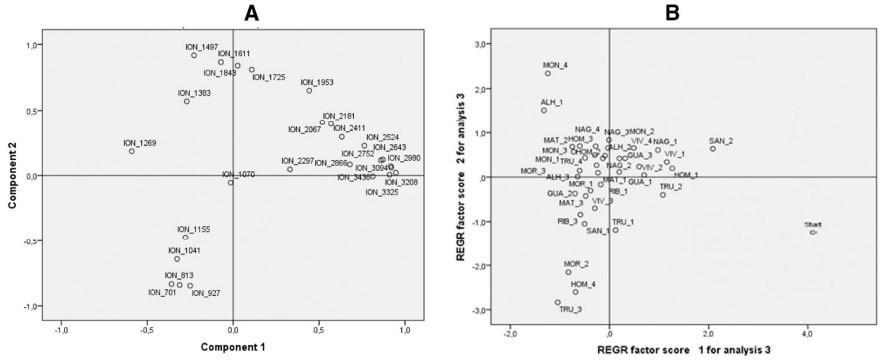

Figure 3.6: Principal Component Analysis plots of experiments in the Ebro river basin. Ions are indicated by their m/z. (A) Loadings plot; (B) Scores plot.

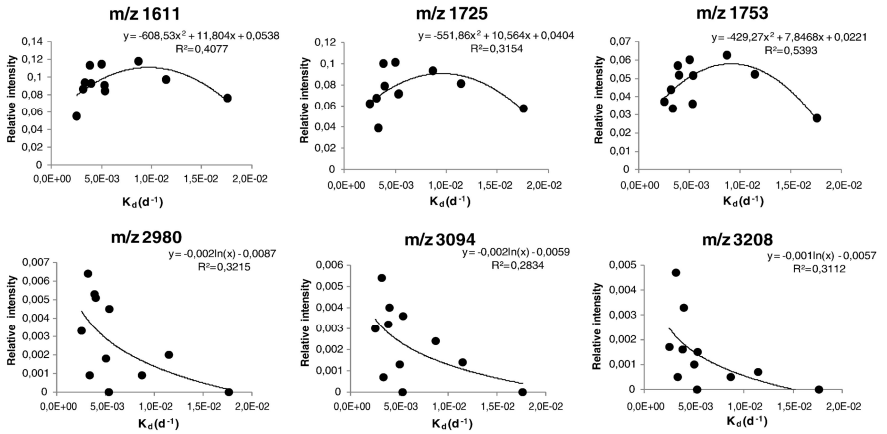

Figure 3.7: Correlation between of polymer weight loss (expressed as Kd) and intensities of some representative peaks.

3.9 Conclusions

The study of degradation of synthetic organic matter by freshwater ecosystems can be approached by means of polymer probes, used in a similar way as natural organic materials (leaf litter, wood sticks, etc.), yielding thus a complementary information on river metabolism. PCP 1250 can be effectively used as a probe and its transformation conveniently monitored by MALDI-TOF/MS. The interpretation of field results in terms of environmental conditions remains elusive, probably reflecting the influence of multiple concurrent factors (Sabater et al., 2016). In that respect, the use of MALDI-TOF/MS IMAGING techniques might open new possibilities (Rivas et al., 2016). In any case, the use of probes based on polymer degradation characterized by MALDI-TOF/MS seems a novel and promising tool whose potential uses are not restricted to river ecosystems, but can be applied as well to other biological systems such as wastewater treatment plants.

3.10 Aknowledgements

This study has been financially supported by the EU through the FP7 project GLOBAQUA (Grant agreement No 603629), and by the Generalitat de Catalunya (Consolidated Research Groups "2014 SGR 418—Water and Soil Quality Unit" and 2014 SGR 291—ICRA). It reflects only the author's views. The Community is not liable for any use that may be made of the information contained therein. The authors are thankful to Maria Casellas (Experimental Streams Facility, Catalan Institute for Water Research, Girona, Spain) for her technical help in the operation of the artificial streams.

3.11 References Chapter 3

Aparna C, Latha NM, Supriya P, Gowrisankar D. A REVIEW ON MATRIX ASSISTED LASER DESORPTION/INOZATION MASS SPECTROSCOPY. Asian Journal of Pharmaceutical and Clinical Research 2015; 8.

Arroita M, Aristi I, Flores L, Larrañaga A, Díez J, Mora J, et al. The use of wooden sticks to assess stream ecosystem functioning: Comparison with leaf breakdown rates. Science of the Total Environment 2012; 440: 115-122.

Artham T, Doble M. Biodegradation of aliphatic and aromatic polycarbonates. Macromolecular bioscience 2008; 8: 14-24.

Bahr U, Deppe A, Karas M, Hillenkamp F, Giessmann U. Mass spectrometry of synthetic polymers by UV-matrix-assisted laser desorption/ionization. Analytical Chemistry 1992; 64: 2866-2869.

Bernhard M, Eubeler JP, Zok S, Knepper TP. Aerobic biodegradation of polyethylene glycols of different molecular weights in wastewater and seawater. Water Research 2008; 42: 4791-4801

Bunn SE, Davies PM, Mosisch TD. Ecosystem measures of river health and their response to riparian and catchment degradation. Freshwater Biology 1999; 41: 333-345.

Ccanccapa A, Masiá A, Navarro-Ortega A, Picó Y, Barceló D. Pesticides in the Ebro River basin: Occurrence and risk assessment. Environmental Pollution 2016; 211: 414-424.

Costanza R, d'Arge R, de Groot R, Farber S, Grasso M, Hannon B, et al. The value of the world's ecosystem services and natural capital. Nature 1997; 387: 253-260.

Elosegi A, Díez J, Mutz M. Effects of hydromorphological integrity on biodiversity and functioning of river ecosystems. Hydrobiologia 2010; 657: 199-215.

Eubeler JP, Zok S, Bernhard M, Knepper TP. Environmental biodegradation of synthetic polymers I. Test methodologies and procedures. TrAC - Trends in Analytical Chemistry 2009; 28: 1057-1072.

Eubeler JP, Bernhard M, Knepper TP. Environmental biodegradation of synthetic polymers II. Biodegradation of different polymer groups. TrAC - Trends in Analytical Chemistry 2010; 29: 84-100.

Favier A, Ladavière C, Charreyre M-T, Pichot C. MALDI-TOF MS Investigation of the RAFT Polymerization of a Water-Soluble Acrylamide Derivative. Macromolecules 2004; 37: 2026-2034.

Feio M, Alves T, Boavida M, Medeiros A, Graça M. Functional indicators of stream health: a river-basin approach. Freshwater Biology 2010; 55: 1050-1065.

Feld CK, Birk S, Bradley DC, Hering D, Kail J, Marzin A, et al. Chapter Three - From Natural to Degraded Rivers and Back Again: A Test of Restoration Ecology Theory and Practice. In: Guy W, editor. Advances in Ecological Research. Volume 44. Academic Press, 2011, pp. 119-209.

Friberg N, Bonada N, Bradley DC, Dunbar MJ, Edwards FK, Grey J, et al. Biomonitoring of Human Impacts in Freshwater Ecosystems. The Good, the Bad and the Ugly. Advances in Ecological Research. 44, 2011, pp. 1-68.

Gessner MO, Chauvet E. A case for using litter breakdown to assess functional stream integrity. Ecological applications 2002; 12: 498-510.

Glass J, Swift G. Agricultural and synthetic polymers, biodegradation and utilization. ACS symposium series. 433, 1989, pp. 9-64.

Göpferich A. Mechanisms of polymer degradation and erosion. Biomaterials 1996; 17: 103-114.

Imberger SJ, Thompson RM, Grace MR. Searching for effective indicators of ecosystem function in urban streams: Assessing cellulose decomposition potential. Freshwater Biology 2010; 55: 2089-2106.

Katayama H, Kamigaito M, Sawamoto M. MALDI-TOF-MS analysis of living cationic polymerization of vinyl ethers. III. Polymerization with SnCl4 and TiCl4 in the absence of additives. Journal of Polymer Science Part A: Polymer Chemistry 2001; 39: 1258-1267.

Kumagai T, Kagawa C, Aota H, Takeda Y, Kawasaki H, Arakawa R, et al. Specific Polymerization Mechanism Involving β-Scission of Mid-Chain Radical Yielding Oligomers in the Free-Radical Polymerization of Vinyl Ethers. Macromolecules 2008; 41: 7347-7351.

Liu J, Loewe RS, McCullough RD. Employing MALDI-MS on poly (alkylthiophenes): analysis of molecular weights, molecular weight distributions, end-group structures, and end-group modifications. Macromolecules 1999; 32: 5777-5785.

López-Serna R, Petrović M, Barceló D. Occurrence and distribution of multi-class pharmaceuticals and their active metabolites and transformation products in the Ebro River basin (NE Spain). Science of the Total Environment 2012; 440: 280-289.

Lucas N, Bienaime C, Belloy C, Queneudec M, Silvestre F, Nava-Saucedo JE. Polymer biodegradation: Mechanisms and estimation techniques. Chemosphere 2008; 73:429-442

McTammany ME, Benfield EF, Webster JR. Effects of agriculture on wood breakdown and microbial biofilm respiration in southern Appalachian streams. Freshwater Biology 2008; 53: 842-854.

Molero C, de Lucas A, Rodríguez JF. Recovery of polyols from flexible polyurethane foam by "split-phase" glycolysis: Study on the influence of reaction parameters. Polymer Degradation and Stability 2008; 93: 353-361.

Monroy S, Menéndez M, Basaguren A, Pérez J, Elosegi A, Pozo J. Drought and detritivores determine leaf litter decomposition in calcareous streams of the Ebro catchment (Spain). Science of the Total Environment 2016 (this issue); http://dx.doi.org/10.1016/j.scitotenv.2016.07.209

Montaudo G, Samperi F, Montaudo MS. Characterization of synthetic polymers by MALDI-MS. Progress in Polymer Science 2006; 31: 277-357.

Nielen MWF. Maldi time-of-flight mass spectrometry of synthetic polymers. Mass Spectrometry Reviews 1999; 18: 309-344.

Palmer MA, Febria CM. The heartbeat of ecosystems. Science 2012; 336: 1393-1394.

Pitt CG, Zhong-wei G. Modification of the rates of chain cleavage of poly(ϵ-caprolactone) and related polyesters in the solid state. Journal of Controlled Release 1987; 4: 283-292.

Ponsatí L, Corcoll N, Petrović M, Picó Y, Ginebreda A, Tornés E, et al. Multiple-stressor effects on river biofilms under different hydrological conditions. Freshwater Biology 2016.

Rivas D., Ginebreda A., Pérez S., Quero C., Barceló D. MALDI-TOF MS Imaging evidences spatial differences in thedegradation of solid polycaprolactone diol in water under aerobic and denitrifying conditions. Science of the Total Environment 2016; 566–567: 27–33

Rizzarelli P, Carroccio S. Modern mass spectrometry in the characterization and degradation of biodegradable polymers. Analytica Chimica Acta 2014; 808: 18-43.

Roig N, Sierra J, Nadal M, Moreno-Garrido I, Nieto E, Hampel M, et al. Assessment of sediment ecotoxicological status as a complementary tool for the evaluation of surface water quality: The Ebro river basin case study. Science of the Total Environment 2015; 503-504: 269-278.

Sabater S, Barceló D, De Castro-Català N, Ginebreda A, Kuzmanovic M, Petrovic M, et al. Shared effects of organic microcontaminants and environmental stressors on biofilms and invertebrates in impaired rivers. Environmental Pollution 2016; 210: 303-314.

Schriemer DC, Li L. Detection of High Molecular Weight Narrow Polydisperse Polymers up to 1.5 Million Daltons by MALDI Mass Spectrometry. Analytical Chemistry 1996; 68: 2721-2725.

Shah AA, Hasan F, Hameed A, Ahmed S. Biological degradation of plastics: A comprehensive review. Biotechnology Advances 2008; 26: 246-265.

Sweeney BW, Bott TL, Jackson JK, Kaplan LA, Newbold JD, Standley LJ, et al. Riparian deforestation, stream narrowing, and loss of stream ecosystem services. Proceedings of the National Academy of Sciences of the United States of America 2004; 101: 14132-14137.

Swift G. Non-medical biodegradable polymers: environmentally degradable polymers. Handbook of biodegradable polymers. Hardwood Academic, Amsterdam 1997: 473-511.

Tank JL, Winterbourn MJ. Microbial activity and invertebrate colonisation of wood in a New Zealand forest stream. New Zealand Journal of Marine and Freshwater Research 1996; 30: 271-280.

Tiegs SD, Langhans SD, Tockner K, Gessner MO. Cotton strips as a leaf surrogate to measure decomposition in river floodplain habitats. Journal of the North American Benthological Society 2007; 26: 70-77.

Tokiwa Y, Calabia B. Biodegradability and biodegradation of polyesters. Journal Polymer Environment 2007; 15: 259-267

Trimpin S, Eichhorn P, Räder HJ, Müllen K, Knepper TP. Recalcitrance of poly(vinylpyrrolidone): evidence through matrix-assisted laser desorption–ionization time-of-flight mass spectrometry. Journal of Chromatography A 2001; 938: 67-77.

Vörösmarty CJ, McIntyre PB, Gessner MO, Dudgeon D, Prusevich A, Green P, et al. Global threats to human water security and river biodiversity. Nature 2010; 467: 555-561.

Weidner S, Kuehn G, Werthmann B, Schroeder H, Just U, Borowski R, et al. A new approach of characterizing the hydrolytic degradation of poly (ethylene terephthalate) by MALDI-MS. Journal of Polymer Science Part A: Polymer Chemistry 1997; 35: 2183-2192.

Young RG, Matthaei CD, Townsend CR. Organic matter breakdown and ecosystem metabolism: functional indicators for assessing river ecosystem health. Journal of the North American Benthological Society 2008; 27: 605-625.

3.12 Supporting information

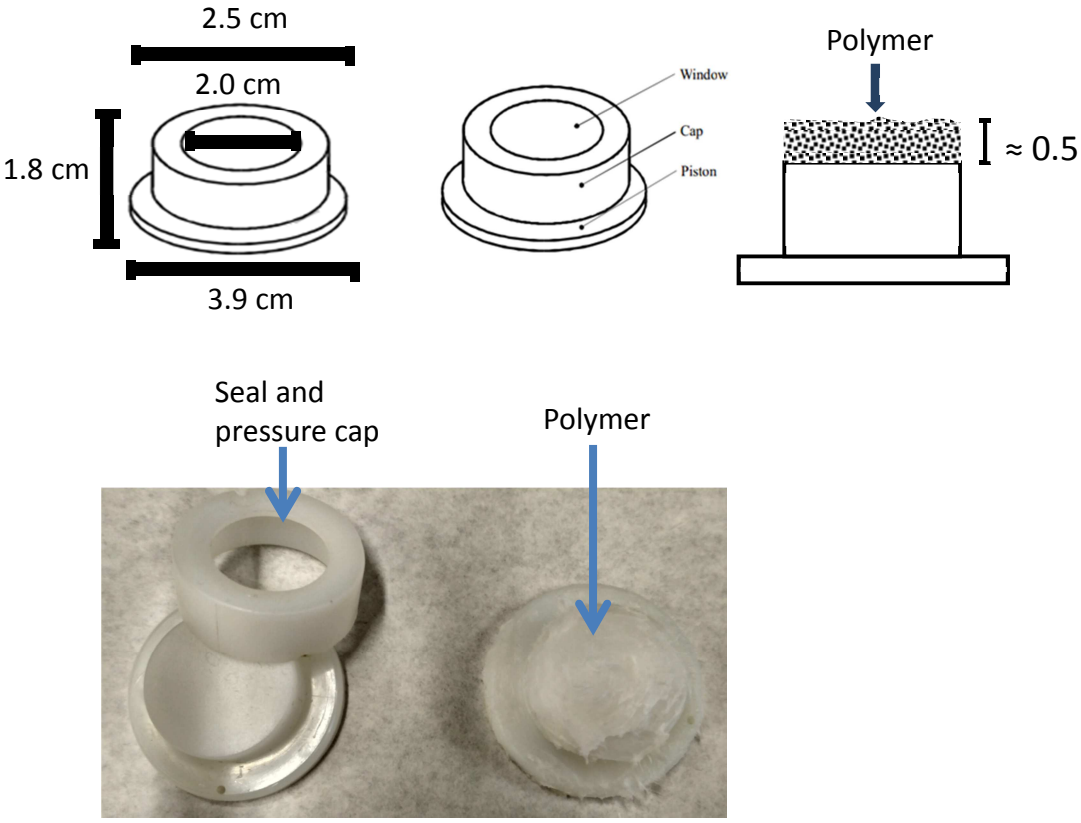

Figure S3.1 Capsules used in exposure experiments

Table S3.1. Environmental variables measured in mesocosm experiments. According to the settings of the experiment, the differences between both treatments (nutrients vs. without nutrients) are perceptible for parameters $P\text{-}PO_4$ and $N\text{-}NH_4$

NUTRIENTS

Time (WEEK)	Conductivity ($\mu S\ cm^{-1}$)	pH	Temperature (ºC)	DOC[a] ($mg\ L^{-1}$)	Oxygen ($mg\ L^{-1}$)	Oxygen (%)	$N\text{-}NO_3$ ($mg\ N\ L^{-1}$)	$P\text{-}PO_4$ ($mg\ P\ L^{-1}$)	$N\text{-}NH_4$ ($mg\ N\ L^{-1}$)
0	319	8.53	20.5	3.324	10.5	116.6	1.992	0.007[b]	<LOQ[b]
1	360	8.40	20.2	2.980	8.8	100.5	2.423	0.038	0.035
2	357	8.38	20.5	3.149	9.9	111.8	2.069	0.012	0.005
3	351	8.26	20.6	3.065	10.1	115.2	2.185	0.026	0.027
4	336	8.37	20.5	4.679	10.2	114.3	1.671	0.026	<LOQ

a)Dissolved Organic Carbon

b) Values before nutrient addition

WHITOUT NUTRIENTS

Time (WEEK)	Conductivity ($\mu S\ cm^{-1}$)	pH	Temperature (ºC)	DOC[a] ($mg\ L^{-1}$)	Oxygen ($mg\ L^{-1}$)	Oxygen (%)	$N\text{-}NO_3$ ($mg\ N\ L^{-1}$)	$P\text{-}PO_4$ ($mg\ P\ L^{-1}$)	$N\text{-}NH_4$ ($mg\ N\ L^{-1}$)
0	335	8.33	20.6	2.723	9.8	114.3	2.212	0.008	<LOQ
1	362	8.47	20.4	2.824	8.6	100.2	2.421	0.009	<LOQ
2	372	8.42	20.4	2.832	10.2	114.3	2.060	0.003	<LOQ
3	348	8.69	20.6	3.085	9.9	116.8	2.192	0.007	<LOQ
4	340	8.59	20.5	6.187	10.0	110.9	1.822	<LOQ	<LOQ

a)Dissolved Organic Carbon

All measurements (AFDW, Chl-a, Yeff and F) were carried out as in (Ponsatí et al., 2016).

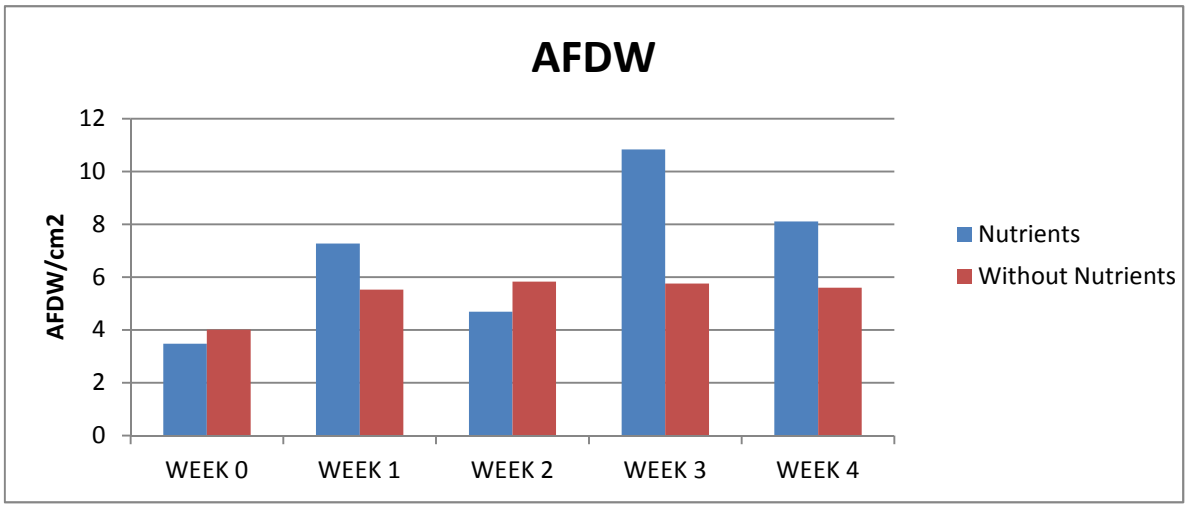

Figure S3.2 Total organic mass measured weekly in mesocosms experiments (with nutrients and without nutrients).

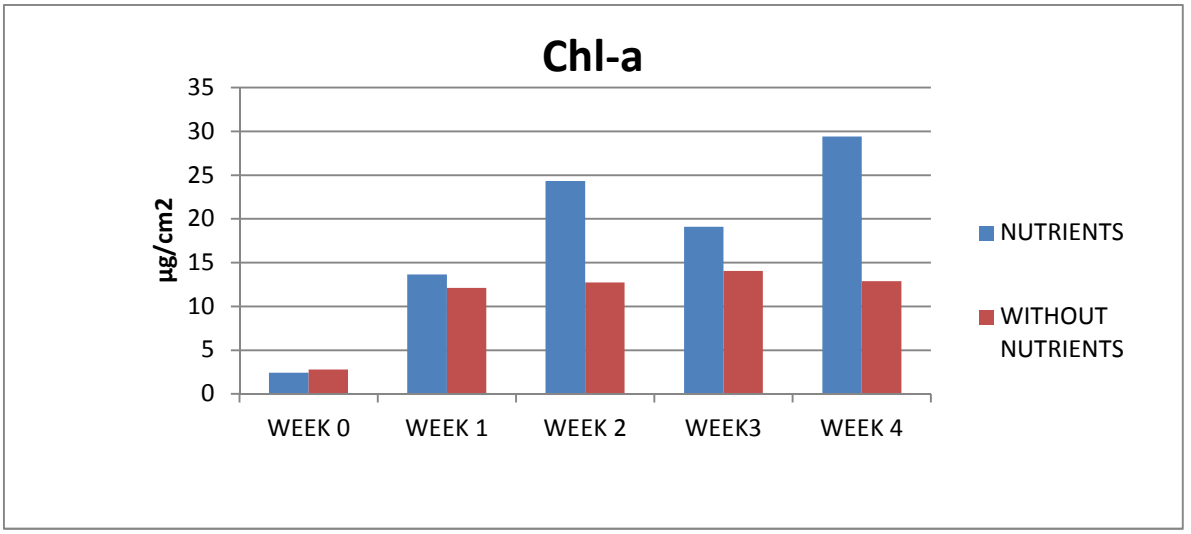

Figure S3.3 Chlorophyll – a measured weekly in mesocosms experiments (with nutrients and without nutrients).

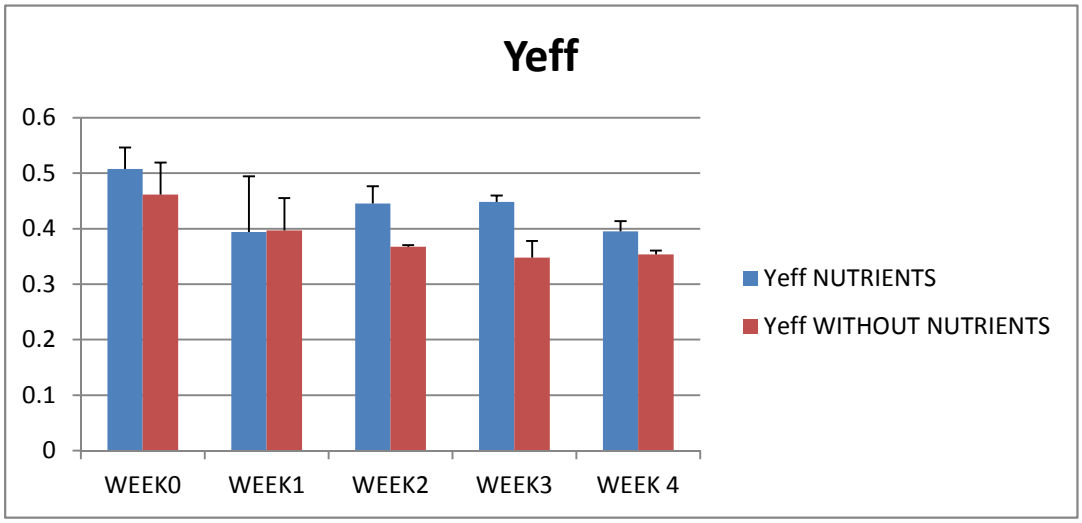

Figure S3.4 Effective photosynthetic capacity measured weekly in mesocosms experiments (with nutrients and without nutrients). Error bars correspond to ± standard deviation (n=3).

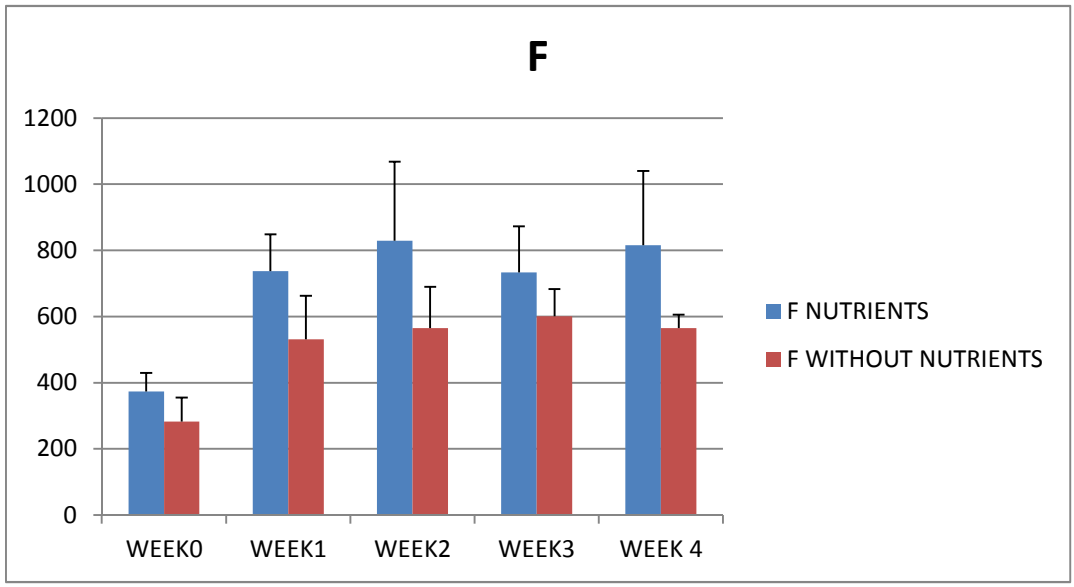

Figure S3.5 Fluorescence measured weekly in mesocosms experiments (with nutrients and without nutrients). Error bars correspond to ± standard deviation (n=3).

Table S3.2. Environmental variables measured in the studied rivers of the Ebro basin (from Monroy et al. 2016).

Stream name	Conductivity (µS/cm)	pH	Dissolved Oxygen (mg/L)	Dissolved Oxygen (%)	$N\text{-}NO_3^-$ (µg/L)	$N\text{-}NH_4^+$ (µg/L)	$N\text{-}NO_2^-$ (µg/L)	DIN (µg/L)	SRP (µg/L)	Flow (L/s)	Temp Mean (ºC)
San Antón	443	8.3	11.3	102.3	1120.1	91.6	1.61	1213.2	6.47	281.7	7.8
Moradillo	430	8.1	11.6	112.0	510.1	58.7	1.35	570.2	4.67	267.9	8.7
Homino	568	8.4	12.0	106.3	11239.8	40.8	4.27	11284.9	13.67	143.5	5.8
Alhama	505	8.5	11.9	106.1	4354.1	58.7	3.30	4416.1	6.40	355.3	**4.3**
Ribota	635	8.1	10.7	97.6	4451.6	39.9	2.91	4494.4	18.80	94.2	6.0
Monegrillo	801	8.1	9.6	91.1	737.4	96.7	1.75	835.8	12.00	14.6	9.4
Nájima	659	8.0	9.9	90.1	5613.9	49.3	4.22	5667.5	2.27	41.9	6.6
Vivel	812	7.9	7.2	66.9	350.1	56.6	19.30	426.0	14.80	84.0	5.8
Guadalope	545	8.3	10.9	101.7	699.6	60.2	6.41	766.2	15.07	237.4	5.2
Truchas	449	8.0	10.5	95.4	131.9	34.4	1.44	167.8	15.20	680.0	3.7
Matarraña	460	8.3	10.3	106.4	289.7	24.0	1.30	315.0	13.80	586.0	12.9

Table S3.3. Weight loss (%) and K_d of the different Ebro streams.

Stream name	Weight loss (%)	K_d (d^{-1})
San Antón	32,42	3,18E-03
Moradillo	61,40	1,76E-02
Homino	49,44	5,36E-03
Alhama	68,01	8,70E-03
Ribota	30,45	3,35E-03
Monegrillo	43,20	5,02E-03
Nájima	31,16	3,85E-03
Vivel	31,96	3,97E-03
Guadalope	75,88	1,15E-02
Truchas	18,10	2,52E-03
Matarraña	40,59	5,31E-03

Table S3.4. Best correlations between relative peak intensities and environmental variables in the Ebro basin sites.

Y Peak m/z (Relative Intensity)	X	Equation	
1269	Temperature (˚C)	$y = 0.0029x + 0.089$	$R^2 = 0.2882$
2181	Temperature (˚C)	$y = -0.0003x^2 + 0.0027x + 0.0234$	$R^2 = 0.3151$
2411	Temperature (˚C)	$y = -0.0004x^2 + 0.0041x + 0.0049$	$R^2 = 0.4751$
2524	Temperature (˚C)	$y = -5E\text{-}05x^2 + 0.0003x + 0.0048$	$R^2 = 0.3339$
2643	Temperature (˚C)	$y = -0.0009x + 0.0133$	$R^2 = 0.2137$
2752	Temperature (˚C)	$y = -9E\text{-}05x^2 + 0.0006x + 0.0065$	$R^2 = 0.5024$
2866	Temperature (˚C)	$y = -0.0003x^2 + 0.0036x + 0.0022$	$R^2 = 0.3822$
3094	Temperature (˚C)	$y = -5E\text{-}05x^2 + 0.0005x + 0.0014$	$R^2 = 0.2540$

Y Peak m/z (Relative Intensity)	X	Equation	
813	Conductivity (µS/cm)	$y = 6E\text{-}07x^2 - 0.0008x + 0.3216$	$R^2 = 0.4342$
927	Conductivity (µS/cm)	$y = 3E\text{-}07x^2 - 0.0005x + 0.2116$	$R^2 = 0.2973$
1497	Conductivity (µS/cm)	$y = 0.0294\ln(x) - 0.0756$	$R^2 = 0.2716$
1611	Conductivity (µS/cm)	$y = 0.0432\ln(x) - 0.1802$	$R^2 = 0.2977$
1725	Conductivity (µS/cm)	$y = 0.0439\ln(x) - 0.2165$	$R^2 = 0.5358$
1843	Conductivity (µS/cm)	$y = -2E\text{-}07x^2 + 0.0003x - 0.0608$	$R^2 = 0.5641$
1953	Conductivity (µS/cm)	$y = -2E\text{-}07x^2 + 0.0003x - 0.0437$	$R^2 = 0.3289$
2181	Conductivity (µS/cm)	$y = -2E\text{-}07x^2 + 0.0003x - 0.0606$	$R^2 = 0.2798$
2411	Conductivity (µS/cm)	$y = -2E\text{-}07x^2 + 0.0003x - 0.0688$	$R^2 = 0.3643$
2524	Conductivity (µS/cm)	$y = -4E\text{-}08x^2 + 6E\text{-}05x - 0.017$	$R^2 = 0.3811$
2866	Conductivity (µS/cm)	$y = -1E\text{-}07x^2 + 0.0002x - 0.0524$	$R^2 = 0.2672$

Y Peak m/z (Relative Intensity)	X	Equation	
813	Flow (L/s)	$y = 9E\text{-}05x + 0.0245$	$R^2 = 0.3985$
1041	Flow (L/s)	$y = 7E\text{-}08x^2 + 2E\text{-}05x + 0.0643$	$R^2 = 0.2436$
1497	Flow (L/s)	$y = -0.007\ln(x) + 0.1464$	$R^2 = 0.4021$
1611	Flow (L/s)	$y = -0.009\ln(x) + 0.1409$	$R^2 = 0.3579$
1843	Flow (L/s)	$y = -0.009\ln(x) + 0.1051$	$R^2 = 0.5221$
1953	Flow (L/s)	$y = -0.005\ln(x) + 0.0719$	$R^2 = 0.2426$
2181	Flow (L/s)	$y = -1E\text{-}08x^2 - 1E\text{-}05x + 0.0315$	$R^2 = 0.2249$
2411	Flow (L/s)	$y = 1E\text{-}08x^2 - 3E\text{-}05x + 0.02$	$R^2 = 0.3146$
2524	Flow (L/s)	$y = 2E\text{-}08x^2 - 2E\text{-}05x + 0.0065$	$R^2 = 0.2668$
2866	Flow (L/s)	$y = 8E\text{-}09x^2 - 2E\text{-}05x + 0.0154$	$R^2 = 0.2432$
Y Peak m/z (Relative Intensity)	**X**	**Equation**	
813	N-NH4+ (µg/L)	$y = 1E\text{-}05x^2 – 0.0022x + 0.1245$	$R^2 = 0.2996$
1041	N-NH4+ (µg/L)	$y = -0.0006x + 0.1097$	$R^2 = 0.2533$
1155	N-NH4+ (µg/L)	$y = 2E\text{-}05x^2 – 0.0028x + 0.1808$	$R^2 = 0.413$
1383	N-NH4+ (µg/L)	$y = 8E\text{-}06x^2 – 0.0006x + 0.1133$	$R^2 = 0.2784$
1497	N-NH4+ (µg/L)	$y = 2E\text{-}06x^2 - 4E\text{-}05x + 0.1039$	$R^2 = 0.2163$
1953	N-NH4+ (µg/L)	$y = -5E\text{-}06x^2 + 0.0008x + 0.0188$	$R^2 = 0.215$
2181	N-NH4+ (µg/L)	$y = -8E\text{-}06x^2 + 0.0012x – 0.011$	$R^2 = 0.331$

Y Peak m/z (Relative Intensity)	X	Equation	
1070	DIN (µg/L)	$y = 5E\text{-}11x^2 + 3E\text{-}07x + 0.0022$	$R^2 = 0.3766$
2181	DIN (µg/L)	$y = 0.004\ln(x) - 0.0018$	$R^2 = 0.2843$
2411	DIN (µg/L)	$y = 0.0032\ln(x) - 0.0083$	$R^2 = 0.3182$
2643	DIN (µg/L)	$y = 8E\text{-}11x^2 - 1E\text{-}07x + 0.0059$	$R^2 = 0.2645$
Y Peak m/z (Relative Intensity)	**X**	**Equation**	
1041	SRP (µg/L)	$y = 0.0003x^2 - 0.0036x + 0.0723$	$R^2 = 0.2472$
1155	SRP (µg/L)	$y = 0.0005x^2 - 0.0072x + 0.0996$	$R^2 = 0.3448$
1383	SRP (µg/L)	$y = -0.0006x^2 + 0.0107x + 0.0844$	$R^2 = 0.7497$
1725	SRP (µg/L)	$y = -0.0003x^2 + 0.0048x + 0.0683$	$R^2 = 0.3317$

Chapter 4

Capítulo 4. MALDI-TOF MS Imaging evidences spatial differences in the degradation of solid polycaprolactone diol in water under aerobic and denitrifying conditions

This chapter is based on the article:

Rivas D, Ginebreda A, Pérez S, Quero C, Barceló D. MALDI-TOF MS Imaging evidences spatial differences in the degradation of solid polycaprolactone diol in water under aerobic and denitrifying conditions. Science of The Total Environment 2016; 566–567: 27-33.

4.1 Highlights

• Solid polycaprolactone diol degrades when exposed to different water environments.

• Major changes occurred under denitrifying conditions.

• Degradation of a solid oligomer in water is studied by MALDI IMAGING technique.

• MALDI IMAGING enables visualizing changes occurred on the sample surface.

4.2 Abstract

Degradation of solid polymers in the aquatic environment encompasses a variety of biotic and abiotic processes giving rise to heterogeneous patterns across the surface of the material, which cannot be investigated using conventional Matrix-assisted laser desorption ionization time-of-flight mass spectrometry (MALDI-TOF-MS) that only renders an "average" picture of the sample. In that context, MALDI-TOF MS Imaging (MALDI MSI) provides a rapid and efficient tool to study 2D spatial changes occurred in the chemical composition of the polymer surface.

Commercial polycaprolactone diol (average molecular weight of 1250 Da) was selected as test material because it had been previously known to be amenable to biological degradation. The test oligomer probe was incubated under aerobic and denitrifying conditions using synthetic water and denitrifying mixed liquor obtained from a wastewater treatment plant respectively. After ca. seven days of exposure the mass spectra obtained by MALDI MSI showed the occurrence of chemical modifications in the sample surface. Observed heterogeneity across the probe's surface indicated significant degradation and suggested the contribution of biotic processes. The results were investigated using different image processing tools. Major changes on the oligomer surface were observed when exposed to denitrifying conditions.

4.3 Graphical Abstract

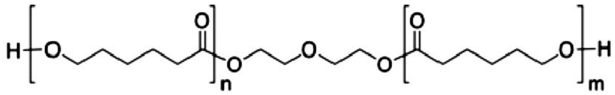

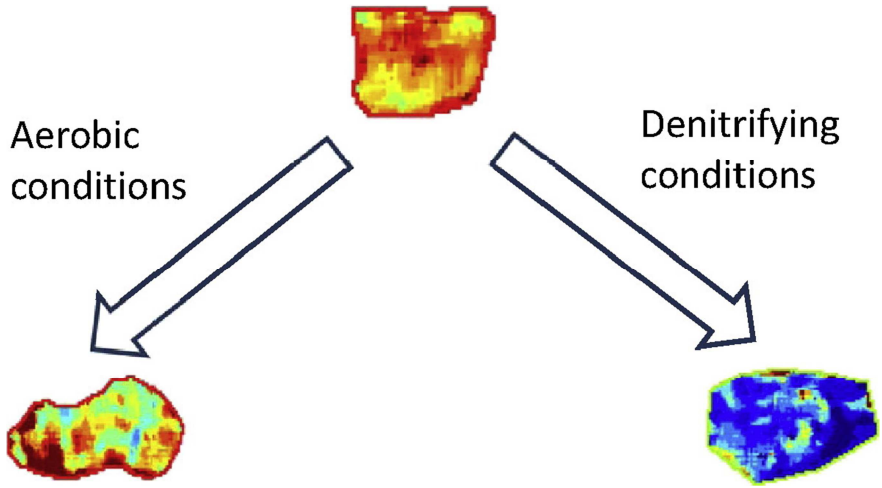

4.4 Introduction

There is an increasing concern on the effects caused by synthetic polymers in the environment. Most of today's synthetic polymers are persistent (Eubeler et al., 2009) thus generating significant sources of environmental pollution potentially harmful to wildlife when they are dispersed in nature (Scott, 2000). For example, the disposal of non-degradable plastic bags adversely affects sea-life (Siracusa et al., 2014). It is widely accepted that the use of long-lasting polymers in products with a short life-span, such as engineering applications, packaging, catering, surgery, and hygiene, is not environmentally adequate (Siracusa et al., 2008). Moreover, incineration of plastic waste is often limited due to economic viability (Li et al., 1995) and in certain cases may give rise to toxic emissions of environmental concern. On the other hand, plastic recycling shows a negative eco-balance in nearly all cases as well. As plastics represent a large part of the waste collection at the local, regional, and national levels, institutions are now aware of the significant savings that compostable or biodegradable materials would generate (Gross and Kalra, 2002). Therefore

replacement of conventional plastic by degradable polymers, particularly for short-term applications (packaging, biomedicine) (Baruah and Dutta, 2009; Silvestre et al., 2011), is of major interest to the society. However, till now, degradable polymers have not found extensive applications to largely replace conventional plastic materials, reasons being their high production costs and sometimes their inadequate properties (Narayan, 2001). Therefore, investigation of polymer degradation has become a topic of major interest.

Polymer degradation encompasses a variety of abiotic (mechanical, thermal, chemical, photolysis) and biotic (biodeterioration, biofragmentation) degradation processes that might take place simultaneously (Göpferich, 1996; Molero et al., 2008). Studies of polymer degradation include both the measurement of physical-chemical and rheological properties, such as intrinsic viscosities and average molecular weights (Pitt and Zhong-wei, 1987), and the use of chemical analytical methods as well. The most commonly used analytical techniques for monitoring the degradation of polymers include GC–MS, LC-MS, NMR and Matrix-assisted laser desorption ionization time-of-flight mass spectrometry (MALDI-TOF MS) (Eubeler et al., 2009). These techniques give information on the molecular structure of polymers, and allow observing the changes occurred over time. MALDI-TOF MS, first developed to study peptides and proteins has also been applied to synthetic polymers analysis (Favier et al., 2004). This technique allows the analysis of polymers with very different absolute molecular weight, although for an optimal characterization, this technique requires that the polymer has a relatively low mass in order to obtain high resolution and good mass accuracy (Nielen, 1999; Schriemer and Li, 1996). MALDI-TOF MS is ideally suited for polymer analysis because of simple acquisition of the mass spectra which show mainly single-charged quasi-molecular ions with hardly any fragmentation (Rizzarelli and Carroccio, 2014). Simple sample preparation, fast analysis times, the variety of available matrices and low sample consumption are other advantages of this technique (Montaudo et al., 2006). Despite these advantages, MALDI-TOF MS has been seldom used in the study of polymer degradation in water. For example some authors studied the hydrolytic degradation of poly (ethylene terephthalate) by MALDI-MS in water (Weidner et al., 1997). The aerobic biodegradation of poly(vinylpyrrolidone) polymer was monitored on a laboratory-scale fixed-bed bioreactor run with river water applying MALDI-TOF MS (Trimpin et al., 2001).

All the foregoing analytical methods (NMR, GC–MS, LC-MS and MALDI-TOF-MS) are reliable but they involve a homogenization step so that they yield only information

relative to the sample under study as a whole. In other words, the spatial information is lost. In contrast, biological mediated processes tend to proceed on a rather heterogeneous way across space, so that their proper characterization requires the use of imaging techniques. MALDI MS Imaging (MALDI MSI) consists of the use of MALDI as a mass spectrometry imaging technique. The sample is scanned in two dimensions at a preselected spatial resolution while the mass spectrum is recorded. Advantages, like measuring the spatial distribution of a large number of analytes almost simultaneously without destroying the sample, make it a useful method in solid-surface study (Crecelius et al., 2014). Other technical and operational advantages of MALDI MSI deserving to be mentioned include fastness, robustness and direct analysis of samples, thus introducing a minimum perturbation on the structure. However, the analytical process requires some optimization regarding sample preparation and matrix selection and deposition (Kaletaş et al., 2009; Fröhlich et al., 2014; Crecelius et al., 2014; Klerk et al., 2007; Astigarraga et al., 2008).

The present study aims at exploring the possibilities of MALDI MSI as a semi-quantitative and qualitative method for the study of polymer degradation in water under different environmental conditions, namely aerobic and denitrifying conditions. To that end, synthetic river water and denitrifying mixed liquor obtained from a wastewater treatment plant (WWTP) were used. Polycaprolactone diol, aliphatic polyester, was selected as testing material owing to its physical-chemical properties, commercial affordability and degradability.

4.5 Methods

4.5.1 Materials

Polycaprolactonediol homopolymer (MW = 1250 Da) used in the degradation experiments was purchased from Polysciences (Warrington, USA). The matrix trans-2-[3-(4-tert-Butylphenyl)-2-methyl-2-propenylidene]malononitrile (DCTB) was purchased from Aldrich (Steinheim, Germany).

The caps units were purchased from Exposmeter AB (Tavelsjo, Sweden). Each capsule unit consists of a plastic piston and a plastic cap with a window 2 cm in diameter.

4.5.2 Degradation experiments

Degradation experiments were carried out by placing capsules filled with polycaprolactonediol (3–6 g) in the reactors under two different water conditions, as explained below.

4.5.3 Aerobic conditions

To simulate the degradation conditions on a real an artificial stream (mesocosm) located at the indoor Experimental Streams Facility of the Catalan Institute for Water Research (Girona, Spain) was used.

Physicochemical conditions were designed to mimic those of natural streams. The artificial stream was 2 m long, had a rectangular cross-section of 50 cm^2 and was set up as an open system with constant slope and steady, uniform flow. Artificial stream operated with water with a constant flow of 60 mL s^{-1}, resulting in mean water velocity of 0.88 ± 0.03 cm s^{-1}, and a water depth over the plane bed between 2.2 and 2.5 cm. The artificial stream was filled with approximately 100 L of sand (mean diameter = 0.37 mm). Sand was sterilized in a Presoclave-II 30 L autoclave (120 °C for 20 min) (JP Selecta S.A., Barcelona, Spain), then it was evenly distributed in the artificial stream to create a plane bed that facilitated the growth of the epipsammic biofilm. Biofilm inocula were obtained from an unpolluted segment of Segre River (Puigcerdà, Girona, Spain), after scraping 10–12 cobbles. New inocula were provided twice a week to each channel during the firsts 3 weeks of the colonization period.

Source water for the artificial stream was rainwater collected in a tank before being filtered through activated carbon filters. Concentrations of phosphate and ammonium were raised as average (0.022 mg L^{-1} $P\text{-}PO_4^{3-}$ and 0.014 mg L^{-1} $N\text{-}NH_4^+$), by means of injection of concentrated solutions (KH_2PO_4 and NH_4Cl, respectively) and using a peristaltic pump (IPC Ismatec, Glattbrugg, Switzerland). Daily cycles of photosynthetic active radiation (PAR) were defined as 9-h daylight + 15-h darkness. PAR was held constant at 150 μE m^{-2} s^{-1} during the daytime. Water temperature was held constant at 20 °C by means of a cryo-compact circulator (Julabo CF-31, Seelbach, Germany). Total exposure time was 5 days.

4.5.4 Denitrifiying Conditions

To compare aerobic and anaerobic denitrifying degradation conditions, liquor collected from the denitrifying tank of a nearby WWTP was used. The capsules filled with polycaprolactonediol (3–6 g per capsule) were placed in a 5 L Erlenmeyer flask filled with 2.5 L of denitrifying liquor agitated with a magnetic stirrer. Anaerobic conditions were ensured by keeping the system under a stream of nitrogen. When necessary (day 3), the concentration of nitrate was increased by injecting a solution of $NaNO_3$ at a concentration of 50 mg L^{-1}. The oxygen concentration was monitored using a portable oximeter probe (Ysi Inc., Ohio, United States) to maintain the anaerobic denitrifying conditions along the experiment. After a total exposure time of 7 days, samples were collected and processed as explained below (Section 4.6).

Moreover, in both experiments the following parameters were monitored: temperature, pH, conductivity, dissolved oxygen, nitrates and nitrites (see Supplementary data Tables S4.1 and S4.2).

4.6 MALDI MSI

4.6.1 Sample preparation

For MALDI-TOF measurements, the tested oligomer was taken out from the capsules and dried in a desiccator for 15 min. Slices of 14–16 μm were cut in a cryo-microtome and placed onto indium-tin oxide (ITO) coated glass slides (Sigma Aldrich). The samples were placed in a desiccator for 15 min before sublimation. The matrix was coated using a sublimation device (Fisher Scientific, Madrid, Spain) using 30 mg DCTB. Sublimation conditions were 100 mTorr pressure at 140 °C during 15 min. Sample slice was externally cooled with ice.

4.6.2 Mass spectrometry

All experiments were performed using an AutoFlex III MALDI-TOF/TOF instrument (Bruker Daltonik GmbH, Bremen, Germany) equipped with a Smartbeam laser at 200 Hz laser at the "medium focus" setting and were controlled using FlexControl 3.0 (Bruker Daltonik GmbH, Bremen, Germany).

The analytical conditions for the MALDI MSI analysis were set as follows: positive reflector ion mode; ion source 1 V, 19 kV; ion source 2 V, 16 kV; lens voltage, 8.5 kV; and mass range, m/z 600–4000. Laser irradiance was maintained slightly above

threshold. Mass spectra were acquired with spatial resolution set at 200 μm. For each pixel, 250 laser shots were measured per position as a sum of 25 consecutive laser shots in 10 random walk shot steps.

4.7 Image processing

Raw spectra were analyzed with FlexImaging 4.0 software (Bruker Daltonik GmbH, Bremen, Germany) after baseline subtraction and Root Mean Square (RMS) normalization. Ion density maps were created for ions observed from the skyline projection spectrum. Masses were manually selected with a mass accuracy set to ± 0.1% (manual peak picking). Regions of interest (ROIs) were manually defined by using both the sample image and MSI data.

Image processing and data analysis were done using different multivariate statistical treatments such as Correlation of Peaks or Hierarchical Cluster Analysis (SCiLS Lab software, Bremen, Germany) allowing identification and quantification of the altered areas.

4.8 Results and discussion

Average MALDI-TOF MS spectra (range m/z 700 to 2300) of the starting material and the two exposed samples are shown in Figs. 4.1A–C at different attenuation factors. The starting material and the sample exposed to aerobic conditions exhibit very similar mass spectra with only slight differences in the intensities of the heavier ions (Fig. 4.1A and B), thus reflecting a different distribution of the chain lengths, the latter showing a shift of the maximum towards longer chains (i.e., from m/z 1155.7 to 1383.8). Peak spacing (m/z 114.1) is consistent with increasing number of monomer units (Fig. 4.1A insert). In contrast, in the spectrum of the sample obtained under denitrifying conditions exposure (Fig. 4.1C) pronounced differences suggested the occurrence of deeper structural changes. While the peaks present in the native sample still appear, their relative intensities have changed with the maximum of distribution shifted to lower molecular weights. The presence of a second series of oligomers, likewise spaced by m/z 114.1 (m/z 1069.6, 1183.6 and 1297.7), is visible in the spectra of the original oligomer and in its degradation samples (see Fig. 4.1A, B and C). With respect to their abundance in the spectrum of the starting material (Fig. 4.1A), their relative intensities have increased during the exposure (Fig. 4.1B). These peaks could be tentatively explained by oxidation of the two terminal hydroxyl groups to

carboxylic acid of the parent peaks m/z 1041.6, 1155.7 and 1269.7 respectively, entailing a mass increment of 28. Such transformation pathway is observed, for instance, in the degradation of terminal $–CH_2OH$ groups in polyethyleneglycols (Bernhard et al., 2008; Eubeler et al., 2010). In order to gain insight into the spatial pattern of the degradation process, MALDI MSI techniques were used. They allow generating 2D images across the oligomer surface using selected ions. As an example, Fig. 4.2 A1, A2, A3 shows the images generated using the main ion of the starting material spectrum (m/z 1155.7) on the three samples analyzed. As expected, the three images show notable differences on the uniformity (homogeneity) of the spatial distribution. Whereas the starting material shows a smooth and highly homogeneous spatial distribution (Fig. 4.2 A1) there is an increasing heterogeneity when going through the aerobic conditions exposed sample (Fig. 4.2 A2) and finally to the sample kept under denitrifying conditions (Fig. 4.2 A3). In this latter case the almost total disappearance of the peak concerned is evidenced from the predominant "black" areas. Polyesters and specifically polycaprolactones are reported to undergo degradation under both aerobic and anaerobic conditions (Eubeler et al., 2010). To better investigate the changes occurred in that sample, we first proceeded to record the average spectra until lower mass ranges (Fig. 4.3A and B). The first image (Fig. 4.3A) corresponds to the spectrum of the initial polycaprolactonediol, and the second is the result after 5 days of exposure in water under denitrifying conditions (Fig. 4.3B), thus revealing several peaks: (a) those at m/z 500, 750 and 1000 which are due to the clusters formed by the matrix DCTB and (b) the standard material presents peaks at ca. m/z 462.8 and 669.7 that presumably correspond to impurities already present (Fig. 4 3A), while the sample obtained under denitrifying conditions exhibits one new peak (m/z 395.1) which could be attributed to the sodium adduct of $C_{18}H_{28}O_8$ whose possible structure is shown in Fig. 4.3B. The presence of sodium ions at m/z 23.0 is observed in both spectra as well. The practical absence of low molecular weight (i.e., below m/z 300) degradation products in the MALDI MSI spectra is likely due to their dissolution in water during exposure (Park, 1994).

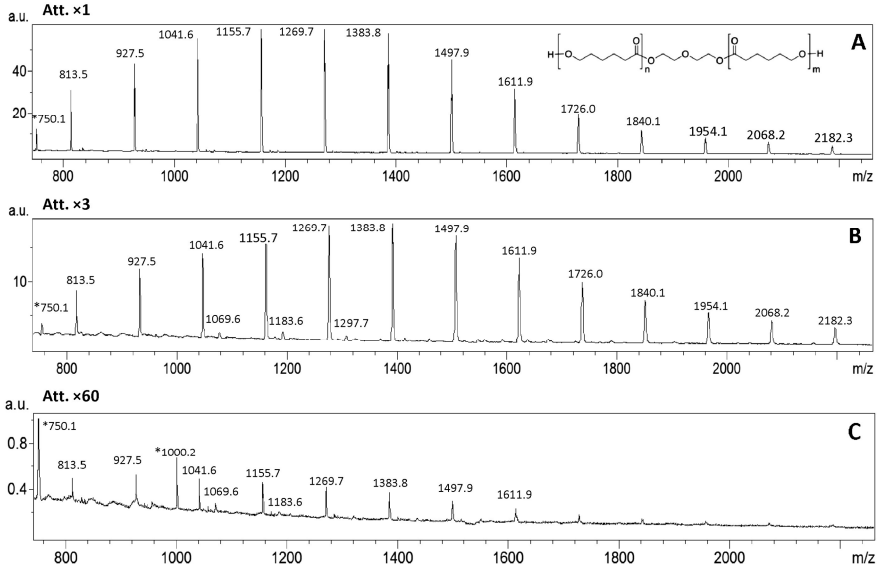

Figure 4.1: Overall average MALDI MSI spectra of polycaprolactonediol (chemical structure shown in the insert). A) Standard polycaprolactonediol; B) after 7 days of exposure in water under aerobic conditions; C) after 5 days of exposure in water under denitrifying conditions. Note that the intensity scales of the three spectra are different (i.e., different attenuation factors are used): A) × 1; B) × 3 and C) × 60. Peaks at (m/z) 750.1 and 1000.2 marked with * correspond to the matrix DCTB. Ions shown are sodium adducts $[M + Na]^+$.

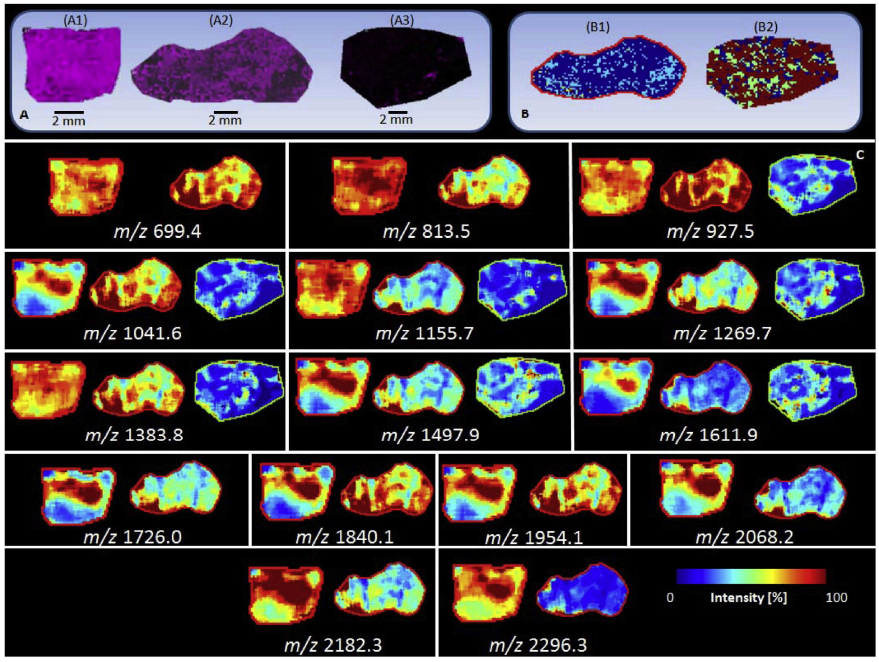

Figure 4.2: A) MALDI MSI sections plotting ion 1155.7 (m/z) (main ion of the standard). (A1) Standard polycaprolactonediol; (A2) after 7 days of exposure in water under aerobic conditions; (A3) after 5 days of exposure in water under denitrifying conditions. B) Images obtained by hierarchical cluster analysis using all ions, after data processing with Flex Imaging 4.0 software (Bruker Daltonik GmbH, Bremen, Germany). Equally colored areas denote pixels having same average spectra. (B1) after 7 days of exposure in water under aerobic conditions; (B2) after 5 days of exposure in water under denitrifying conditions. C) Comparison of images corresponding to standard, aerobic and denitrifying exposure samples using different single ions, after data processing with Flex Imaging 4.0 software (Bruker Daltonik GmbH). Some images of the denitrifying conditions sample are missing because the corresponding ion was not present. Spatial differences among pixels using the different ions are visible across the surface of the samples. Ions shown are sodium adducts $[M + Na]^+$.

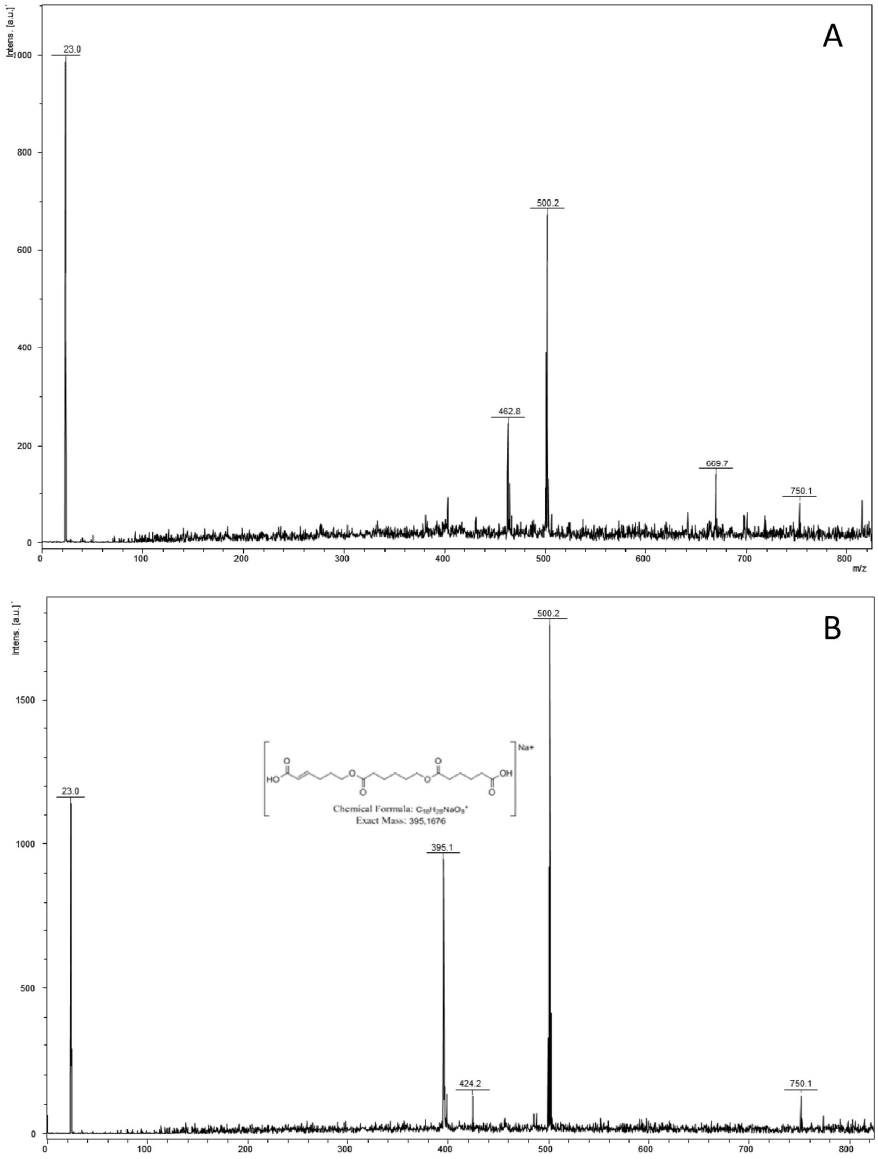

Figure 4.3: MALDI MSI average spectra obtained for the range (m/z) 0-700. (A) Starting polycaprolactonediol and (B) after 5 days of exposure in water under denitrifying conditions. Peaks at (m/z) 500.2 and 750.1 correspond to the matrix DCTB. Ions shown are sodium adducts $[M + Na]^+$. Peak at (m/z) 395.1 is tentatively attributed to the sodium adduct of $C_{18}H_{28}O_8$ (chemical structure shown in the insert).

Direct MALDI MSI images obtained as described above were improved upon treatment with image processing software (see Fig. 4.2C). These images provide ion based maps, using the intensities of the selected ion in each pixel (pixels are set at a spatial resolution of 200 × 200 μm, and for each pixel 250 random spectra are averaged). Examples of such maps using ions m/z 699.4, 813.5, 927.5, 1041.6, 1155.7, 1269.7, 1383.8, 1497.9, 1611.9, 1726.0, 1840.1, 1954.1, 2068.2, 2182.3 and 2296.3 are represented in Fig. 4.2C. They enable identifying what are the most relevant ones on each sample as well as how are spatially distributed the sites in which the degradation processes are located. Heterogeneity of the changes produced across the sample surface suggests a contribution of biotic mediated processes. The extent of the changes is maximal in the sample exposed at denitrifying conditions in which some common ions in the other two are lacking (i.e., m/z 699.4, 813.5, 1726.0, 1840.1, 1954.1, 2068.2, 2182.3, 2296.3). Furthermore, the information resulting from the whole spectra (not only a single ion) of each pixel can be combined using hierarchical cluster analysis. The so obtained clustering highlights similar areas based on spectra coincidences among pixels (i.e., equally colored areas denote pixels having same average spectra). To gain some insight on the extent of changes occurred in a given sample, correlations between the intensities of all peak pairs in each pixel were computed. The matrices of correlation coefficients for starting polymer, aerobic and denitrifying exposure are shown in Fig. 4.4 A, B and C respectively. Representative examples of such correlations using different pairs of ions are presented in Fig. 4.4D and E (the examples given correspond to correlations between ions m/z 1269.7 vs. m/z 1041.6 and 1611.9 vs. m/z 1041.6 and are traced in the corresponding correlation matrices by a colored circle; every pixel is represented by a '×' in the plot). Increasing heterogeneity among pixels translates into decreasing correlation coefficients (taking as reference those of the starting reference material). In general the correlations followed, as expected, the rank starting material > anaerobic > denitrifying. This provides a semi-quantitative measure of the extent of changes occurred in the oligomer surface, thus confirming that the sample exposed to denitrifying conditions has undergone the greatest structural transformations.

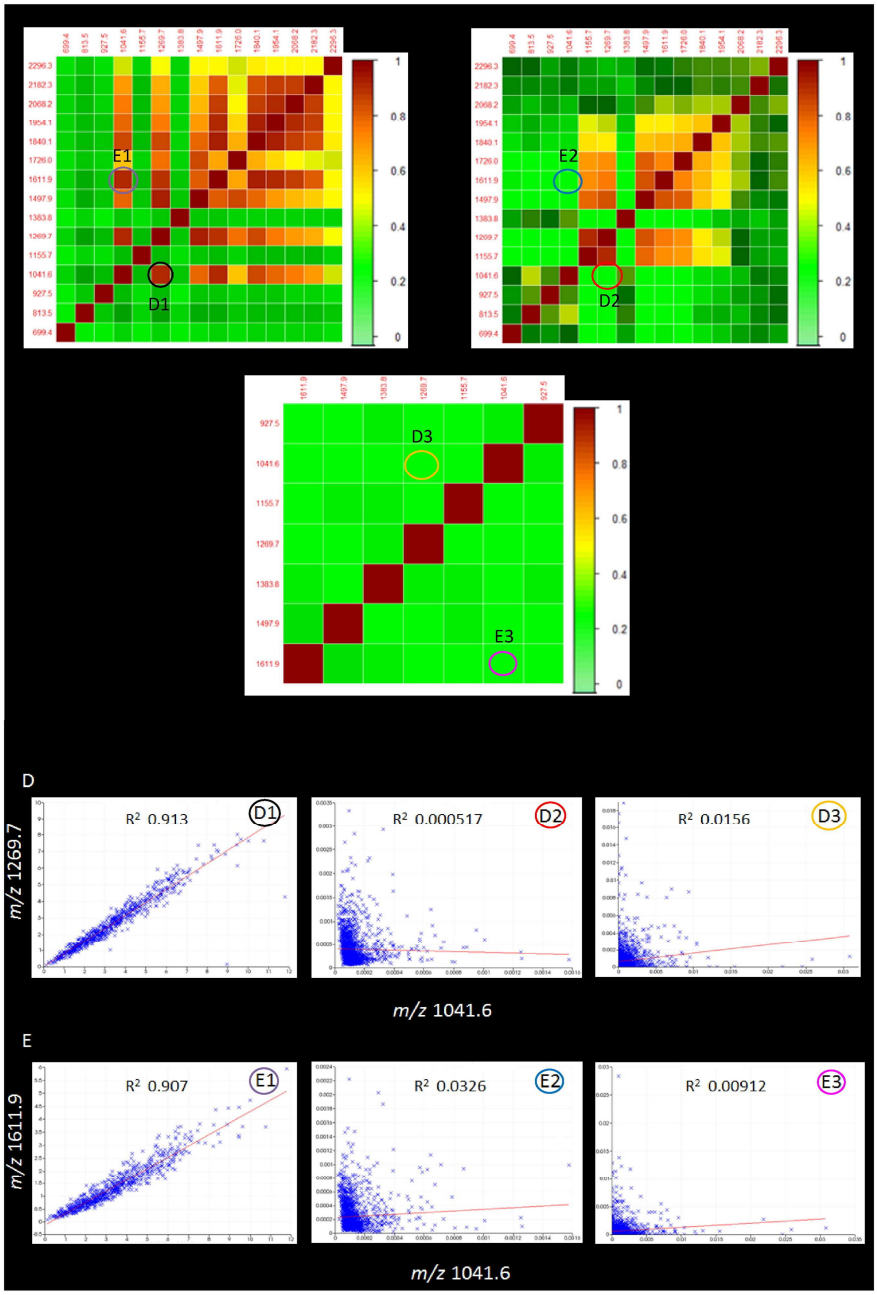

Figure 4.4: Matrices of correlation coefficients between ion pairs in the pixels of a given sample. Correlations are obtained using the intensities of the respective peak pairs of all pixel spectra recorded for the sample concerned. (A) Standard polycaprolactonediol; (B) after 7 days of exposure in water under aerobic conditions; (C) after 5 days of exposure in water under denitrifying conditions. Selected examples of the correlation plots are shown

in panels D and E (examples deployed are circled in the corresponding correlation matrices A, B, C): Correlation plots between ion m/z 1269.7 vs. ion m/z 1041.6 (plots D1, D2 and D3) and ion m/z 1611.9 vs.1041.6 (plots E1, E2, E3). Every pixel is indicated with a colored circle on the plots. (D1) and (E1) Standard polycaprolactonediol; (D2) and (E2) after 7 days of exposure in water under aerobic conditions; (D3) and (E3) after 5 days of exposure in water under denitrifying conditions. Correlation plots were obtained using Flex Imaging 4.0 software (Bruker Daltonik GmbH, Bremen, Germany).

4.9 Conclusions

MALDI MSI reveals as a rapid and efficient tool to investigate structural changes occurred across the surface of a polyester oligomer exposed to different aquatic environments. The resulting images indicate that the degradation proceeds on a rather spatial heterogeneous manner, thus supporting the contribution of biotic processes. Moreover, MALDI MSI allows to clearly differentiating (qualitatively and semi-quantitatively) in terms of chemical structure changes between aerobic and denitrifying conditions. Further work is in progress.

4.10 Acknowledgements

This study has been financially supported by the EU through the FP7 project GLOBAQUA (Grant agreement No 603629), and by the Generalitat de Catalunya (Consolidated Research Groups “2014 SGR 418—Water and Soil Quality Unit” and "2014 SGR 291—ICRA"). It reflects only the author's views. The Community is not liable for any use that may be made of the information contained therein. The authors are thankful to Dr. P. Eichhorn for his critical reading of the manuscript and the valuable comments provided and to Maria Casellas (Experimental Streams Facility, Catalan Institute for Water Research, Girona, Spain) for her technical help in the operation of the artificial stream.

4.11 References Chapter 4

Astigarraga E, Barreda-Gómez G, Lombardero L, Fresnedo O, Castaño F, Giralt MT, et al. Profiling and Imaging of Lipids on Brain and Liver Tissue by Matrix-Assisted Laser Desorption/Ionization Mass Spectrometry Using 2-Mercaptobenzothiazole as a Matrix. Analytical Chemistry 2008; 80: 9105-9114.

Baruah S, Dutta J. Nanotechnology applications in pollution sensing and degradation in agriculture: a review. Environmental Chemistry Letters 2009; 7: 191-204.

Bernhard M, Eubeler JP, Zok S, Knepper TP. Aerobic biodegradation of polyethylene glycols of different molecular weights in wastewater and seawater. Water Research 2008; 42: 4791-4801.

Crecelius AC, Vitz J, Schubert US. Mass spectrometric imaging of synthetic polymers. Analytica Chimica Acta 2014; 808: 10-17.

Eubeler JP, Bernhard M, Knepper TP. Environmental biodegradation of synthetic polymers II. Biodegradation of different polymer groups. TrAC Trends in Analytical Chemistry 2010; 29: 84-100.

Eubeler JP, Zok S, Bernhard M, Knepper TP. Environmental biodegradation of synthetic polymers I. Test methodologies and procedures. TrAC - Trends in Analytical Chemistry 2009; 28: 1057-1072.

Favier A, Ladavière C, Charreyre M-T, Pichot C. MALDI-TOF MS Investigation of the RAFT Polymerization of a Water-Soluble Acrylamide Derivative. Macromolecules 2004; 37: 2026-2034.

Fröhlich SM, Archodoulaki V-M, Allmaier G, Marchetti-Deschmann M. MALDI-TOF Mass Spectrometry Imaging Reveals Molecular Level Changes in Ultrahigh Molecular Weight Polyethylene Joint Implants in Correlation with Lipid Adsorption. Analytical Chemistry 2014; 86: 9723-9732.

Göpferich A. Mechanisms of polymer degradation and erosion. Biomaterials 1996; 17: 103-114.

Gross RA, Kalra B. Biodegradable Polymers for the Environment. Science 2002; 297: 803-807.

Kaletaş BK, van der Wiel IM, Stauber J, Lennard JD, Güzel C, Kros JM, et al. Sample preparation issues for tissue imaging by imaging MS. PROTEOMICS 2009; 9: 2622-2633.

Klerk LA, Broersen A, Fletcher IW, van Liere R, Heeren RMA. Extended data analysis strategies for high resolution imaging MS: New methods to deal with extremely large image hyperspectral datasets. International Journal of Mass Spectrometry 2007; 260: 222-236.

Li C-T, Lee W-J, Mi H-H, Su C-C. PAH emission from the incineration of waste oily sludge and PE plastic mixtures. Science of The Total Environment 1995; 170: 171-183.

Molero C, de Lucas A, Rodríguez JF. Recovery of polyols from flexible polyurethane foam by "split-phase" glycolysis: Study on the influence of reaction parameters. Polymer Degradation and Stability 2008; 93: 353-361.

Montaudo G, Samperi F, Montaudo MS. Characterization of synthetic polymers by MALDI-MS. Progress in Polymer Science 2006; 31: 277-357.

Narayan R. Drivers for biodegradable/compostable plastics and role of composting in waste management and sustainable agriculture. Bioprocessing of Solid Waste and Sludge 2001; 11.

Nielen MWF. Maldi time-of-flight mass spectrometry of synthetic polymers. Mass Spectrometry Reviews 1999; 18: 309-344.

Park TG. Degradation of poly(d,l-lactic acid) microspheres: effect of molecular weight. Journal of Controlled Release 1994; 30: 161-173.

Pitt CG, Zhong-wei G. Modification of the rates of chain cleavage of poly(ϵ-caprolactone) and related polyesters in the solid state. Journal of Controlled Release 1987; 4: 283-292.

Rizzarelli P, Carroccio S. Modern mass spectrometry in the characterization and degradation of biodegradable polymers. Analytica Chimica Acta 2014; 808: 18-43.

Scott G. 'Green' polymers. Polymer Degradation and Stability 2000; 68: 1-7.

Schriemer DC, Li L. Detection of High Molecular Weight Narrow Polydisperse Polymers up to 1.5 Million Daltons by MALDI Mass Spectrometry. Analytical Chemistry 1996; 68: 2721-2725.

Silvestre C, Duraccio D, Cimmino S. Food packaging based on polymer nanomaterials. Progress in Polymer Science 2011; 36: 1766-1782.

Siracusa V, Ingrao C, Lo Giudice A, Mbohwa C, Dalla Rosa M. Environmental assessment of a multilayer polymer bag for food packaging and preservation: An LCA approach. Food Research International 2014; 62: 151-161.

Siracusa V, Rocculi P, Romani S, Rosa MD. Biodegradable polymers for food packaging: a review. Trends in Food Science & Technology 2008; 19: 634-643.

Trimpin S, Eichhorn P, Räder HJ, Müllen K, Knepper TP. Recalcitrance of poly(vinylpyrrolidone): evidence through matrix-assisted laser desorption–ionization time-of-flight mass spectrometry. Journal of Chromatography A 2001; 938: 67-77.

Weidner S, Kuehn G, Werthmann B, Schroeder H, Just U, Borowski R, et al. A new approach of characterizing the hydrolytic degradation of poly (ethylene terephthalate) by MALDI-MS. Journal of Polymer Science Part A: Polymer Chemistry 1997; 35: 2183-2192.

4.12 Supporting information

Table S4.1. Parameters monitored daily in during the aerobic conditions exposure experiment.

Ti	(µS cm⁻¹)		(°C)	(mg L⁻¹)	(mg L⁻¹)	(%)	(mg N L⁻¹)	(mg P L⁻¹)	(mg N L⁻¹)
1	319	8,53	20,5	3,324	10,5	116,6	1,992	0,007	<LOQ
2	360	8,40	20,2	2,980	8,8	100,5	2,423	0,038	0,035
3	357	8,38	20,5	3,149	9,9	111,8	2,069	0,012	0,005
4	351	8,26	20,6	3,065	10,1	115,2	2,185	0,026	0,027
5	336	8,37	20,5	4,679	10,2	114,3	1,671	0,026	<LOQ

a) Dissolved Organic Carbon

Table S4.2. Parameters monitored daily during the denitrifying conditions exposure experiment.

Time (days)	Conductivity (µS cm^{-1})	pH	Temperature (ºC)	Oxygen (mg L^{-1})	Oxygen (%)	ORP (mV)	$N\text{-}NO_3$ (mg N L^{-1})	(mg N L^{-1})
1	n.a.	n.a.	19,9	n.a.	n.a.	n.a.	13	<LOQ
2	1916	6,74	19,4	<LOQ	<LOQ	-119,8	25	1
3	2213	7,57	22,7	<LOQ	<LOQ	-140,5	25	1
4	2185	6,89	22,8	<LOQ	<LOQ	-214,0	50	40
5	2154	6,69	21,5	<LOQ	<LOQ	-277,3	50	40
6	2207	6,85	22,6	<LOQ	<LOQ	-278,4	25	20
7	2301	6,89	23,5	<LOQ	<LOQ	-293,7	25	10

Chapter 5

Capítulo 5. Using MALDI-TOF MS imaging and LC-HRMS for the investigation of the degradation of polycaprolactone diol exposed to different wastewater treatments

This chapter is based on the article:

Rivas D, Zonja B, Eichhorn P, Ginebreda A, Pérez S, Barceló D. Using MALDI-TOF MS imaging and LC-HRMS for the investigation of the degradation of polycaprolactone diol exposed to different wastewater treatments. Analytical and Bioanalytical Chemistry 2017: 1-11.

5.1 Highlights

• Solid polycaprolactone diol degrades when exposed to different water environments.

• Major changes occurred under denitrifying conditions.

• Degradation of a solid oligomer in water is studied by MALDI IMAGING technique.

• MALDI IMAGING enables visualizing changes occurred on the sample surface.

5.2 Abstract

Polymers are used in high amounts in a wide range of applications from biomedicine to industry. Because of the growing awareness of the increasing amounts of plastic wastes in the aquatic environment during recent years, the evaluation of their biodegradability deserves special attention. In the past, most efforts were dedicated to studying the biodegradation of polyesters in soil and compost, while very little research has been conducted on their fate in wastewater. Here, we assessed the ability of bacterial communities residing in the aerobic and denitrification tank from a wastewater treatment plant (WWTP) to degrade the polymeric ester polycaprolactone diol (PCLD; average molecular weight of 1250 Da). Following the incubation of the solid polymer in WWTP tanks, matrix-assisted laser desorption/ionization-mass spectrometry imaging (MALDI-MSI) was used to provide evidence for hydrolytic reactions and to study differences in the spatial degradation on the PCLD surface. It was demonstrated that regardless of the wastewater type, the chemical structure on the PCLD surface underwent modifications after 7 days of exposure. Apart from the parent PCLD peak series in MALDI-MSI mass spectra, the presence of a second oligomer series with mass peaks spaced by m/z 114 (as in PCLD) was observed. It was proposed to correspond to polycaprolactone (PCL) originating from the hydrolytic cleavage of the diethylene glycol from PCLD. Their ion masses were detected at m/z 104 below the PCLD peaks and their structures were proposed as PCL cyclized oligomers. Differences in the spatial distribution of low MW ions (<800) between the aerobic and denitrifying exposed samples in MALDI MSI were also noticeable. While the ions at m/z 221.1, 247.1 and 449.2 predominated in the aerobic exposed sample, those at m/z 475.5 and 677.4 were characteristic of the denitrifying one. The MALDI-MSI measurements in the low mass range were complemented with LC-HRMS analysis to determine plausible structures of the major degradation products. Ten transformation products (TPs) were detected in the denitrifying wastewater experiment, five of them were the result of ester hydrolysis forming caprolactone oligomers (TPs 220, 334, 448, 562, and 676) while the other series corresponded to formation of PCL chain with a terminal diethylene glycol, likewise formed by ester hydrolysis (TPs 246, 360, 474, 588, and 702).

5.3 Graphical Abstract

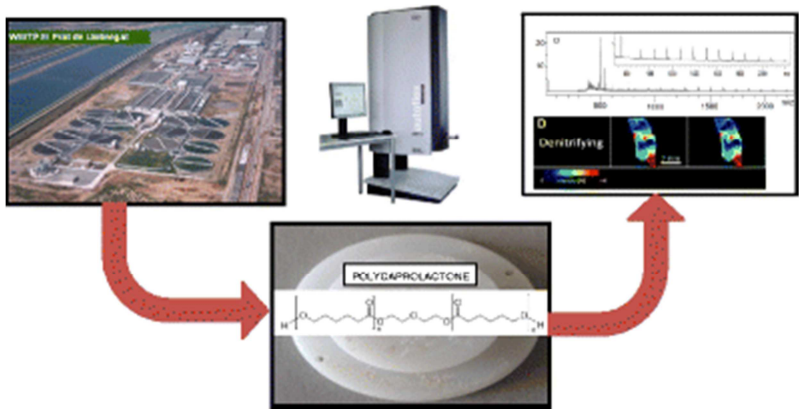

Figure 5.1: Investigation of the polymer degradation in WWTPs by MALDI-MSI and LC-HRMS

5.4 Introduction

Polycaprolactone diol (PCLD) is an aliphatic polyester in which two polycaprolactone (PCL) chains are linked via a diethylene glycol molecule. The low molecular weight PCLD is widely used in the manufacture of biodegradable polyurethanes [1, 2]. From the point of view of stability, PCLD is known be to biodegradable making it attractive for specific applications in biomedicine, e.g., drug delivery, in medical devices, and as degradable sutures [3, 4, 5]. Recently, PCL-related polymers have been proved useful as carbon source and biofilm carrier for denitrifying microorganisms in tertiary wastewater treatments [6]. Thus, they can directly contribute to the release of synthetic polymers in wastewater treatment plants (WWTP). WWTPs essentially consist of a sequence of treatment steps designed to remove both organic matter and nutrients. Typically, they include a biological treatment under aerobic conditions designed to reduce organic load, followed by a tertiary treatment with nitrification/denitrification process to remove ammonium and nitrate. Each treatment step is characterized by specific conditions (aerobic or anoxic), which result in the development of adapted microorganisms consortia [7]. It is well known that the degradation pathways and kinetics of synthetic organic compounds largely depend on the conditions (aerobic or anaerobic) under which the wastewater bacteria are striving. For instance, synthetic polyesters have been reported to display higher degradation rates under aerobic conditions than under anaerobic ones [6, 7, 8, 9].

Table 5.1: High mass range (MW > 800 Da) transformation product structures identified by in the different polymer samples studied. Structures on the right column are those of the starting polycaprolactone diol (PCLD) polymer, while those in the left column correspond to polycaprolactone (PCL) polymer formed as transformation product under denitrifying conditions

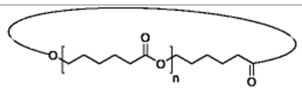		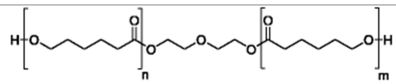	
m/z of $[M+Na]^+$	**n+1**	***m/z of* $[M+Na]^+$**	**n+m**
		813.5	6
822.6	7	927.5	7
937.4	8	1041.6	8
1051.6	9	1155.7	9
1165.2	10	1269.7	10
1278.3	11	1383.8	11
1393.2	12	1497.9	12
1506.6	13	1611.9	13
1621.0	14	1726.0	14
1736.0	15	1840.1	15
1850.1	16	1954.1	16
1963.3	17	2068.2	17
2077.7	18	2182.3	18
2192.2	19	2296.3	19
2306.5	20	2411.2	20
2420.9	21	2524.9	21
2536.8	22	2640.8	22
2650.2	23	2754.2	23

Table 5.2: Low mass transformation product structures identified by either LC-HRMS, MALDI MSI or both in the different polycaprolactone diol samples studied

m/z of $[M+H]^+$	Error	Detected by LC-HRMS	Detected by MALDI-MSI	Sterile control	Aerobic wastewater	Denitrifying wastewater
221.1382	−0.7	X	X		X	X
247.1538	−0.7	X	X		X	X
335.2059	−1.7	X (2)[a]	X		X	X
					X	X
361.2214	−1.8	X			X	X
449.2738	−1.6	X (2)[a]	X		X	X
					X	X
475.2897	−1.0	X	X		X	X
					X	X
563.342	−1.0	X (3)[a]	X		X	X
					X	X
589.3577	−0.9	X			X	X
						X
677.4101	−0.8	X (3)[a]	X			X
						X
703.4255	−1.1	X			X	X

[a]Number of peaks

A plethora of mass spectrometric analytical techniques have been used for evaluating the degradation of synthetic polymers [10]. The main drawback of the techniques used to date (gas chromatography coupled to mass spectrometry (MS), liquid chromatography-MS, and matrix-assisted laser desorption/ionization time of flight MS (MALDI-ToF-MS) is the loss of spatial information that occurs in the preparation of a liquid sample (extract). This loss is due to the homogenization and dissolution of the sample, a step that can be obviated by employing MALDI-MS imaging (MALDI MSI) on the intact solid sample. By two-dimensional scanning of the sample surface with the laser beam following deposition of a suitable matrix, analyte ions are being desorbed from the surface and extracted into the ToF analyzer for mass spectral recording. Due to the large m/z operating range of the ToF-MS, high molecular weight components of the polymer under investigation can easily be studied. Characterization of polymers [11], polymeric dialyzer membranes [12], and polymers used for joint implants [13] have been performed by MALDI-ToF-MSI. However, the

accuracy of MALDI average molecular weights has often been discussed. When MALDI-ToF-MSI is compared to high-resolution MS (HRMS) instruments commonly used in environmental laboratories for identification of small molecules, e.g., Orbitrap-MS [14], it presents limited MS/MS capability relative to its lower mass resolving power and mass accuracy [15].

Several studies have evaluated the biodegradability of polymers in soil, compost [6], wastewaters [16], and marine environments [17]; however, less attention has been paid to the biodegradation of polyesters in wastewaters. Recently, we performed a comparative study on the degradation of a polyester, PCLD, in two aquatic environments, a river and a laboratory mesocosm, applying MALDI-ToF-MS [18]. In a follow-up study [19], we explored the capability of MALDI-MSI as an analytical tool for investigating modifications in the chemical composition at the polymer surface after exposure to either sterile, aerobic, or denitrifying conditions, using PCLD as a probe polymer. Whereas the acquisition of the MALDI mass spectral data and the subsequent image processing proved a powerful technique for studying 2D spatial degradation patterns of the polymer surface, its mass resolution capability turned out to be insufficient for assigning chemical structures to the mass peaks attributed to a series of emerging transformation products [20]. This limitation prompted us to undertake a third study of PCLD degradation exploiting in parallel the spatial capabilities of MALDI-MSI and the identification power of LC-HRMS [11].

The objective of the present study was to investigate the degradation of PCLD following exposure to wastewater bacteria in the aerobic and denitrifying reactor tanks of a municipal WWTP. We set out to identify the chemical changes in the polymer structure leading to degradation products and to determine their spatial distribution on the surface. This was accomplished by making use of LC-HRMS and MALDI-MSI, respectively.

5.5 Materials and methods

5.5.1 Chemical reagents and materials

Polycaprolactone diol homopolymer (average MW = 1250 Da) used in the degradation experiments was purchased from Polysciences (Warrington, PA, USA). The matrix trans-2-[3-(4-tert-butylphenyl)-2-methyl-2-propenylidene] malononitrile (DCTB) was purchased from Aldrich (Steinheim, Germany). PCLD was placed in the capsule units (Lancaster, UK) used as polymer holders in the biodegradation experiments; they were

purchased from Exposmeter AB (Tavelsjo, Sweden). Each capsule unit consisted of a plastic piston and a plastic cap with a window 2 cm in diameter (see Electronic Supplementary Material (ESM), Fig. 5S1). Acetonitrile and water were purchased from Fisher Scientific (Geel, Belgium). Formic acid (98–100%) was ACS grade and purchased from Sigma-Aldrich (Schnelldorf, Germany).

5.6 Degradation experiments

5.6.1 Wastewater treatment plant

The wastewater generated by the southern district of Barcelona reaches the WWTP located in Prat de Llobregat (see ESM, Fig. 5.S2) through several pumping stations after a pretreatment for the elimination of sand and grease it passes through an activated sludge biological treatment plant. About 60% of the treated water is discharged into the sea through 3.2 km long emissary. The remaining 40% is subjected to tertiary treatment for nutrient removal and subsequent reuse (environmental flow and irrigation). Main technical characteristics of the plant are reported in the ESM, Table 5.S1.

5.6.2 Degradation experiments in WWTP

Degradation experiments were carried out by placing three capsules filled with PCLD (3–6 g) in the secondary (aerobic) and denitrifying reactors. Samples were collected after 7 days of exposure and analyzed as explained below. Moreover, the following parameters were routinely monitored as part of the regular in-process operational WWTP control: suspended solid, BOD, COD, nitrates, nitrites, phosphor, nitrogen, conductivity, and pH. Data corresponding to the days in which the experiment took place are given (see ESM, Table 5.S1).

5.6.3 Control experiments at lab scale

For control and comparison purposes, a parallel blank experiment was carried out in the lab, in which capsules containing the polymer were exposed to sterilized water at room temperature during the same period of time (7 days). Furthermore, a polymer sample standard (i.e., non-exposed) was analyzed as explained below.

5.7 Maldi MSI

5.7.1 Sample preparation

For MALDI-TOF-MS measurements, the polymer was removed from the capsules and dried in a dessicator for 15 min. Slices of 12–16 μm were cut in a cryo-microtome (Leica CM3050S, Nußloch, Germany) and placed onto indium-tin oxide (ITO)-coated glass slides (Sigma-Aldrich). The samples were placed in a desiccator for 15 min before matrix deposition. The section was coated with 30 mg of DCTB using a sublimation device (Fisher Scientific, Madrid, Spain). Sublimation conditions were 100 mTorr pressure at 140 °C during 15 min. The sample slice was externally cooled with ice.

5.7.2 Mass spectrometry

All experiments were performed using an AuToFlex III MALDI-TOF/TOF instrument (Bruker Daltonik GmbH, Bremen, Germany) equipped with a Smartbeam laser at 200 Hz laser at the "medium focus" setting and were controlled using FlexControl 3.0 (Bruker Daltonik GmbH). The analytical conditions for the MALDI MSI analysis were set as follows: positive reflector ion mode; ion source 1 voltage, 19 kV; ion source 2 voltage, 16 kV; lens voltage, 8.5 kV; and mass range m/z 100–3000. Laser irradiance was maintained slightly above threshold. Mass spectra were acquired with spatial resolution set at 200 μm. For each pixel, 250 laser shots were measured per position as a sum of 25 consecutive laser shots in 10 random walk shot steps.

5.7.3 Image processing

Raw spectra were analyzed with Flex Imaging 4.0 software (Bruker Daltonik GmbH, Bremen, Germany) after baseline subtraction and root mean square (RMS) normalization. Ion density maps were created for ions observed from the skyline projection spectrum. Masses were manually selected with a mass accuracy set to ±0.1% (manual peak picking). Regions of interest were manually defined by using both the sample image and MSI data. Image processing and data analysis were done using SCiLS Lab software (Bremen, Germany) allowing identification and quantification of the altered areas.

5.8 LC - HRMS

Clean cuts of the polymer exposed in wastewater tanks at the WWTP were dissolved in methanol and then diluted with water (95:5 water:methanol) to achieve the initial concentration of 1 mgL^{-1} of the polymer. The samples were injected directly (10 µL) into LC-HRMS. A generic LC-HRMS method was applied to detect and identify TPs of the PCLD using an Acquity UPLC coupled to Q-Exactive (Thermo Scientific, Bremen, Germany). Electrospray ionization (ESI) interface was operated in both positive and negative ionization mode to obtain the exact masses of the TPs. The chromatographic separation was performed using an Acquity UPLC C18 column (100 × 2.1 mm, 1.7 µm) proceeded by a pre-column of the same packing material (5 × 2.1 mm, 1.7 µm). The mobile phases for the chromatographic run were as follows: (a) acetonitrile with 0.1% formic acid and (b) water (0.1% formic acid). The total chromatographic run was 15 min with a flow rate of 300 $\mu L\ min^{-1}$. The elution was accomplished with the following solvent gradient: 0 min (10% A)–1 min (10% A)–11 min (95% A) and 13 min (95% A)—13.5 min (10% A) and stabilized until 15 min. The column temperature was set to 40 °C. For the detection method, a data dependent scan was applied with the following parameters: full scan and data-dependant MS^2 were set to resolution of 35,000 [full width at half maximum (FWHM)], with the full scan range of m/z 100–1000. In the data-dependent scan, the isolation window was m/z 2 and the normalized collision energy was (NCE) either 15 or 35. Both positive and negative ionization mode runs were used and then compared to a blank sample (containing only the parent homopolymer dissolved in pure water and methanol (95:5)) with the degraded samples using SIEVE 2.2 (Thermo Fisher).

5.9 Results and discussion

5.9.1 Maldi mass spectra of polymer section

Representative average MALDI-TOF mass spectra (mass range up to m/z 2600) of sections of the starting material, the sterile control, and the two samples exposed to aerobic and denitrifying wastewater are shown in Fig. 5.1A–D at different attenuation factors. Highest mass range (m/z 700–2600) is consistent with the starting polymer structure with increasing number of monomer (caprolactone) units (peak spacing m/z 114). Overall, there is a general decrease of the relative peak intensities in the exposed samples (Fig. 5.1B–D) as well as differences in the peak distribution, thus suggesting a different distribution of the chain lengths.

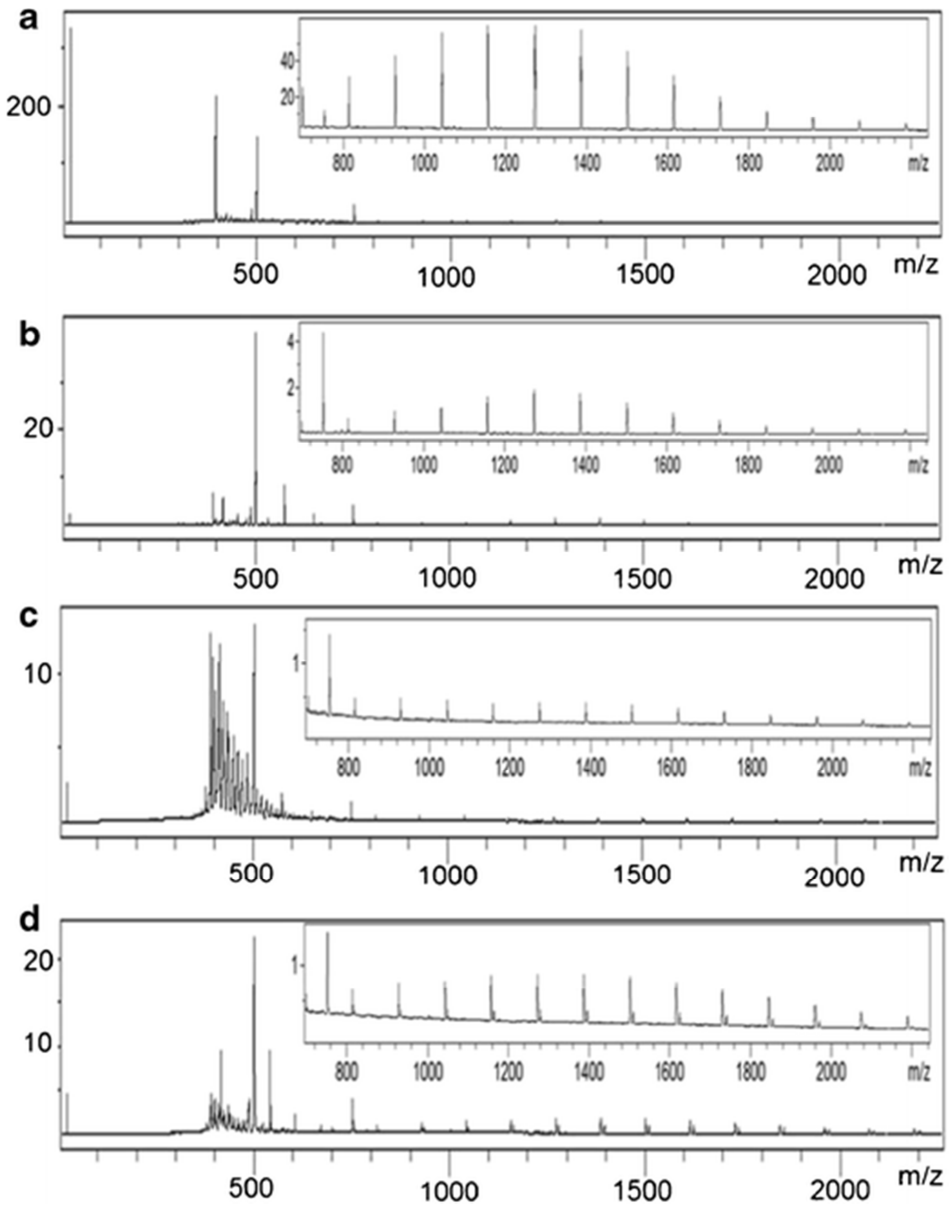

Figure 5.2: Average MALDI-ToF mass spectra recorded in the positive reflectron mode, showing a polycaprolactone diol series $[M+Na]^+$ in the range from m/z 23 to 2600. The differences in the intensity scales: (A) standard polycaprolactone diol; (B) after 7 days of exposure in sterile water. (C) After 7 days of exposure in water under aerobic conditions (WWTP secondary treatment tank); (D) after 7 days of exposure in water under denitrifying conditions (WWTP tertiary treatment tank).

This trend is more pronounced in the samples exposed to aerobic and denitrifying conditions (Fig. 5.1C, D). In addition, in the spectrum of the latter sample (Fig. 5.1D), the presence of a second series of oligomers, likewise, spaced by m/z 114 (i.e., m/z 1051.6 and 1165.6) and separated from the homolog peaks of the main series by m/z 104. It was attributed to PCL (Table 5.1) formally corresponding to a loss of the diethylenglycol unit from PCLD polymer and they were identified as PCL cyclic oligomers [21, 22, 23, 24], previously reported as a possible degradation pathway of PCL (Fig. 5.1) [25].

As regards the lower mass range series (m/z < 800), with the peak at m/z 500 corresponding to the matrix DCTB, there is also evidence in the degraded polymer samples (Fig. 5.1C–D) of peaks attributable to degradation of the standard material as well. Again, this is detected in the polymer exposed to aerobic and denitrifying conditions. The structural identification of these peaks was further investigated in detail using LC-HRMS (see "Identification of transformation products using LC-HRMS"). Overall, the above findings are indicative of degradation processes affecting the exposed samples. This is consistent with the fact that polyesters and specifically polycaprolactones are reported to undergo degradation under both aerobic and anaerobic conditions [6].

5.9.2 Identification of transformation products using LC-HRMS

Since there was no qualitative difference between the runs in the positive and negative ionization mode, transformation products (TPs) were identified using the positive ESI. For the identification of polymer TPs, the product ion spectra of the TPs were recorded to determine the most likely elemental compositions and to identify structures of the fragment ions.

All compounds detected were formed as the result of ester hydrolysis of the parent homopolymer (Fig. 5.2). In total, ten TPs were detected and identified in LC-HRMS (see ESM, Tables S5.1 and S5.2). Five were the result of ester hydrolysis forming caprolactone oligomers (see ESM, Table S5.1 in the homologous series TPs 220, 334, 448, 562, and 676) while the other series detected corresponded to formation of PCL chain with a terminal diethylene glycol (see ESM, Table S5.2), via (again) ester hydrolysis (TPs 246, 360, 474, 588, and 702). In all cases, the difference between the polymer series was the repeating unit of m/z 114.0681 (6-hydroxyhexanecarbonyl,

HOCH2-(CH2)5-CO-) (see ESM, Fig. 5S3). In general, all TPs were predominantly detected as ionized sodium adducts and [M+H]+.

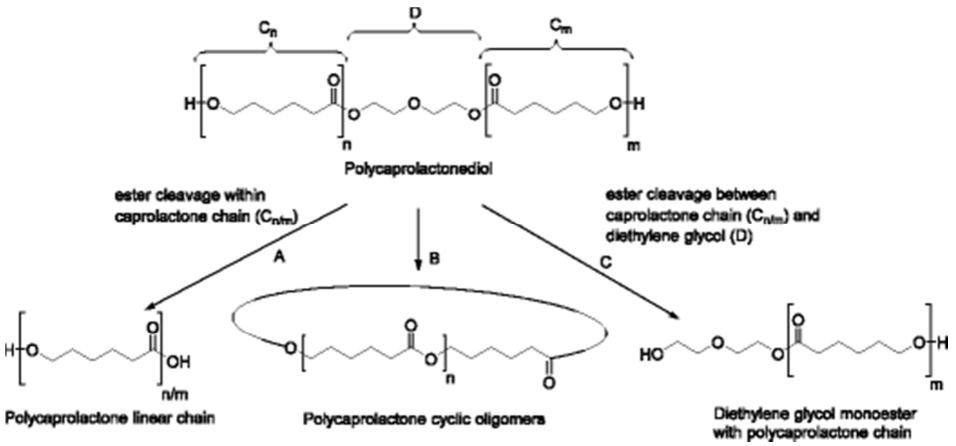

Figure 5.3: Proposed degradation pathway of polycaprolactone diol: (A) formation of polycaprolactone (PCL) linear oligomers; (B) formation of cyclic oligomers and (C) formation of polycaprolactone-diethylene glycol monoester

The fragmentation of TP 220 started with a water loss followed by loss of m/z 44.0262 (C_2H_4O). Its homolog series followed the same pattern (see ESM, Table S5.1). As for the other series, their fragmentation pattern again was the water loss in combination with loss of C_2H_4O, after the initial water loss from the acid itself. Detailed fragmentation pattern and mass spectra can be found in the ESM on Tables S5.1 and S5.2. A summary of the main peaks identified in "MALDI mass spectra of polymer sections" and "Identification of transformation products using LC-HRMS," together with their proposed structure is given in Tables 5.1 and 5.2 for low mass range (MW < 800 Da) and high mass range (MW > 800 Da) TPs, respectively.

UPLC-HRMS chromatograms corresponding to the low mass range TPs of the denitrifying exposed sample are shown in Fig. 5.3. Peaks corresponding to polycaprolactone (PCL) fragments (Fig. 5.3A; TPs 246, 360, 474, 588, and 702) are single as expected from the hydrolysis pattern, while those of polycaprolactone-diethylene glycol monoesters (Fig. 5.3B: TPs 220, 334, 448, 562, and 676) appear resolved totally or partially in more than one peak (Table 5.2), tentatively pointing to the presence of isomer mixtures. However, their HRMS-(ESI)-mass spectra (Fig. 5.4) cannot confirm this hypothesis.

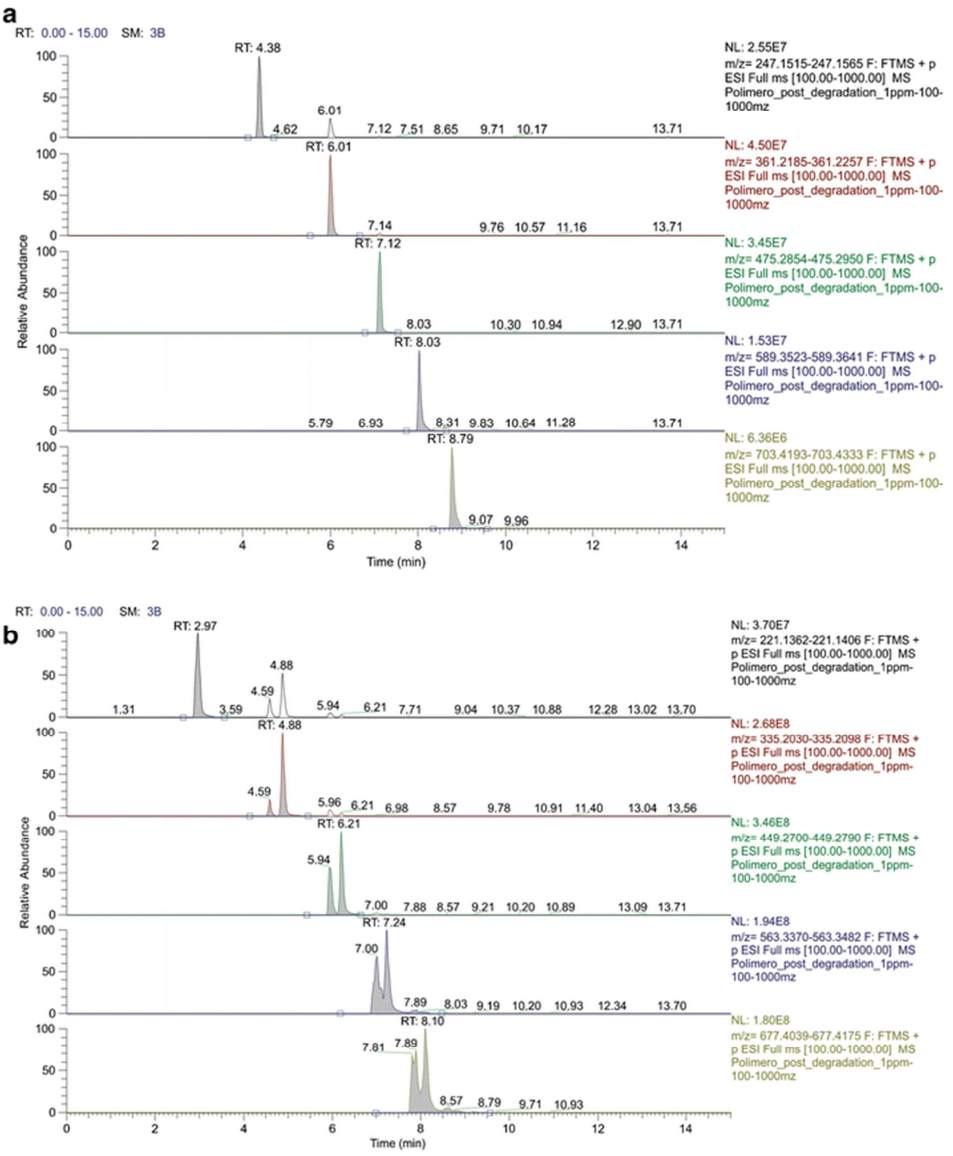

Figure 5.4: UPLC-HRMS chromatogram of the TPs in the low mass range (m/z < 800); (A) formed by ester hydrolysis and (B) formation of polycaprolactone-diethylene glycol monoester in degradation sample at t 7 days (see also Fig. 5.2)

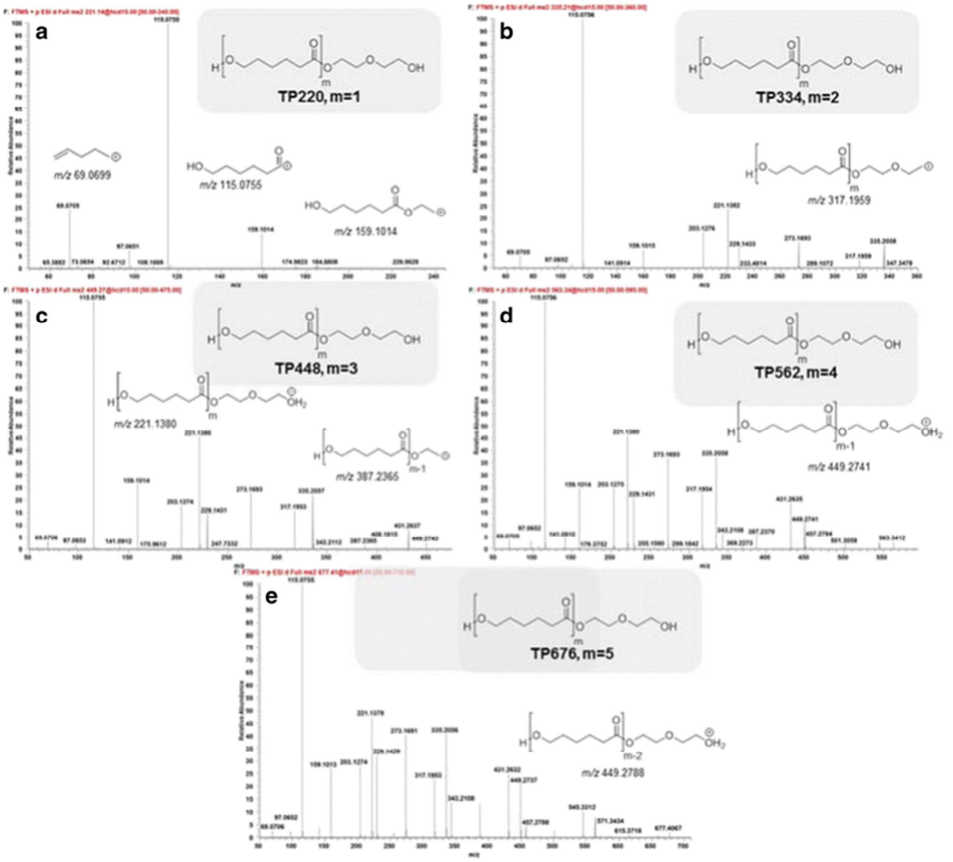

Figure 5.5: HRMS-(ESI)-mass spectra of (A) TP220, (B) TP334, (C) TP448, (D) TP562, and (E) TP676

5.9.3 Spatial distribution of polymer degradation patterns by MALDI MSI

Biotic-mediated processes taking place in the surface of polymer samples exposed in the WWTP environment were expected to exhibit large spatial heterogeneity, especially if they are associated to the formation of biofilm colonies in the surface of the exposed material. This fact should be correspondingly reflected in the surface composition pattern of the exposed polymer probes. To investigate it, MALDI MSI appears as a suitable technique since it allows generating 2D images across the probe surface using selected ions. In Fig. 5.5A–D, MALDI MSI images generated from polymer cuts of the four samples analyzed using the main ions characteristic of the

starting polymer (m/z 1155.7, 1269.7, 1383.8, and 1497.9) are shown as an example. They exhibit notable differences in the spatial distribution on both intensity and uniformity (homogeneity). Whereas the standard polymer (Fig. 5.5A) shows a highly uniform and intense distribution, exposed samples (Fig. 5.5B–D) deploy increasingly heterogeneous spatial patterns with a decreasing intensity in the order sterile->aerobic->denitrifying. In the latter case (Fig. 5.5D), the disappearance of the peak monitored is almost complete in some parts (deep blue colored areas). These findings are fully consistent with those derived from the average MALDI MS exposed in "MALDI mass spectra of polymer sections."

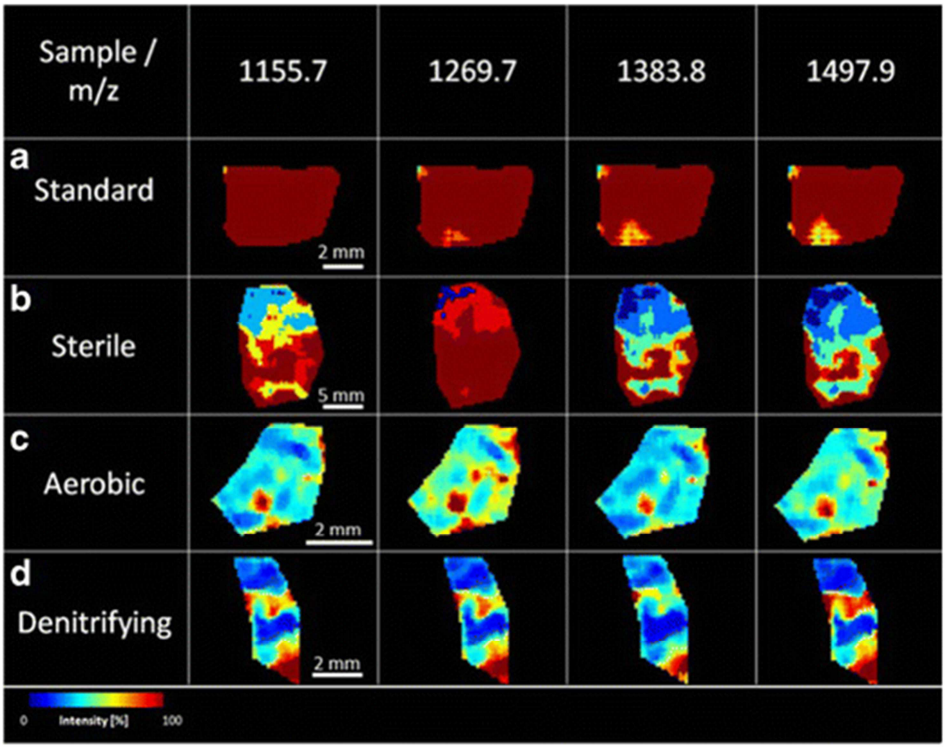

Figure 5.6: Comparison of MALDI-ToF images corresponding to sections of (A) PCDL standard, (B) control sample kept in sterilized water, (C) sample exposed to aerobic wastewater, and (D) sample exposed to denitrifying wastewater. Images were obtained by data processing with Flex Imaging 4.0 software. Spatial differences among pixels using the different ions are visible across the surface of the samples. Ions shown are sodium adducts $[M + Na]^+$

The spatial pattern of second oligomer series predominantly formed in the denitrifying exposed sample was investigated using MALDI MSI as well. The images corresponding to the main parent oligomer and the second series formed by hydrolytic loss of the diethylene glycol moiety are shown in Fig. 5.5. In each compartment, the transformed polymer peak is shown on the right side while the formally parent peak is on the left side. Their MW differs on m/z 104, which corresponds to the diethylene glycol fragment lost. The images corresponding to the main parent oligomer and the second series formed by internal "back-biting" cyclization are shown in Fig. 5.6. In each compartment, the cycled analog ion distribution is shown on the left side while the formally parent peak ion distribution is on the right side. It is worth noting that the transformation polymer is highly unevenly distributed across the sample, appearing mostly located in the upper part and it is roughly complementary to the starting polymer. Such pattern is approximately repeated for all peaks shown in Fig. 5.6.

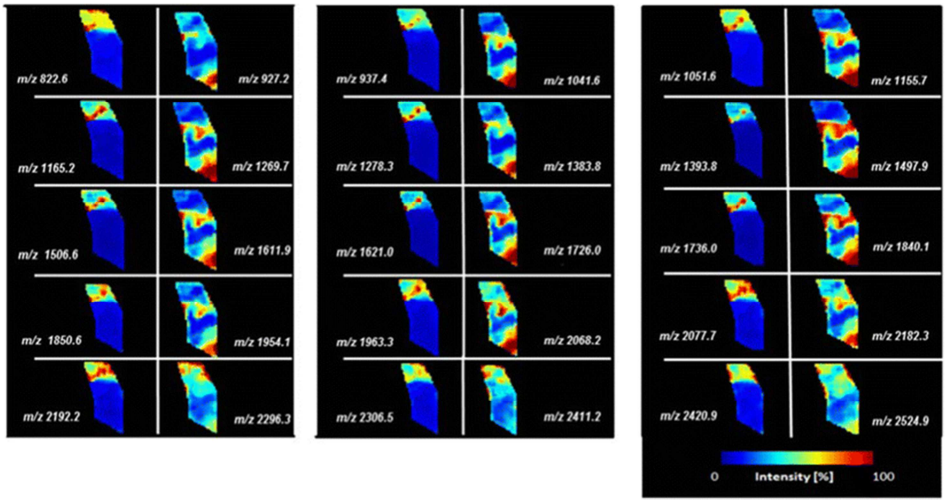

Figure 5.7: Comparison of MALDI-ToF images corresponding to sections of samples exposed to denitrifying wastewater. Images were obtained by data processing with Flex Imaging 4.0 software. Each pair of images shown corresponds (right) to the peaks of the starting polycaprolactone diol polymer PCDL (M) and (left) the cyclic polycaprolactone analog (M-104). Ions shown are sodium adducts $[M + Na]^+$

We finally studied the spatial distribution of low MW range ions (i.e., below m/e 700). Their structures are reported in Table 5.2. Most of them were confirmed by LC-HRMS as explained above. Comparing the aerobic and denitrifying exposed sample images, some differences are perceptible. Whereas ions m/z 221.1, 247.1, and 449.2 seem to predominate in the aerobic exposed sample, those at m/z 475.5 and 677.4 are

characteristic for the denitrifying exposed sample. Remarkably, while the surface distribution of the latter one (m/z 677.4) follows a similar spatial pattern than those observed for the aforementioned transformation polymer (Fig. 5.7, right side images, upper part), the former (m/z 475.5) fits the opposite and complementary distribution (Fig. 5.7, right side images, lower part).

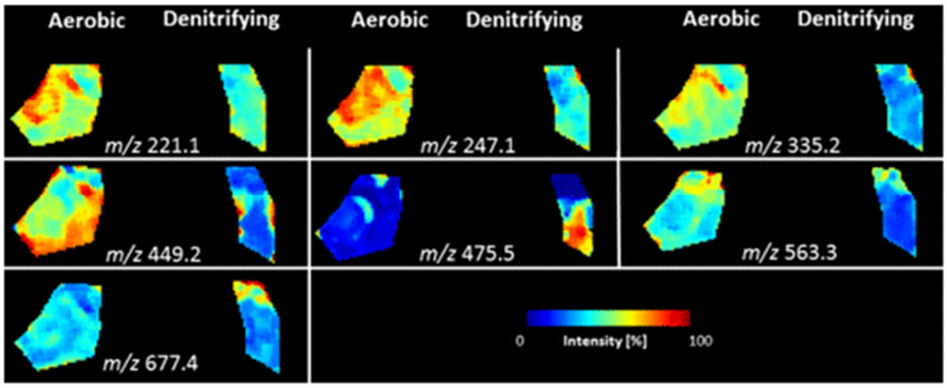

Figure 5.8: Comparison of MALDI-ToF images corresponding to sections of samples exposed to aerobic (left) and denitrifying (right) wastewater using characteristic ions (m/z < 800). Images were obtained by data processing with Flex Imaging 4.0 software.

5.10 Conclusions

This study has been demonstrated the complementarity of the MSI and UPLC-HRMS techniques for the determination of the biodegradation products of polycaprolactone diol. Whereas UPLC-HRMS has higher sensitivity thus allowing the unequivocal identification of degradation products through their exact masses, MALDI MSI technique shows how these degradation products are distributed across the surface of the exposed sample.

In addition, different transformation products of the starting polycaprolactone diol oligomer were identified in both the low and high molecular weight mass ranges. On the other hand, there is evidence of three different degradation processes as well, namely (a) the hydrolytic cleavage of the diethylenglycol-polycaproic ester bond, (b) another one taking place on the polyester bonds of the polycaprolactone units, and (c) the cyclization of polycaprolactone oligomers via internal ester formation. The former one seems specific of the denitrifying exposed samples. On the other hand, there is evidence of two different ester hydrolysis processes as well, namely the cleavage of the diethylenglycol-polycaproic ester bond and another one taking place on the polyester

bonds of the polycaprolactone moiety. The former one seems specific of the denitrifying exposed samples. Both processes were traced through the corresponding degradation products.

Finally, the study of MALDI MSI images reveal the spatial complexity and specificity of the degradation processes taking place in the exposed polymer surface, which allow clearly differentiation between aerobic and denitrifying environments as found in conventional engineered systems. Such differential behavior is better highlighted in comparison with a sample kept under sterile conditions. Whereas abiotic processes seem to be present as well, it clearly supports the contribution of biotic processes acting on the aerobic and denitrifying exposed samples.

5.11 Acknowledgements

This study has been financially supported by the EU through the FP7 project GLOBAQUA (Grant Agreement No 603629), and by the Generalitat de Catalunya (Consolidated Research Groups "2014 SGR 418—Water and Soil Quality Unit" and 2014 SGR 291—ICRA). It reflects only the author's views. The Community is not liable for any use that may be made of the information contained therein.

5.12 References Chapter 5

1. Rattanapan S, Pasetto P, Pilard JF, Tanrattanakul V. Preparation and properties of bio-based polyurethane foams from natural rubber and polycaprolactone diol. J Polym Res. 2016;23(9) doi:10.1007/s10965-016-1081-7.

2. Nadjiadjim G, Sheibat-Othman N, Févotte G, Dupuy J. Development and monitoring of a continuous polyurethane pilot reactor. Chem Eng Technol. 2010;33(11):1900–8. doi:10.1002/ceat.201000296.

3. Tehrani AD, Parsamanesh M. Preparation, characterization and drug delivery study of a novel nanobiopolymeric multidrug delivery system. Mater Sci Eng C. 2017;73:516–24.

4. Schek RM, Taboas JM, Segvich SJ, Hollister SJ, Krebsbach PH. Engineered osteochondral grafts using biphasic composite solid free-form fabricated scaffolds. Tissue Eng. 2004;10(9–10):1376–85.

5.Munj HR, Lannutti JJ, Tomasko DL. Understanding drug release from PCL/gelatin electrospun blends. J Biomater Appl. 2016;31:933–49.

6.Eubeler JP, Bernhard M, Knepper TP. Environmental biodegradation of synthetic polymers II. Biodegradation of different polymer groups. TrAC Trends Anal Chem. 2010;29(1):84–100.

7. Wang J, Chu L. Biological nitrate removal from water and wastewater by solid-phase denitrification process. Biotechnol Adv. 2016;34(6):1103–12.

8.Li P, Zuo J, Wang Y, Zhao J, Tang L, Li Z. Tertiary nitrogen removal for municipal wastewater using a solid-phase denitrifying biofilter with polycaprolactone as the carbon source and filtration medium. Water Res. 2016;93:74–83.

9.Abou-Zeid D-M, Müller R-J, Deckwer W-D. Biodegradation of aliphatic homopolyesters and aliphatic-aromatic copolyesters by anaerobic microorganisms. Biomacromolecules. 2004;5(5):1687–97.

10. Rizzarelli P, Carroccio S. Modern mass spectrometry in the characterization and degradation of biodegradable polymers. Anal Chim Acta. 2014;808:18–43. doi:10.1016/j.aca.2013.11.001.

11. Weidner SM, Falkenhagen J. Imaging mass spectrometry for examining localization of polymeric composition in matrix-assisted laser desorption/ionization samples. Rapid Commun Mass Spectrom. 2009;23(5):653–60. doi:10.1002/rcm.3919.

12. Krueger K, Terne C, Werner C, Freudenberg U, Jankowski V, Zidek W, Jankowski J. Characterization of polymer membranes by MALDI mass-spectrometric imaging techniques. Anal Chem. 2013;85(10):4998–5004. doi:10.1021/ac4002063.

13.Fröhlich SM, Archodoulaki V-M, Allmaier G, Marchetti-Deschmann M. MALDI-TOF mass spectrometry imaging reveals molecular level changes in ultrahigh molecular weight polyethylene joint implants in correlation with lipid adsorption. Anal Chem. 2014;86(19):9723–32. doi:10.1021/ac5025232.

14.Trim PJ, Snel MF. Small molecule MALDI MS imaging: current technologies and future challenges. Methods. 2016;104:127–41. doi:10.1016/j.ymeth.2016.01.011.

15.Verhaert PDEM, Pinkse MWH, Strupat K, Conaway MCP. Imaging of similar mass neuropeptides in neuronal tissue by enhanced resolution MALDI MS with an ion trap – OrbitrapTM hybrid instrument. In: Rubakhin SS, Sweedler JV, editors. Mass spectrometry imaging: principles and protocols. Totowa: Humana Press; 2010. p. 433–49. doi:10.1007/978-1-60761-746-4_25.

16.Otal E, Mantzavinos D, Delgado MV, Hellenbrand R, Lebrato J, Metcalfe IS, Livingston AG. Integrated wet air oxidation and biological treatment of polyethylene glycol-containing wastewaters. J Chem Technol Biotechnol. 1997;70(2):147–56. doi:10.1002/(SICI)1097-4660(199710)70:2<147::AID-JCTB747>3.0.CO;2-3.

17.Staples CA, Williams JB, Craig GR, Roberts KM. Fate, effects and potential environmental risks of ethylene glycol: a review. Chemosphere. 2001;43(3):377–83.

18.Rivas D, Ginebreda A, Pérez S, Quero C, Barceló D. MALDI-TOF MS imaging evidences spatial differences in the degradation of solid polycaprolactone diol in water under aerobic and denitrifying conditions. Sci Total Environ. 2016;566–567:27–33.

19.Rivas D, Ginebreda A, Elosegi A, Pozo J, Pérez S, Quero C, Barceló D. Using a polymer probe characterized by MALDI-TOF/MS to assess river ecosystem functioning: from polymer selection to field tests. Sci Total Environ. 2016;573:532–40.

20.Dopstadt J, Vens-Cappell S, Neubauer L, Tudzynski P, Cramer B, Dreisewerd K, Humpf H-U (2016) Localization of ergot alkaloids in sclerotia of Claviceps purpurea by matrix-assisted laser desorption/ionization mass spectrometry imaging. Anal Bioanal Chem :1–10.

21.Kricheldorf HR, Langanke D, Stricker A, Räder HJ. Polylactones, 53: formation of cyclic polyesters in the combined ring-expansion polymerization/ring-opening polycondensation of lactones. Macromol Chem Phys. 2002;203(2):405–12. doi:10.1002/1521-3935(20020101)203:2<405::AID-MACP405>3.0.CO;2-N.

22.Kricheldorf HR, Stricker A, Langanke D. Polylactones, 52. Tin carboxylates as initiators of ε-caprolactone. Macromol Chem Phys. 2001;202(15):2963–70.

23.Báez JE, Martínez-Richa A, Marcos-Fernández A. One-step route to α-hydroxyl-ω-(carboxylic acid) polylactones using catalysis by decamolybdate anion. Macromolecules. 2005;38(5):1599–608. doi:10.1021/ma0491098.

24.Ahmed H, Trathnigg B, Oliver Kappe C, Saf R. Characterization of poly(ethylene glycol)-b-poly(ε-caprolactone) by liquid chromatography under critical conditions: influence of catalysts and reaction conditions on product composition. Eur Polym J. 2009;45(8):2338–47. doi:10.1016/j.eurpolymj.2009.05.001.

25.Bankova M, Kumar A, Impallomeni G, Ballistreri A, Gross RA. Mass-selective lipase-catalyzed poly(ε-caprolactone) transesterification reactions. Macromolecules. 2002;35(18):6858–66. doi:10.1021/ma0202282.

5.13 Supporting information

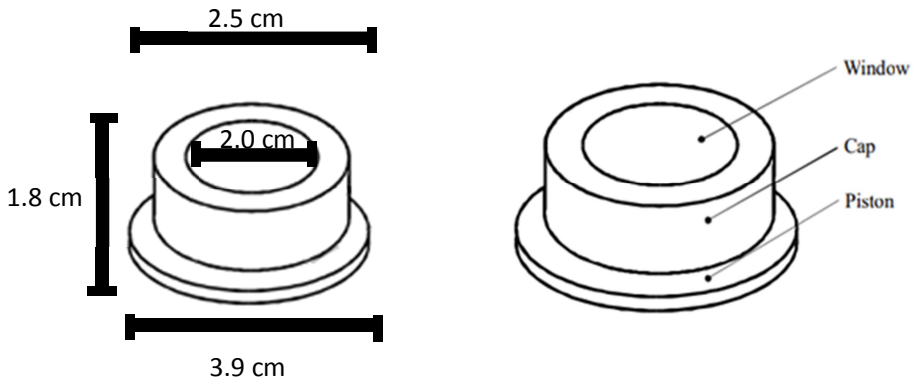

Figure S5.1 Description of DGT. Each capsule unit consist of a plastic piston and a plastic cap

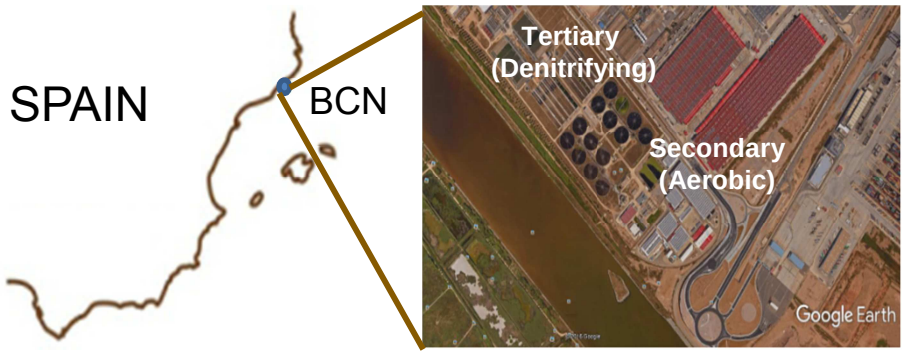

Figure S5.2 Location of WWTP El Prat de Llobregat. Sampling sites of WWTP El Prat de Llobregat

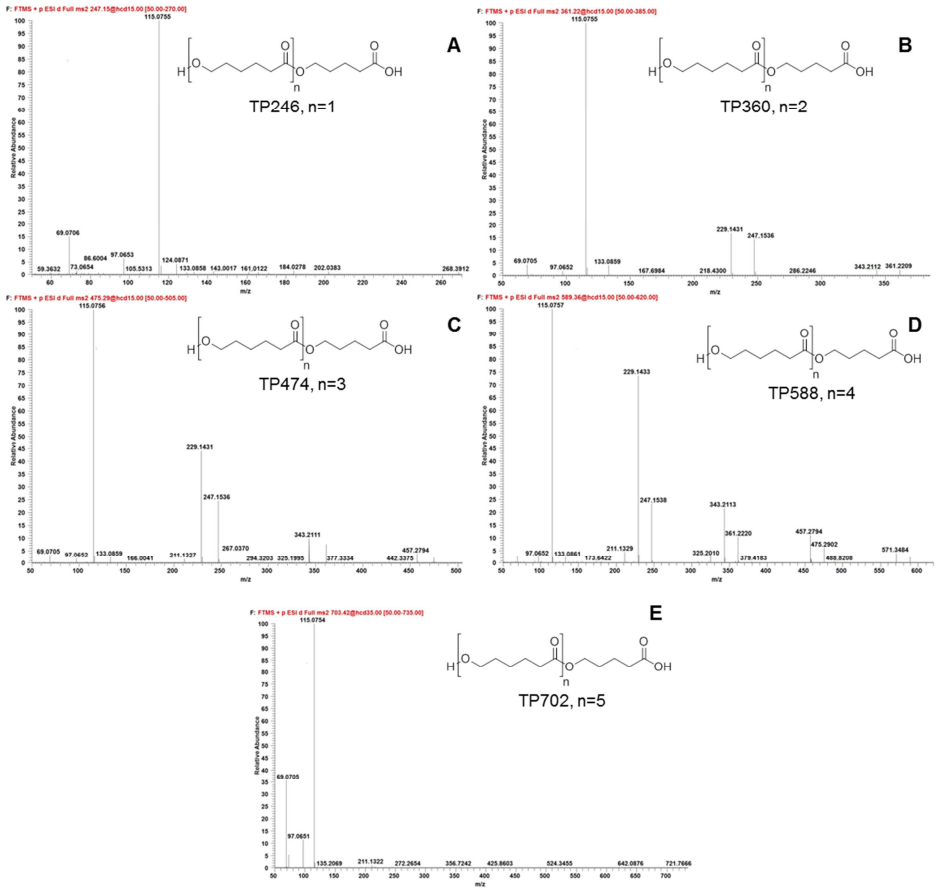

Figure S5.3 HRMS-(ESI)-mass spectra of (A) TP246, (B) TP360, (C) TP474, (D) TP588 (E) TP702.

Table S5.1. Parameters monitored daily in the WWTP(El Prat de Llobregat, Barcelona) for aerobic and denitrifying conditions.

	Inlet								
	mg/l	mg/l	mg/l	mg/l	mg/l	mg/l	µS/cm	NTU	uph
Time (Days)	Suspended solids	BOD5	COD	N-NH_4	NT	P total	Conductivity	TURB	pH
1	157						2.3	155	7,2
2	160						2.43	155	7,2
3	160						2.55	136	7,4
4	155						2.5	140	7,7
5	141		424	53	63,1	9,4	2.45	147	7,9
TOTAL									
MEAN	161	221	428	49,5	63,4	8,7	2.429	152	7,6
MAX	188	253	530	59,4	75,9	10,8	2.78	184	8
MIN	115	203	157	34,7	46,9	4,2	1.438	96	7,1

*Total nitrogen kjeldahl

Secondary outlet							Denitrifying outlet					
mg/l	mg/l	mg/l	NTU	µS/cm	mg/l	mg/l	mg/l	mg/l	mg/l	mg/l	mg/l	uph
Suspended solids	BOD5	COD	TURB.	Conductivity	$N\text{-}NH_4$	NTK*	$N\text{-}NO_2$	$N\text{-}NO_3$	NT	P total	pH	
11		34	3	1.486	2,9	4,3	0,3	1,3	5,9	4	7,1	
9		39	3	1.601	5,1	6,5	0,6	1,9	9	2,7	6,9	
9			2	1.891							7,6	
9			3	2.22							7,8	
12		30	5	1.836	1,6	3,6	0,2	2,7	6,5	3,9	7,9	
10	5	37	3,8	1.941	3,2	4,6	0,6	3,1	8,3	4,2	7,6	
29	16	55	12	2.38	7,2	8,7	4	5	11,6	7,7	8,1	
5	3	30	2	1.486	1,6	1,8	0,2	0,5	5,5	2,7	6,9	

*Total nitrogen kjeldahl

PopulationServed (inhabitants)	Remote pump stations	Collectors (Km)	Q design (m^3/d)	Q design N/P reductions (m^3/d)
2275000	6	48.3	420000	325000

Table S5.2. List of generic fragment ions of TPs identified as diethylene glycol PCL monoesters

Ion	Generic structure	m	TP220	TP334	TP448	TP562	TP676
677.4107	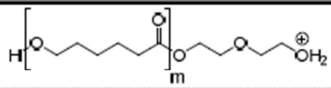	5					X*
659.4001	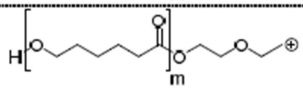	5					X
615.3739	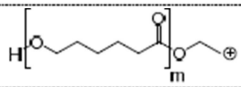	5					X
571.3477	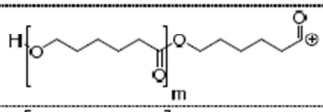	4					X
563.3426	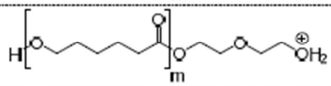	4				X*	X
545.3320	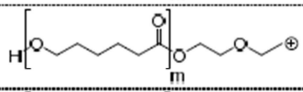	4				X	X
501.3058	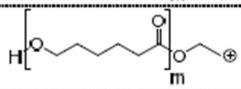	4				X	X
457.2796	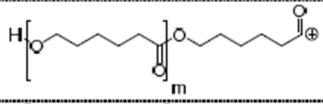	3				X	X
449.2745	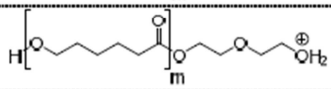	3			X*	X	X
431.2639	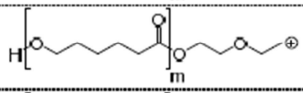	3			X	X	X
387.2377	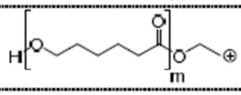	3			X	X	X
343.2115	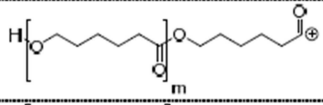	2			X	X	X
335.2064	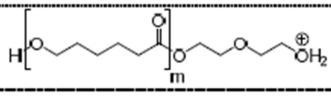	2		X*	X	X	X

Ion	Generic structure	m	TP220	TP334	TP448	TP562	TP676
317.1959	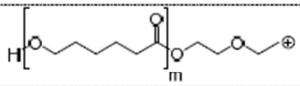	2		X	X	X	X
273.1697	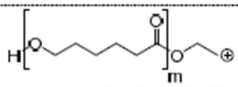	2		X	X	X	X
229.1434	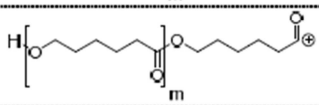	1		X	X	X	X
221.1384	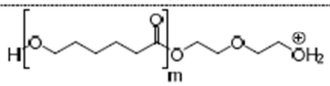	1	X	X	X	X	X
203.1278	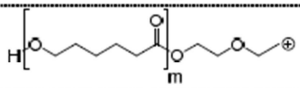	1	X	X	X	X	X
159.1016	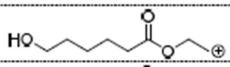	1	X		X	X	X
115.0754	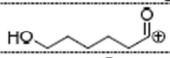	-	X	X	X	X	X
97.0648	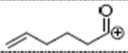	-	X	X	X	X	X
69.0699	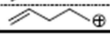	-	X	X	X	X	x

Table S5.3.List of generic fragment ions of TPs identified as polycaproic oligomers

Ion	Generic structure	n	TP246	TP360	TP474	TP588	T702
703.4263	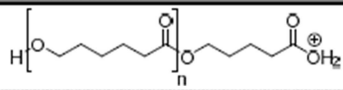	5					X*
685.4158	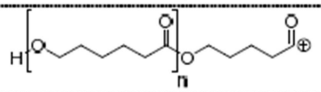	5					X
589.3582	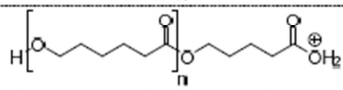	4				X	X
571.3477	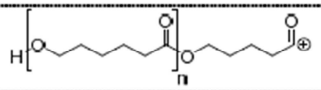	4				X	X
475.2902	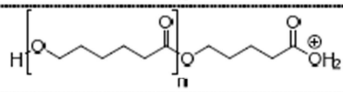	3			X	X*	X
457.2796	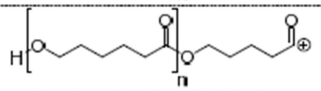	3			X	X	X
361.2221	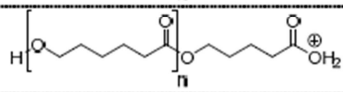	2		X	X*	X	X
343.2115	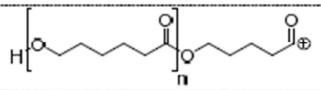	2		X	X	X	X
247.1540	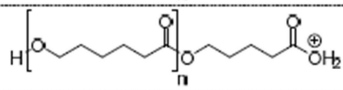	1	X	X	X	X	X
229.1434	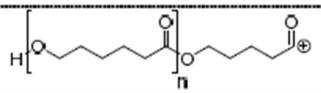	1	X	X	X	X	X
211.1329	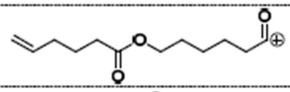	-	X	X	X	X	X
115.0754	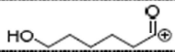	-	X	X	X	X	X
97.0648	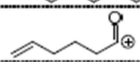	-	X	X	X	X	X
69.0699	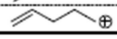	-	X	X	X	X	x

Chapter 6

Capítulo 6. General Discussion

In this work, we aimed at studying the degradation of organic synthetic matter either in natural or engineered sytems (fluvial ecosystems and waste water treatment plants). t by the development of a synthetic material probe to study The device is based on a commercial polymer exposed for a while to different aquatic environments (aerobic, anaerobic) and the changes occurred measured using advanced mass spectrometric techniques, such as MALDI-TOF/MS, MALDI IMAGING and HPLC-MS.

A large number of studies have been published about stream ecosystem functioning, comprising structural and functional aspects (Gessner and Chauvet, 2002) (Palmer and Febria, 2012). Leaf-litter breakdown has been used to investigate responses of streams to acid mine drainage and acid rain, disturbance by logging, temperature and nutrient and gradients of agricultural development (Ferreira et al.,2015) Indeed, leaf-litter breakdown and organic matter decomposition have been proposed as a useful method for assessing the functional integrity of streams (Feio et al., 2010); (Gessner and Chauvet,2002). However, there are other studies that prefer the use of standardized materials for routine monitoring such as cotton strips and wooden sticks (Imberger et al., 2010); (Tiegs et al.,2007) ;(McTammany et al., 2008); (Tank andWinterbourn, 1996);(Young et al., 2008);(Arroita et al., 2012). While all these substrates reflect the decomposition of natural organic matter, they yield little information about the degradation of synthetic organic matter. Industries, urban sewage, landfills and agricultural production are sources of anthropogenic pollution that contaminates river ecosystems. The use of a polymeric probe is presented as an appropriate tool for observing the degradation of synthetic organic matter. In this regard, a search was conducted in chapter 3, taking into consideration commercial affordability, n physical-chemical properties (notably its solubility), and manipulation feasibility. MALDI-TOF/MS analysis methods were developed for several candidates (….). FInally, PCLD was selected as the most suitable polymer for conducting the experiments(Rivas et al., 2016). An experimental setup was performed in two artificial

streams (with nutrients and without nutrients), to study the polymer biodegradation. Mesocosm degradation experiments were carried out by placing capsules filled with PCLD 1250 (20–80 mg) in two artificial streams (mesocosm) (see section 3.5.2). Total exposure time was 28 days. Samples (three capsules) were collected every 7 days and finally analyzed by MALDI-TOF/MS.

In the last years the use of synthetic polymers has increased exponentially (Eubeler et al., 2009). Most of these synthetic polymers present a low biodegradability. Owing to that the synthetic polymers can accumulate in the different ecosystems contaminating and altering the life that surrounds them. For these reasons, several authors have focused their research on the degradation of plastics and their transformation products (Li et al., 1995) (Gross and Kalra, 2002) (Siracusa et al., 2014). Polymer degradation encompasses a variety of abiotic and biotic degradation processes that might take place simultaneously in the polymer. The most commonly used analytical techniques for monitoring the degradation of polymers include GC–MS, LC-MS, NMR and MALDI-TOF/MS (Eubeler et al., 2009).

Polymer biodegradation has been the object of several reviews (Swift, 1997; Shah et al., 2008;

Lucas et al., 2008; Eubeler et al., 2010). However, most of these experiments were performed in different experimental set ups or using other polymers, which have different physical and chemical properties. For example, some authors studied the hydrolytic degradation of poly (ethylene terephthalate) by MALDI-MS in water (Weidner et al., 1997). The aerobic biodegradation of poly(vinylpyrrolidone) polymer was monitored on a laboratory-scale fixed-bed bioreactor run with river water applying MALDI-TOF MS (Trimpin et al., 2001).

Thus, it is generally difficult to compare results due to many factors that can affect the experimental measurements.

In the artificial streams experiment, we focused on the possible role of nutrients. Principal Component Analysis (see figure 3.3) plots of mesocosms experiments show in the loading plot ions three distinct groups: low (m/z 700–1700), medium (m/z 1700–2800) and high masses (m/z N 2800) but in the scores plot did not differentiate samples neither in terms of exposure time nor treatment (nutrient concentration). However, the starting material seemed different from the rest, indicating that exposed samples had undergone some structural changes. These changes of the polymer

composition can be observed as well in the studies of Weidner and Trimpin (Weidner et al., 1997) (Trimpin et al., 2001). Depending on the polymer, there are different chemical changes (oxidation, reductions etc.)..

The most remarkable result of the test (ANOVA, Levene test p b 0.05), that shows the differences in relative intensities between a given ion of an exposed sample with respect to the standard material at different exposure times, was observed in the fourth week. At that exposure time the number of statiscally different ion intensities with respect to the standard material increased. These changes were more remarkably in the stream with presence of nutrients. In this stream, 11 different peaks intensities appeared, meanwhile in the stream without nutrients only 3 different peaks could be observed. These differences in the degradation of polycaprolactonediol attributable to the presence of nutrients were seemingly statistically relevant only at longest exposure times. Once the degradation device was evaluated in the mesocosm study, a decomposition experiment was performed at 11 sites across the Ebro River basin. Three caps filled with PCLD 1250 (20–80 mg/caps) were deployed at each of 11sites, and subsequently recovered after 97 days. Sites were selected so that river ecosystems of different characteristics were covered (flow, river morphology etc.).After exposure were analyzed by MALDI TOF/MS. The results obtained by the analysis of principal components were very similar to those obtained in the mesocosm experiment. The 3 groups of ions (low, medium and high) were clearly identifiable (see figure 3.5). As observed in the mesocosm experiments, the PCA scores plot allowed differentiating samples among sites. All the points of the Ebro river presented different behavior. The MALDI-TOF/MS spectra obtained from the different sites of the river are completely different. This data confirms the results obtained from principal component analysis.

The use of polymer probes for the study of the synthetic organic matter degradation in freshwater ecosystems is presented as complementary tool to use together with leaf litter or wood sticks.(von Schiller et al., 2017) PCLD 1250 can be effectively used as a probe and its transformation conveniently monitored by MALDI-TOF/MS. However, it was not fully satisfactoryto to differentiate among samples. This study agrees with the observations (Weidner et al., 1997) (Trimpin et al., 2001). MALDI-TOF/MS must be investigated further for a quantitative assessment to ascertain the relative amounts of generated species in a mixture. In addition, it has been demonstrated that MALDI TOF/MS is a robust and unequivocal technique for determination of PCDL 1250 degradation in an environmental matrix such as river water.

These investigations showed that MALDI-TOF/MS can be used as an extended detection method PCDL 1250 experiments and thereby enlarges the analytical window regarding polymeric analytes making them accessible for environmental fate studies

In that respect, the use of MALDI-TOF/MS IMAGING techniques might open new possibilities.

In chapter 4 the use of MSI technique for first time in the study of polymer degradation in water under different environmental conditions (aerobic and denitrifying) presents the next advantages: it does not involve an homogenization step of the polymer, it measures the spatial distribution of a large number of analytes and is a useful method to analyze the sample in solid-surface study.

Degradation experiments at lab scale were carried out by placing capsules filled with PCLD (3–6 g) in the reactors under two different water conditions (aerobic and denitrifying) (Rivas et al., 2016). The samples were collected and analyzed by MSI technique. Overall average MSI spectra of PCLD were compared among them (standard PCLD, aerobic PCLD and denitrifying PCLD) (see figure 4.1). The standard PCLD and aerobic PCLD exhibited very similar spectra while denitrifying PCLD exposure showed pronounced differences thus suggesting the occurrence of deeper structural changes.

For the first time, these deeper structural changes are present in the comparison of images corresponding to standard, aerobic and denitrifying exposure samples using different single ions (see figure 4.2 C).

Another way to observe the degradation occurring in the samples is to check the matrices of correlation coefficients between ion pairs in the pixels of a given sample (see figure 4.4).The lower mass average spectra allowed the identification of clusters formed by the matrix DCTB, impurities from the standard PCLD and peak (m/z 395.1) which could be attributed to the sodium adduct of C18H28O8.(see chemical structure in figure 4.3).

As it is reported in chapter 4, MSI is an efficient tool to investigate the structural changes occurred across the surface of the samples. Images show how the degradation proceeds on a rather spatial heterogeneous manner thus supporting the hypothesis of contribution of biotic processes.

WWTPs essentially consists of a sequence of treatment steps designed to remove both organic matter and nutrients. Typically, they include a biological treatment under aerobic conditions designed to reduce organic load, followed by a tertiary treatment with nitrification/ denitrification process to remove ammonium and nitrate. Each treatment step is characterized by specific conditions (aerobic or anoxic), which results in the development of adapted microorganisms consortia.

According to the transformation products found in chapter 4 and the impossibility to identify them further research was focused on the use of LC-HRMS combined with MSI for making a degradation experiment with the polymer PLCD subjected to the different treatments (aerobic and denitrifying) of WWTP.

MSI and LC-HRMS are two complementary techniques to facilitate the observation of a compound along the surface of the sample and allows the identification of degradation products.

The most remarkable results in this experiment were the evidence of three different degradation processes of the starting PCLD 1250. In particular the ester hydrolysis through cleavage of the diethylenglycol-polycaproic ester bond seems specific

of the denitrifying exposed samples.

Furthermore, as discussed in the previous chapter, MSI images reveal the spatial complexity of the degradation processes in the polymer surface, as well as the possibility of identifying aerobic and denitrifying conditions. These 'markers' can be very interesting to know what type of biodegradation is happening on a particular site. Future work in progress aims at studying more WWTP's with the polymer devices, and to observe if the same degradation pattern occurs. Moreover an analysis of the DNA in the samples and in the medium, would provide information regarding the bacterial species involved in the biodegradation.

The future for obtaining better results in this kind of experiments is to improve the ionization sources, as well as the process of obtaining images. The software developers will soon offer a database to be able to compare the polymers analyzed and to be able to observe the impurities generated by the degradation of products or the matrix interferences (Ràfols et al., 2016). In order to obtain more information, the software that will be developed to be a complementary tool, for example, in a mixture of polymers will be able to perfectly appreciate the interface of the different polymers

that compose the sample, and thus to observe perfectly how they are distributed along the surface of the sample. A very important aspect to develop with the MSI technique is the quantification of the sample. Particularly in the polymer industry, it is required to create new materials by mixing compounds. The main challenge in the short term is seeing how these compounds behave among them and be able to perform and accurate quantification. However, there are semi-quantitative methods as used in the study of (Zhang et al., 2016) that make in situ analysis of gangliosides in brain or that use a semi-quantitative method for analyzing drugs in brain.

The quantification of polymers is very interesting in order to observe the degradation of polymeric material over time or subjected to various stressors.

Certainly in the next few years, another of the main goals to improve the MALDI MSI technique is to increase spatial resolution. The commercial companies manage year after year to reduce the laser size of the laser, these equipment's are currently used to analyze metabolites in tissues (Jones et al., 2017; Shi et al., 2016)) and surely they will be implemented in the future in the analysis of polymers. The other strategy to improve the spatial resolution is the sample deposition, where different robots appear in the market that for achieve a completely homogenous matrix deposition, offering several parameters to modify according to the selected matrix.

Since its initial applications in plants and pharmaceutical imaging, MSI has gained acceptance as a valuable tool for drug and metabolite localization studies. Multiple ionization techniques ensure a variety of options for imaging drugs and metabolites in multiple tissue types at different spatial resolutions. The ability to directly and rapidly map the distribution of drugs is a clear benefit. However, probably the greatest value offered by MSI technique is the ability to acquire images of both parent drug and multiple metabolites in a single imaging experiment. Although sample preparation for MALDI MSI is complicated, matrix-free ionization methods like nanostructure-initiator mass spectrometry (NIMS) and ambient methods like desorption electrospray ionization (DESI) and laser ablation electrospray ionization (LAESI) simplify sample preparation, but these techniques are suitable for small molecule imaging. MALDI, DESI, and NIMS have been employed to image drugs and metabolites in animal tissues while SIMS has been heavily utilized for pharmaceutical detection in drug release systems.

The use of non-target analysis can provide a good knowledge to study the main transformation products that occur in the polymer degradation in the different environmental compartments, however high-resolution mass spectrometry techniques needed, are expensive and experiments in natural environments have many parameters that are difficult to control and therefore the experiments are not easily reproducible.

Finally, the future work should be oriented to the test of new polymeric materials in different environmental compartments. DNA analysis of colonies of bacteria that produce biodegradation is presented as a challenge to be achieved.

Improvements in the ionization sources, spatial resolution, sample preparation and data analysis software will allow a more comprehensive understanding of the degradation of polymeric materials

In Summary all this information makes it possible to manufacture a polymeric device.This device would be left in an environmental compartment for a long time andwill be later collected and easily analyzed, obtaining, in an easy, fast and cheap way, the type of degradation that it suffered.

Chapter 7

Capítulo 7. Conclusions

The general main conclusions extracted from the research conducted in this Thesis are summarized as follows:

- Different commercially available homopolymers were examined as possible candidates to be used as synthetic probes. On the basis of affordability, physical-chemical properties and operational manipulation Polycaprolactonediol 1250 was finally selected as suitable material for further experiments.
- MALDI-TOF, MALDI IMGAING and HPLC-MS analytical methods for the characterization of polycaprolactonediol were developed and optimized.
- To test the proposed approach different exposition experiments of polycaprolactone probes were performed under different aquatic conditions first in laboratory, and subsequently in real systems, such as natural and wastewater treatment plants.
- Preliminary exposure experiments of polycaprolactonediol probes were carried out in different sites of the Ebro River, measured by MALDI-TOF/MS. The results were compared with those obtained simultaneously using conventional methods based on leaf tree decomposition and no significant difference was observed, however it could be used in parallel to obtain complementary information on river metabolism.
- These preliminary experiments showed that conventional MALDI-TOF/MS measurements only provide a crude picture of the transformations occurred in polycaprolactonediol. To have a better insight on the degradation processes occurred in the probe MALDI IMAGING was identified as a better technique, since it enables the 2D spatial characterization of the polymer's sample surface.
- A second series of experiments carried out under sterile, aerobic and denitrifying conditions were carried out, using MALDI IMAGING as analytical measurement technique.

- Observed heterogeneity across the probe's surface of exposed samples indicated significant degradation and suggested the contribution of biotic processes by comparison to a reference sample kept under sterile conditions.
- The MSI spectra obtained from degraded areas allows the characterization of the transformation products.
- The chemical structures of some transformation products were confirmed and semi-quantified by HPLC-MS.
- Image processing using different statistical tools, allows observing and quantifying spatial differences between degraded and non-degraded areas.
- MALDI-TOF MS IMAGING provides a reliable, fast and efficient technique for the characterization of polymers and its transformation after exposure to different aquatic environments.

- Overall, MSI provides a new and promising method to study the degradation of synthetic organic matter both in natural (river)and engineered systems (WWTPs), which has significant advantages in terms of the information provided over the classical methods used today in field ecology or in the control of WWTPs.

Bibliografía

Albertsson A-C, Varma IK. Aliphatic polyesters: synthesis, properties and applications. Degradable Aliphatic Polyesters. Springer, 2002, pp. 1-40.

Altelaar AM, Klinkert I, Jalink K, de Lange RP, Adan RA, Heeren RM, et al. Gold-enhanced biomolecular surface imaging of cells and tissue by SIMS and MALDI mass spectrometry. Analytical chemistry 2006; 78: 734-742.

Anderson DM, Carolan VA, Crosland S, Sharples KR, Clench MR. Examination of the distribution of nicosulfuron in sunflower plants by matrix-assisted laser desorption/ionisation mass spectrometry imaging. Rapid communications in mass spectrometry 2009; 23: 1321-1327.

Andres PR, Schubert US. Metallo-Polymerization/-Cyclization of a C16-Bridged Di-Terpyridine Ligand and Iron (II) Ions. Macromolecular rapid communications 2004; 25: 1371-1375.

Arroita M, Aristi I, Flores L, Larrañaga A, Díez J, Mora J, et al. The use of wooden sticks to assess stream ecosystem functioning: Comparison with leaf breakdown rates. Science of the Total Environment 2012; 440: 115-122.

Ashcroft A, Brenton G, Monaghan J. Recent developments in polymer characterization using mass spectrometry. Advances in Mass Spectrometry: Plenary and Keynote Lectures of the 16th International Mass Sepctrometry Conference. 16. Elsevier, 2004, pp. 215.

Atkinson SJ, Loadman PM, Sutton C, Patterson LH, Clench MR. Examination of the distribution of the bioreductive drug AQ4N and its active metabolite AQ4 in solid tumours by imaging matrix-assisted laser desorption/ionisation mass spectrometry. Rapid communications in mass spectrometry 2007; 21: 1271-1276.

Aziz M, Sturtevant D, Winston J, Collakova E, Jelesko J, Chapman K. MALDI-MS Imaging of Urushiols in Poison Ivy Stem. Molecules 2017; 22: 711.

Bahr U, Deppe A, Karas M, Hillenkamp F, Giessmann U. Mass spectrometry of synthetic polymers by UV-matrix-assisted laser desorption/ionization. Analytical Chemistry 1992; 64: 2866-2869.

Balzer W. Organic matter degradation and biogenic element cycling in a nearshore sediment (Kiel Bight). Limnol. Oceanogr 1984; 29: 1231-1246.

Bärlocher F. Leaf mass loss estimated by litter bag technique. Methods to study litter decomposition. Springer, 2005, pp. 37-42.

Barner-Kowollik C, Delaittre G, Gründling T. and Thomas Paulöhrl. Mass Spectrometry in Polymer Chemistry 2012: 373.

Bauer BJ, Guttman CM, Liu D-W, Blair WR. Tri-Alpha-Napthyl Benzene as a Crystalline or Glassy MALDI Matrix. Polymer 2002.

Belu A, Mahoney C, Wormuth K. Chemical imaging of drug eluting coatings: combining surface analysis and confocal Raman microscopy. Journal of Controlled Release 2008; 126: 111-121.

Benabdellah F, Touboul D, Brunelle A, Laprévote O. In situ primary metabolites localization on a rat brain section by chemical mass spectrometry imaging. Analytical chemistry 2009; 81: 5557-5560.

Bertrand P, Lallier-Vergès E. Past sedimentary organic matter accumulation and degradation controlled by productivity. Nature 1993; 364: 786-788.

Bivehed E, Strömvall R, Bergquist J, Bakalkin G, Andersson M. Region-specific bioconversion of dynorphin neuropeptide detected by in situ histochemistry and MALDI imaging mass spectrometry. Peptides 2017; 87: 20-27.

Bouslimani A, Bec N, Glueckmann M, Hirtz C, Larroque C. Matrix-assisted laser desorption/ionization imaging mass spectrometry of oxaliplatin derivatives in heated intraoperative chemotherapy (HIPEC)-like treated rat kidney. Rapid Communications in Mass Spectrometry 2010; 24: 415-421.

Brentan Silva D, Aschenbrenner A-K, Lopes N, Spring O. Direct Analyses of Secondary Metabolites by Mass Spectrometry Imaging (MSI) from Sunflower (Helianthus annuus L.) Trichomes. Molecules 2017; 22: 774.

Bunn SE, Davies PM, Mosisch TD. Ecosystem measures of river health and their response to riparian and catchment degradation. Freshwater Biology 1999; 41: 333-345.

Burrell M, Earnshaw C, Clench M. Imaging matrix assisted laser desorption ionization mass spectrometry: a technique to map plant metabolites within tissues at high spatial resolution. Journal of experimental botany 2006; 58: 757-763.

Calderón-Preciado D, Matamoros V, Bayona JM. Occurrence and potential crop uptake of emerging contaminants and related compounds in an agricultural irrigation network. Science of the total environment 2011; 412: 14-19.

Canfield DE, Thamdrup B, Hansen JW. The anaerobic degradation of organic matter in Danish coastal sediments: iron reduction, manganese reduction, and sulfate reduction. Geochimica et Cosmochimica Acta 1993; 57: 3867-3883.

Castellino S, Groseclose MR, Wagner D. MALDI imaging mass spectrometry: bridging biology and chemistry in drug development. 2011.

Cha S, Song Z, Nikolau BJ, Yeung ES. Direct profiling and imaging of epicuticular waxes on Arabidopsis thaliana by laser desorption/ionization mass spectrometry using silver colloid as a matrix. Analytical chemistry 2009; 81: 2991-3000.

Chacon A, Zagol-Ikapitte I, Amarnath V, Reyzer ML, Oates JA, Caprioli RM, et al. On-tissue chemical derivatization of 3-methoxysalicylamine for MALDI-imaging mass spectrometry. Journal of Mass Spectrometry 2011; 46: 840-846.

Chan C-M, Weng L-T, Lau Y-TR. Polymer surface structures determined using ToF-SIMS. Reviews in Analytical Chemistry 2014; 33: 11-30.

Chaurand P, Sanders ME, Jensen RA, Caprioli RM. Proteomics in diagnostic pathology: profiling and imaging proteins directly in tissue sections. The American journal of pathology 2004; 165: 1057-1068.

Chen R, Hui L, Sturm RM, Li L. Three dimensional mapping of neuropeptides and lipids in crustacean brain by mass spectral imaging. Journal of the American Society for Mass Spectrometry 2009; 20: 1068-1077.

Cheung Z-L, Weng L-T, Chan C-M, Hou WM, Li L. Morphology-driven surface segregation in a blend of poly (ε-caprolactone) and poly (vinyl chloride). Langmuir 2005; 21: 7968-7970.

Costanza R, d'Arge R, de Groot R, Farber S, Grasso M, Hannon B, et al. The value of the world's ecosystem services and natural capital. Nature 1997; 387: 253-260.

Cotter RJ, Gardner BD, Iltchenko S, English RD. Tandem time-of-flight mass spectrometry with a curved field reflectron. Analytical chemistry 2004; 76: 1976-1981.

Crecelius AC, Baumgaertel A, Schubert US. Tandem mass spectrometry of synthetic polymers. Journal of mass spectrometry 2009; 44: 1277-1286.

Crecelius AC, Hölscher D, Hoffmann T, Schneider B, Fischer TC, Hanke MV, et al. Spatial and Temporal Localization of Flavonoid Metabolites in Strawberry Fruit (Fragaria × ananassa). Journal of Agricultural and Food Chemistry 2017a; 65: 3559-3568.

Crecelius AC, Michalzik B, Potthast K, Meyer S, Schubert US. Tracing the fate and transport of secondary plant metabolites in a laboratory mesocosm experiment by employing mass spectrometric imaging. Analytical and Bioanalytical Chemistry 2017b; 409: 3807-3820.

Crecelius AC, Steinacker R, Meier A, Alexandrov T, Vitz Jr, Schubert US. Application of matrix-assisted laser desorption/ionization mass spectrometric imaging for photolithographic structuring. Analytical chemistry 2012; 84: 6921-6925.

Crecelius AC, Vitz J, Schubert US. Mass spectrometric imaging of synthetic polymers. Analytica Chimica Acta 2014; 808: 10-17.

Dalisay DS, Kim KW, Lee C, Yang H, Rübel O, Bowen BP, et al. Dirigent Protein-Mediated Lignan and Cyanogenic Glucoside Formation in Flax Seed: Integrated Omics and MALDI Mass Spectrometry Imaging. Journal of Natural Products 2015; 78: 1231-1242.

Debois D, Jourdan E, Smargiasso N, Thonart P, De Pauw E, Ongena M. Spatiotemporal Monitoring of the Antibiome Secreted by Bacillus Biofilms on Plant Roots Using MALDI Mass Spectrometry Imaging. Analytical Chemistry 2014; 86: 4431-4438.

Deininger S-O, Cornett DS, Paape R, Becker M, Pineau C, Rauser S, et al. Normalization in MALDI-TOF imaging datasets of proteins: practical considerations. Analytical and bioanalytical chemistry 2011; 401: 167-181.

Dekker LJ, van Kampen JJ, Reedijk ML, Burgers PC, Gruters RA, Osterhaus AD, et al. A mass spectrometry based imaging method developed for the intracellular detection of HIV protease inhibitors. Rapid Communications in Mass Spectrometry 2009; 23: 1183-1188.

Delcorte A, Bour J, Aubriet F, Muller J-F, Bertrand P. Sample metallization for performance improvement in desorption/ionization of kilodalton molecules: quantitative evaluation, imaging secondary ion MS, and laser ablation. Analytical chemistry 2003; 75: 6875-6885.

Dilillo M, Ait-Belkacem R, Esteve C, Pellegrini D, Nicolardi S, Costa M, et al. Ultra-High Mass Resolution MALDI Imaging Mass Spectrometry of Proteins and Metabolites in a Mouse Model of Glioblastoma. Scientific Reports 2017; 7: 603.

dos Santos FN, Tata A, Belaz KRA, Magalhães DMA, Luz EDMN, Eberlin MN. Major phytopathogens and strains from cocoa (Theobroma cacao L.) are differentiated by MALDI-MS lipid and/or peptide/protein profiles. Analytical and Bioanalytical Chemistry 2017; 409: 1765-1777.

Drexler DM, Garrett TJ, Cantone JL, Diters RW, Mitroka JG, Conaway MCP, et al. Utility of imaging mass spectrometry (IMS) by matrix-assisted laser desorption ionization (MALDI) on an ion trap mass spectrometer in the analysis of drugs and metabolites in biological tissues. Journal of pharmacological and toxicological methods 2007; 55: 279-288.

Dubey M, Emoto K, Cheng F, Gamble LJ, Takahashi H, Grainger DW, et al. Surface analysis of photolithographic patterns using ToF-SIMS and PCA. Surface and Interface Analysis 2009; 41: 645-652.

Dufresne M, Thomas Al, Breault-Turcot J, Masson J-Fo, Chaurand P. Silver-assisted laser desorption ionization for high spatial resolution imaging mass spectrometry of olefins from thin tissue sections. Analytical chemistry 2013; 85: 3318-3324.

Earnshaw CJ, Carolan VA, Richards DS, Clench MR. Direct analysis of pharmaceutical tablet formulations using matrix-assisted laser desorption/ionisation mass spectrometry imaging. Rapid Communications in Mass Spectrometry 2010; 24: 1665-1672.

Elosegi A, Díez J, Mutz M. Effects of hydromorphological integrity on biodiversity and functioning of river ecosystems. Hydrobiologia 2010; 657: 199-215.

Eswaran H, Van Den Berg E, Reich P. Organic carbon in soils of the world. Soil science society of America journal 1993; 57: 192-194.

Fehniger TE, Végvári Á, Rezeli M, Prikk K, Ross P, Dahlbäck M, et al. Direct demonstration of tissue uptake of an inhaled drug: proof-of-principle study using matrix-assisted laser desorption ionization mass spectrometry imaging. Analytical chemistry 2011; 83: 8329-8336.

Feio M, Alves T, Boavida M, Medeiros A, Graça M. Functional indicators of stream health: a river-basin approach. Freshwater Biology 2010; 55: 1050-1065.

Feld CK, Birk S, Bradley DC, Hering D, Kail J, Marzin A, et al. Chapter Three - From Natural to Degraded Rivers and Back Again: A Test of Restoration Ecology Theory and Practice. In: Guy W, editor. Advances in Ecological Research. Volume 44. Academic Press, 2011, pp. 119-209.

Ferreira V, Castagneyrol B, Koricheva J, Gulis V, Chauvet E, Graça MA. A meta-analysis of the effects of nutrient enrichment on litter decomposition in streams. Biological Reviews 2015; 90: 669-688.

Fisher GL, Belu AM, Mahoney CM, Wormuth K, Sanada N. Three-dimensional time-of-flight secondary ion mass spectrometry imaging of a pharmaceutical in a coronary stent coating as a function of elution time. Analytical chemistry 2009; 81: 9930-9940.

Flinders B, Cuypers E, Porta T, Varesio E, Hopfgartner G, Heeren RMA. Mass Spectrometry Imaging of Drugs of Abuse in Hair. In: Cole LM, editor. Imaging Mass Spectrometry : Methods and Protocols. Springer New York, New York, NY, 2017, pp. 137-147.

Fowble KL, Teramoto K, Cody RB, Edwards D, Guarrera D, Musah RA. Development of "Laser Ablation Direct Analysis in Real Time Imaging" Mass Spectrometry: Application to Spatial Distribution Mapping of Metabolites Along the Biosynthetic Cascade Leading to Synthesis of Atropine and Scopolamine in Plant Tissue. Analytical Chemistry 2017; 89: 3421-3429.

Francese S, Dani FR, Traldi P, Mastrobuoni G, Pieraccini G, Moneti G. MALDI mass spectrometry imaging, from its origins up to today: the state of the art. Combinatorial chemistry & high throughput screening 2009; 12: 156-174.

Friberg N, Bonada N, Bradley DC, Dunbar MJ, Edwards FK, Grey J, et al. Biomonitoring of Human Impacts in Freshwater Ecosystems. The Good, the Bad and the Ugly. Advances in Ecological Research. 44, 2011, pp. 1-68.

Garrett TJ, Prieto-Conaway MC, Kovtoun V, Bui H, Izgarian N, Stafford G, et al. Imaging of small molecules in tissue sections with a new intermediate-pressure MALDI linear ion trap mass spectrometer. International Journal of Mass Spectrometry 2007; 260: 166-176.

Gessner MO, Chauvet E. A case for using litter breakdown to assess functional stream integrity. Ecological applications 2002; 12: 498-510.

Goodwin RJ, Macintyre L, Watson D, Scullion S, Pitt A. A solvent-free matrix application method for matrix-assisted laser desorption/ionization imaging of small molecules. Rapid communications in mass spectrometry 2010; 24: 1682-1686.

Goodwin RJ, Mackay CL, Nilsson A, Harrison DJ, Farde L, Andren PE, et al. Qualitative and quantitative MALDI imaging of the positron emission tomography ligands raclopride (a D2 dopamine antagonist) and SCH 23390 (a D1 dopamine antagonist) in rat brain tissue sections using a solvent-free dry matrix application method. Analytical chemistry 2011; 83: 9694-9701.

Goodwin RJ, Pennington SR, Pitt AR. Protein and peptides in pictures: imaging with MALDI mass spectrometry. Proteomics 2008; 8: 3785-3800.

Goto-Inoue N, Setou M, Zaima N. Visualization of spatial distribution of γ-aminobutyric acid in eggplant (Solanum melongena) by matrix-assisted laser desorption/ionization imaging mass spectrometry. Analytical Sciences 2010; 26: 821-825.

Greene J. Biodegradation of Compostable Plastics in Green Yard-Waste Compost Environment. Journal of Polymers and the Environment 2007; 15: 269-273.

Groseclose MR, Andersson M, Hardesty WM, Caprioli RM. Identification of proteins directly from tissue: in situ tryptic digestions coupled with imaging mass spectrometry. Journal of Mass Spectrometry 2007; 42: 254-262.

Grove KJ, Kansara V, Prentiss M, Long D, Mogi M, Kim S, et al. Application of Imaging Mass Spectrometry to Assess Ocular Drug Transit. SLAS DISCOVERY: Advancing Life Sciences R&D; 0: 2472555217724780.

Gruendling T, Weidner S, Falkenhagen J, Barner-Kowollik C. Mass spectrometry in polymer chemistry: a state-of-the-art up-date. Polymer Chemistry 2010; 1: 599-617.

Guenther S, Römpp A, Kummer W, Spengler B. AP-MALDI imaging of neuropeptides in mouse pituitary gland with 5µm spatial resolution and high mass accuracy. International Journal of Mass Spectrometry 2011; 305: 228-237.

Harvey HR, Fallon RD, Patton JS. The effect of organic matter and oxygen on the degradation of bacterial membrane lipids in marine sediments. Geochimica et Cosmochimica Acta 1986; 50: 795-804.

Hofmann G. Biodegradable implants in traumatology: a review on the state-of-the-art. Archives of orthopaedic and trauma surgery 1995; 114: 123-132.

Holder E, Marin V, Meier MA, Schubert US. A Novel Light-Emitting Mixed-Ligand Iridium (III) Complex with a Terpyridine-Poly (ethylene glycol) Macroligand. Macromolecular rapid communications 2004; 25: 1491-1496.

Hölscher D, Fuchser J, Knop K, Menezes RC, Buerkert A, Svatoš A, et al. High resolution mass spectrometry imaging reveals the occurrence of phenylphenalenone-type compounds in red paracytic stomata and red epidermis tissue of Musa acuminata ssp. zebrina cv. 'Rowe Red'. Phytochemistry 2015; 116: 239-245.

Hölscher D, Shroff R, Knop K, Gottschaldt M, Crecelius A, Schneider B, et al. Matrix-free UV-laser desorption/ionization (LDI) mass spectrometric imaging at the single-cell level: Distribution of secondary metabolites of Arabidopsis thaliana and Hypericum species. The Plant Journal 2009; 60: 907-918.

Hoshi T, Kudo M. High resolution static SIMS imaging by time of flight SIMS. Applied surface science 2003; 203: 818-824.

Hoteling AJ, Kawaoka K, Goodberlet MC, Yu WM, Owens KG. Optimization of matrix-assisted laser desorption/ionization time-of-flight collision-induced dissociation using poly (ethylene glycol). Rapid communications in mass spectrometry 2003; 17: 1671-1676.

Hoteling AJ, Owens KG. Improved PSD and CID on a MALDI ToFMS. Journal of the American Society for Mass Spectrometry 2004; 15: 523-535.

Hsieh Y, Li F, Korfmacher WA. Mapping pharmaceuticals in rat brain sections using MALDI imaging mass spectrometry. Mass Spectrometry Imaging: Principles and Protocols 2010: 147-158.

Hutton G, Haller L, Water S, Organization WH. Evaluation of the costs and benefits of water and sanitation improvements at the global level. 2004.

Ibáñez AJ, Scharte J, Bones P, Pirkl A, Meldau S, Baldwin IT, et al. Rapid metabolic profiling of Nicotiana tabacum defence responses against Phytophthora nicotianae using direct infrared laser desorption ionization mass spectrometry and principal component analysis. Plant methods 2010; 6: 14.

Imberger SJ, Thompson RM, Grace MR. Searching for effective indicators of ecosystem function in urban streams: Assessing cellulose decomposition potential. Freshwater Biology 2010; 55: 2089-2106.

Jackson ST, Short RD. Surface morphology of PVC/PMMA blends. Journal of Materials Chemistry 1992; 2: 259-260.

Jagtap RN, Ambre AH. Overview literature on matrix assisted laser desorption ionization mass spectroscopy (MALDI MS): Basics and its applications in characterizing polymeric materials. Bulletin of Materials Science 2005; 28: 515-528.

Jun JH, Song Z, Liu Z, Nikolau BJ, Yeung ES, Lee YJ. High-spatial and high-mass resolution imaging of surface metabolites of Arabidopsis thaliana by laser desorption-ionization mass spectrometry using colloidal silver. Analytical chemistry 2010; 82: 3255-3265.

Kailas L, Audinot J-N, Migeon H-N, Bertrand P. ToF-SIMS molecular characterization and nano-SIMS imaging of submicron domain formation at the surface of PS/PMMA blend and copolymer thin films. Applied surface science 2004; 231: 289-295.

Kalbitz K, Schwesig D, Schmerwitz J, Kaiser K, Haumaier L, Glaser B, et al. Changes in properties of soil-derived dissolved organic matter induced by biodegradation. Soil Biology and Biochemistry 2003; 35: 1129-1142.

Kalbitz K, Solinger S, Park J-H, Michalzik B, Matzner E. Controls on the dynamics of dissolved organic matter in soils: a review. Soil science 2000; 165: 277-304.

Kawamoto T. Use of a new adhesive film for the preparation of multi-purpose fresh-frozen sections from hard tissues, whole-animals, insects and plants. Archives of histology and cytology 2003; 66: 123-143.

Kawasaki H, Ozawa T, Hisatomi H, Arakawa R. Platinum vapor deposition surface-assisted laser desorption/ionization for imaging mass spectrometry of small molecules. Rapid Communications in Mass Spectrometry 2012; 26: 1849-1858.

Kell RG, Montluçon DB, Prahli FG. organic matter in marine sediments. Nature 1994; 370: 18.

Kertesz V, Van Berkel GJ, Vavrek M, Koeplinger KA, Schneider BB, Covey TR. Comparison of drug distribution images from whole-body thin tissue sections obtained using desorption electrospray ionization tandem mass spectrometry and autoradiography. Analytical chemistry 2008; 80: 5168-5177.

Khatib-Shahidi S, Andersson M, Herman JL, Gillespie TA, Caprioli RM. Direct molecular analysis of whole-body animal tissue sections by imaging MALDI mass spectrometry. Analytical chemistry 2006; 78: 6448-6456.

Kim SH, Kim J, Lee YJ, Lee TG, Yoon S. Sample Preparation of Corn Seed Tissue to Prevent Analyte Relocations for Mass Spectrometry Imaging. Journal of The American Society for Mass Spectrometry 2017; 28: 1729-1732.

Kloninger C, Rehahn M. 1, 1-dimethylsilacyclobutane-mediated living anionic block copolymerization of [1] dimethylsilaferrocenophane and methyl methacrylate. Macromolecules 2004; 37: 1720-1727.

Koeniger SL, Talaty N, Luo Y, Ready D, Voorbach M, Seifert T, et al. A quantitation method for mass spectrometry imaging. Rapid Communications in Mass Spectrometry 2011; 25: 503-510.

Kompauer M, Heiles S, Spengler B. Atmospheric pressure MALDI mass spectrometry imaging of tissues and cells at 1.4-[mu]m lateral resolution. Nat Meth 2017; 14: 90-96.

Kondo T, Sawa S, Kinoshita A, Mizuno S, Kakimoto T, Fukuda H, et al. A plant peptide encoded by CLV3 identified by in situ MALDI-TOF MS analysis. Science 2006; 313: 845-848.

Kono T, Iwase E, Kanamori Y. TOF-SIMS analysis of polystyrene/polybutadiene blend using chemical derivatization and multivariate analysis. Applied Surface Science 2008; 255: 997-1000.

Kooijman PC, Kok S, Honing M. Independent assessment of matrix-assisted laser desorption/ionization mass spectrometry (MALDI-MS) sample preparation quality: Effect of sample preparation on MALDI-MS of synthetic polymers. Rapid Communications in Mass Spectrometry 2017; 31: 362-370.

Kristensen E, Ahmed SI, Devol AH. Aerobic and anaerobic decomposition of organic matter in marine sediment: which is fastest? Limnology and oceanography 1995; 40: 1430-1437.

Kroiss J, Kaltenpoth M, Schneider B, Schwinger M-G, Hertweck C, Maddula RK, et al. Symbiotic streptomycetes provide antibiotic combination prophylaxis for wasp offspring. Nature Chemical Biology 2010; 6: 261-263.

Lanao J, Fraile M. Drug tissue distribution: study methods and therapeutic implications. Current pharmaceutical design 2005; 11: 3829-3845.

Langer O, Muller M. Methods to assess tissue-specific distribution and metabolism of drugs. Current drug metabolism 2004; 5: 463-481.

Lee RFS, Theiner S, Meibom A, Koellensperger G, Keppler BK, Dyson PJ. Application of imaging mass spectrometry approaches to facilitate metal-based anticancer drug research. Metallomics 2017; 9: 365-381.

Lepoittevin B, Dourges M-A, Masure M, Hemery P, Baran K, Cramail H. Synthesis and characterization of ring-shaped polystyrenes. Macromolecules 2000; 33: 8218-8224.

Li Y, Shrestha B, Vertes A. Atmospheric pressure molecular imaging by infrared MALDI mass spectrometry. Analytical Chemistry 2007; 79: 523-532.

Lukowski JK, Weaver EM, Hummon AB. Analyzing Liposomal Drug Delivery Systems in Three-Dimensional Cell Culture Models Using MALDI Imaging Mass Spectrometry. Analytical Chemistry 2017; 89: 8453-8458.

Mahoney CM, Yu J, Fahey A, Gardella JA. SIMS depth profiling of polymer blends with protein based drugs. Applied Surface Science 2006; 252: 6609-6614.

Mains J, Wilson CG, Urquhart A. ToF-SIMS analysis of dexamethasone distribution in the isolated perfused eye. Investigative ophthalmology & visual science 2011; 52: 8413-8419.

Manier ML, Reyzer ML, Goh A, Dartois V, Via LE, Barry CE, et al. Reagent precoated targets for rapid in-tissue derivatization of the anti-tuberculosis drug isoniazid followed by MALDI imaging mass spectrometry. Journal of the American Society for Mass Spectrometry 2011; 22: 1409-1419.

Mantzavinos D, Kalogerakis N. Treatment of olive mill effluents: Part I. Organic matter degradation by chemical and biological processes—an overview. Environment international 2005; 31: 289-295.

Marien J, Ghitti G, Jérôme R, Teyssié P. Potentiality of secondary ion mass spectrometry for chemical, micron-size imaging of multiphase polymer materials. Polymer Bulletin 1993; 30: 435-440.

Marko-Varga G, Fehniger TE, Rezeli M, Döme B, Laurell T, Végvári Á. Drug localization in different lung cancer phenotypes by MALDI mass spectrometry imaging. Journal of proteomics 2011; 74: 982-992.

Marshall P, Toteu-Djomte V, Bareille P, Perry H, Brown G, Baumert M, et al. Correlation of skin blanching and percutaneous absorption for glucocorticoid receptor agonists by matrix-assisted laser desorption ionization mass spectrometry imaging and liquid extraction surface analysis with nanoelectrospray ionization mass spectrometry. Analytical chemistry 2010; 82: 7787-7794.

Martínez A, Pérez J, Molinero J, Sagarduy M, Pozo J. Effects of flow scarcity on leaf-litter processing under oceanic climate conditions in calcareous streams. Science of The Total Environment 2015; 503: 251-257.

McDermott MK, Saylor DM, Casas R, Dair BJ, Guo J, Kim CS, et al. Microstructure and elution of tetracycline from block copolymer coatings. Journal of pharmaceutical sciences 2010; 99: 2777-2785.

McTammany ME, Benfield EF, Webster JR. Effects of agriculture on wood breakdown and microbial biofilm respiration in southern Appalachian streams. Freshwater Biology 2008; 53: 842-854.

Mendoza–Lera C, Larrañaga A, Pérez J, Descals E, Martínez A, Moya O, et al. Headwater reservoirs weaken terrestrial-aquatic linkage by slowing leaf-litter processing in downstream regulated reaches. River Research and Applications 2012; 28: 13-22.

Miyasaka T, Ikemoto T, Kohno T. ToF-SIMS imaging of PE/PP polymer using multivariate analysis. Applied Surface Science 2008; 255: 1576-1579.

Montaudo G, Samperi F, Montaudo MS. Characterization of synthetic polymers by MALDI-MS. Progress in Polymer Science 2006; 31: 277-357.

Moran MA, Sheldon WM, Zepp RG. Carbon loss and optical property changes during long-term photochemical and biological degradation of estuarine dissolved organic matter. Limnology and Oceanography 2000; 45: 1254-1264.

Mouton JW, Theuretzbacher U, Craig WA, Tulkens PM, Derendorf H, Cars O. Tissue concentrations: do we ever learn? Journal of Antimicrobial Chemotherapy 2007; 61: 235-237.

Mullen AK, Clench MR, Crosland S, Sharples KR. Determination of agrochemical compounds in soya plants by imaging matrix-assisted laser desorption/ionisation mass spectrometry. Rapid Communications in Mass Spectrometry 2005; 19: 2507-2516.

Nemes P, Barton AA, Vertes A. Three-dimensional imaging of metabolites in tissues under ambient conditions by laser ablation electrospray ionization mass spectrometry. Analytical Chemistry 2009; 81: 6668-6675.

Neubert H, Knights KA, de Miguel YR, Cowan DA. MALDI TOF post-source decay investigation of alkali metal adducts of apolar polypentylresorcinol dendrimers. Macromolecules 2003; 36: 8297-8303.

Nielen MWF. Maldi time-of-flight mass spectrometry of synthetic polymers. Mass Spectrometry Reviews 1999; 18: 309-344.

Nilsson A, Fehniger TE, Gustavsson L, Andersson M, Kenne K, Marko-Varga G, et al. Fine mapping the spatial distribution and concentration of unlabeled drugs within tissue micro-compartments using imaging mass spectrometry. PloS one 2010; 5: e11411.

NIST. http://maldi.nist.gov/.

Northen TR, Yanes O, Northen MT, Marrinucci D, Uritboonthai W, Apon J, et al. Clathrate nanostructures for mass spectrometry. Nature 2007; 449: 1033.

Nyadong L, Harris GA, Balayssac S, Galhena AS, Malet-Martino M, Martino R, et al. Combining two-dimensional diffusion-ordered nuclear magnetic resonance spectroscopy, imaging desorption electrospray ionization mass spectrometry, and direct analysis in real-time mass spectrometry for the integral investigation of counterfeit pharmaceuticals. Analytical chemistry 2009; 81: 4803-4812.

Oades J. An introduction to organic matter in mineral soils. Minerals in soil environments 1989: 89-159.

Oades JM. Soil organic matter and structural stability: mechanisms and implications for management. Biological Processes and Soil Fertility. Springer, 1984, pp. 319-337.

Organization WH. Guidelines for drinking-water quality: Geneva: world health organization, 2011.

Palmer MA, Febria CM. The heartbeat of ecosystems. Science 2012; 336: 1393-1394.

Parton W, Schimel DS, Cole C, Ojima D. Analysis of factors controlling soil organic matter levels in Great Plains grasslands. Soil Science Society of America Journal 1987; 51: 1173-1179.

Pasch H, Rode K. Use of matrix-assisted laser desorption/ionization mass spectrometry for molar mass-sensitive detection in liquid chromatography of polymers. Journal of Chromatography A 1995; 699: 21-29.

Paschke C, Leisner A, Hester A, Maass K, Guenther S, Bouschen W, et al. Mirion--a software package for automatic processing of mass spectrometric images. Journal of the American Society for Mass Spectrometry 2013; 24: 1296-1306.

Peacock PM, McEwen CN. Mass spectrometry of synthetic polymers. Analytical chemistry 2004; 76: 3417-3428.

Porta T, Grivet C, Kraemer T, Varesio E, Hopfgartner G. Single hair cocaine consumption monitoring by mass spectrometric imaging. Analytical chemistry 2011; 83: 4266-4272.

Powers TW, Neely BA, Shao Y, Tang H, Troyer DA, Mehta AS, et al. MALDI Imaging Mass Spectrometry Profiling of N-Glycans in Formalin-Fixed Paraffin Embedded Clinical Tissue Blocks and Tissue Microarrays. PLOS ONE 2014; 9: e106255.

Prentice BM, Chumbley CW, Caprioli RM. Absolute Quantification of Rifampicin by MALDI Imaging Mass Spectrometry Using Multiple TOF/TOF Events in a Single Laser Shot. Journal of The American Society for Mass Spectrometry 2017; 28: 136-144.

Prideaux B, Staab D, Stoeckli M. Applications of MALDI-MSI to pharmaceutical research. Mass Spectrometry Imaging: Principles and Protocols 2010: 405-413.

Riemann B, Schäfers K, Schober O, Schäfers M. Small animal PET in preclinical studies: opportunities and challenges. The Quarterly Journal of Nuclear Medicine and Molecular Imaging 2008; 52: 215.

Rivas D, Ginebreda A, Pérez S, Quero C, Barceló D. MALDI-TOF MS Imaging evidences spatial differences in the degradation of solid polycaprolactone diol in water under aerobic and denitrifying conditions. Science of The Total Environment 2016; 566–567: 27-33.

Rizzarelli P, Carroccio S. Modern mass spectrometry in the characterization and degradation of biodegradable polymers. Analytica Chimica Acta 2014; 808: 18-43.

Robeson LM. Polymer blends. Hanser, Munich 2007: 24-149.

Robinson S, Warburton K, Seymour M, Clench M, Thomas-Oates J. Localization of water-soluble carbohydrates in wheat stems using imaging matrix-assisted laser desorption ionization mass spectrometry. New Phytologist 2007; 173: 438-444.

Römpp A, Spengler B. Mass spectrometry imaging with high resolution in mass and space. Histochemistry and cell biology 2013; 139: 759-783.

Rossi F, Ferrari R, Castiglione F, Mele A, Perale G, Moscatelli D. Polymer hydrogel functionalized with biodegradable nanoparticles as composite system for controlled drug delivery. Nanotechnology 2014; 26.

Schriemer DC, Li L. Detection of High Molecular Weight Narrow Polydisperse Polymers up to 1.5 Million Daltons by MALDI Mass Spectrometry. Analytical Chemistry 1996; 68: 2721-2725.

Schwartz SA, Reyzer ML, Caprioli RM. Direct tissue analysis using matrix-assisted laser desorption/ionization mass spectrometry: practical aspects of sample preparation. Journal of Mass Spectrometry 2003; 38: 699-708.

Shariatgorji M, Källback P, Gustavsson L, Schintu N, Svenningsson P, Goodwin RJ, et al. Controlled-pH tissue cleanup protocol for signal enhancement of small molecule drugs analyzed by MALDI-MS imaging. Analytical chemistry 2012; 84: 4603-4607.

Shin YG, Dong T, Chou B, Menghrajani K. Determination of loperamide in mdr1a/1b knock-out mouse brain tissue using matrix-assisted laser desorption/ionization mass spectrometry and comparison with quantitative electrospray-triple quadrupole mass spectrometry analysis. Archives of pharmacal research 2011; 34: 1983-1988.

Short RD, Ameen A, Jackson S, Pawson D, O'Toole L, Ward A. 1992 CR Burch prize TOF SIMS in polymer surface studies. Vacuum 1993; 44: 1143-1160.

Shroff R, Vergara F, Muck A, Svatoš A, Gershenzon J. Nonuniform distribution of glucosinolates in Arabidopsis thaliana leaves has important consequences for plant defense. Proceedings of the National Academy of Sciences 2008; 105: 6196-6201.

Sinha TK, Khatib-Shahidi S, Yankeelov TE, Mapara K, Ehtesham M, Cornett DS, et al. Integrating spatially resolved three-dimensional MALDI IMS with in vivo magnetic resonance imaging. Nature methods 2008; 5: 57.

Siracusa V, Ingrao C, Lo Giudice A, Mbohwa C, Dalla Rosa M. Environmental assessment of a multilayer polymer bag for food packaging and preservation: An LCA approach. Food Research International 2014; 62: 151-161.

Solon EG, Schweitzer A, Stoeckli M, Prideaux B. Autoradiography, MALDI-MS, and SIMS-MS imaging in pharmaceutical discovery and development. The AAPS journal 2010; 12: 11-26.

Sosnik A, Sodhi RNS, Brodersen PM, Sefton MV. Surface study of collagen/poloxamine hydrogels by a 'deep freezing' ToF-SIMS approach. Biomaterials 2006; 27: 2340-2348.

Stoeckli M, Staab D, Schweitzer A. Compound and metabolite distribution measured by MALDI mass spectrometric imaging in whole-body tissue sections. International Journal of Mass Spectrometry 2007; 260: 195-202.

Strohalm M, Strohalm Ji, Kaftan F, Krásný Ls, Volný M, Novák P, et al. Poly [N-(2-hydroxypropyl) methacrylamide]-based tissue-embedding medium compatible with MALDI mass spectrometry imaging experiments. Analytical chemistry 2011; 83: 5458-5462.

Sugiura Y, Setou M. Imaging mass spectrometry for visualization of drug and endogenous metabolite distribution: toward in situ pharmacometabolomes. Journal of Neuroimmune Pharmacology 2010; 5: 31-43.

Sweeney BW, Bott TL, Jackson JK, Kaplan LA, Newbold JD, Standley LJ, et al. Riparian deforestation, stream narrowing, and loss of stream ecosystem services. Proceedings of the National Academy of Sciences of the United States of America 2004; 101: 14132-14137.

Takahashi H, Emoto K, Dubey M, Castner DG, Grainger DW. Imaging surface immobilization chemistry: correlation with cell patterning on non-adhesive hydrogel thin films. Advanced functional materials 2008; 18: 2079-2088.

Takai N, Tanaka Y, Inazawa K, Saji H. Quantitative analysis of pharmaceutical drug distribution in multiple organs by imaging mass spectrometry. Rapid Communications in Mass Spectrometry 2012; 26: 1549-1556.

Tank JL, Winterbourn MJ. Microbial activity and invertebrate colonisation of wood in a New Zealand forest stream. New Zealand Journal of Marine and Freshwater Research 1996; 30: 271-280.

Teklezgi BG, Pamreddy A, Baijnath S, Gopal ND, Naicker T, Kruger HG, et al. Post heroin dose tissue distribution of 6-monoacetylmorphine (6-MAM) with MALDI imaging. Journal of Molecular Histology 2017; 48: 285-292.

Thomas J. The role of dissolved organic matter, particularly free amino acids and humic substances, in freshwater ecosystems. Freshwater Biology 1997; 38: 1-36.

Tiegs SD, Langhans SD, Tockner K, Gessner MO. Cotton strips as a leaf surrogate to measure decomposition in river floodplain habitats. Journal of the North American Benthological Society 2007; 26: 70-77.

Torrisi V, Licciardello A, Marletta G. Chemical imaging of self-assembling structures in Langmuir–Blodgett films of polymer blends. Materials Science and Engineering: B 2010; 169: 49-54.

Trim PJ, Djidja M-C, Atkinson SJ, Oakes K, Cole LM, Anderson DM, et al. Introduction of a 20 kHz Nd: YVO4 laser into a hybrid quadrupole time-of-flight mass spectrometer for MALDI-MS imaging. Analytical and bioanalytical chemistry 2010; 397: 3409-3419.

Trimpin S, Eichhorn P, Räder HJ, Müllen K, Knepper TP. Recalcitrance of poly(vinylpyrrolidone): evidence through matrix-assisted laser desorption–ionization time-of-flight mass spectrometry. Journal of Chromatography A 2001; 938: 67-77.

Uner A, Yilmaz F. Efficiency of laundry polymers containing liquid detergents for hard surface cleaning. Journal of Surfactants and Detergents 2015; 18: 213-224.

van Hove ERA, Smith DF, Heeren RM. A concise review of mass spectrometry imaging. Journal of chromatography A 2010; 1217: 3946-3954.

Van Veen J, Kuikman P. Soil structural aspects of decomposition of organic matter by micro-organisms. Biogeochemistry 1990; 11: 213-233.

Végvári Á, Fehniger TE, Gustavsson L, Nilsson A, Andrén PE, Kenne K, et al. Essential tactics of tissue preparation and matrix nano-spotting for successful compound imaging mass spectrometry. Journal of proteomics 2010; 73: 1270-1278.

Veličković D, Herdier H, Philippe G, Marion D, Rogniaux H, Bakan B. Matrix-assisted laser desorption/ionization mass spectrometry imaging: a powerful tool for probing the molecular topology of plant cutin polymer. The Plant Journal 2014; 80: 926-935.

Vorosmarty CJ, McIntyre PB, Gessner MO, Dudgeon D, Prusevich A, Green P, et al. Global threats to human water security and river biodiversity. Nature 2010; 467: 555-561.

Vrkoslav V, Muck A, Cvačka J, Svatoš A. MALDI imaging of neutral cuticular lipids in insects and plants. Journal of the American Society for Mass Spectrometry 2010; 21: 220-231.

Weidner S, Knappe P, Panne U. MALDI-TOF imaging mass spectrometry of artifacts in "dried droplet" polymer samples. Analytical and Bioanalytical Chemistry 2011; 401: 127-134.

Weidner SM, Falkenhagen J. Imaging mass spectrometry for examining localization of polymeric composition in matrix-assisted laser desorption/ionization samples. Rapid Communications in Mass Spectrometry 2009; 23: 653-660.

Welsh DM, Kloeppner LJ, Madrigal L, Pinto MR, Thompson BC, Schanze KS, et al. Regiosymmetric dibutyl-substituted poly (3, 4-propylenedioxythiophene) s as highly electron-rich electroactive and luminescent polymers. Macromolecules 2002; 35: 6517-6525.

Weng L-T, Smith TL, Feng J, Chan C-M. Morphology and Miscibility of Blends of Ethylene− Tetrafluoroethylene Copolymer/Poly (methyl methacrylate) Studied by ToF SIMS Imaging. Macromolecules 1998; 31: 928-932.

Wetzel RG, Hatcher PG, Bianchi TS. Natural photolysis by ultraviolet irradiance of recalcitrant dissolved organic matter to simple substrates for rapidbacterial metabolism. Limnology and Oceanography 1995; 40: 1369-1380.

Wiseman JM, Ifa DR, Zhu Y, Kissinger CB, Manicke NE, Kissinger PT, et al. Desorption electrospray ionization mass spectrometry: Imaging drugs and metabolites in tissues. Proceedings of the National Academy of Sciences 2008; 105: 18120-18125.

Yalcin T, Wallace WE, Guttman CM, Li L. Metal powder substrate-assisted laser desorption/ionization mass spectrometry for polyethylene analysis. Analytical chemistry 2002; 74: 4750-4756.

Yamada Y, Hidefumi K, Shion H, Oshikata M, Haramaki Y. Distribution of chloroquine in ocular tissue of pigmented rat using matrix-assisted laser desorption/ionization imaging quadrupole time-of-flight tandem mass spectrometry. Rapid Communications in Mass Spectrometry 2011; 25: 1600-1608.

Young RG, Matthaei CD, Townsend CR. Organic matter breakdown and ecosystem metabolism: functional indicators for assessing river ecosystem health. Journal of the North American Benthological Society 2008; 27: 605-625.

Yunus S, Delcorte A, Poleunis C, Bertrand P, Bolognesi A, Botta C. A Route to Self-Organized Honeycomb Microstructured Polystyrene Films and Their Chemical Characterization by ToF-SIMS Imaging. Advanced Functional Materials 2007; 17: 1079-1084.

Zaima N, Goto-Inoue N, Hayasaka T, Setou M. Application of imaging mass spectrometry for the analysis of Oryza sativa rice. Rapid Communications in Mass Spectrometry 2010; 24: 2723-2729.

Zavalin A, Todd EM, Rawhouser PD, Yang J, Norris JL, Caprioli RM. Direct imaging of single cells and tissue at sub-cellular spatial resolution using transmission geometry MALDI MS. Journal of Mass Spectrometry 2012; 47: 1473-1481.

Zhang J, Zenobi R. Matrix-dependent cationization in MALDI mass spectrometry. Journal of mass spectrometry 2004; 39: 808-816.